



Skolkovo Institute of Science and Technology

**OPERATIONAL AND UNCERTAINTY AWARE
PLANNING OF POWER SYSTEMS**

Doctoral Thesis

by

VLADIMIR FROLOV

DOCTORAL PROGRAM IN ENGINEERING SYSTEMS

Supervisor

Michael Chertkov, Adjunct Professor, Skoltech
Chair, Program in Applied Mathematics, University of Arizona

Moscow - 2021

©Vladimir Frolov 2021

I hereby declare that the work presented in this thesis was carried out by myself at Skolkovo Institute of Science and Technology, Moscow, except where due acknowledgement is made, and has not been submitted for any other degree.

Candidate (Vladimir Frolov)
Supervisor (Prof. Michael Chertkov)

Abstract

Operational and uncertainty aware power system planning methodology is developed in this thesis. A planning decision is made taking into account future power system operations with new selected equipment installed. Uncertainty and variability of future operational conditions are incorporated into the methodology using two separate approaches.

The first is stochastic programming when variability and uncertainty are represented by a set of deterministic scenarios. A two-stage planning problem with a single set of investment variables for all available operational scenarios and an individual set of operational variables-settings for each scenario is formulated. The sum of CAPEX and OPEX is optimized and demonstrated to be beneficial in a practical setting. Multiple time intervals generalization for gradual investments is also considered by adding an individual set of investment variables for each time interval and proper connection between time frames. Scenario sampling methodology was developed for the representation of the load duration curves for the planning horizon. The optimization framework accounts for the most general AC operational setting. The resulting nonlinear, non-convex, and multiple-scenario multiple-time intervals optimization is resolved through an efficient heuristic algorithm consisting of a sequence of quadratic programmings solved by CPLEX combined with exact AC-PF resolution for each scenario for maintaining feasible operational states during iterations. The developed methodology applicability is demonstrated for the solution of the Flexible Alternating Current Transmission System (FACTS) placement and sizing problem. Long-term planning is demonstrated on the example of a moderate size 30 bus system and practical size Polish network. Efficient non-local and sparse installation of the FACTS is demonstrated to be a good approach for the resolution of congestion problems in the environment with high integration of the renewables, increasing demand levels, and limited transmission expansion opportunities (e.g. in Europe, transmission expansion is severely limited because of political and environmental issues). An investment plan is found for the given horizon considering representable future operational conditions.

The second is probabilistic modeling using chance constraints. This approach was inspired by the Chance-Constrained Optimal Power Flow model and extended/generalized. The main point here is to represent operational conditions not by deterministic samples but by probabilistic clouds. The benefit is that each cloud represents an infinite number of samples, and the whole state space of operational conditions can be represented by several clouds. The future evolution of the operational space is modeled by the movement of the clouds and modification of the sizes-uncertainty levels. This approach increases the complexity of modeling but reduces the dimensionality of the internal operational part of the planning problem. The complexity reduction approach coined Cloud-AC-OPF, which replaces a collection of samples by their compact representation in terms of mean and standard deviation, is introduced. Instead of determining an optimal generation dispatch for each sample individually, we parametrize the generation dispatch as an affine function. The Cloud-AC-OPF is mathematically similar to a generalized Chance-Constrained AC-OPF (CC-AC-OPF) of the

type recently discussed in the literature but conceptually different as it discusses applications to long-term planning. We further propose a tractable formulation and implementation and illustrate our construction on the example of a 30-bus IEEE model. Then Cloud-AC-OPF is extended to Multi-Cluster-AC-OPF setting and tested on RTC-GMLC 73 bus case.

Developed operational and uncertainty aware planning methodology is suitable for the analysis of "what if" scenarios accounting for the cost of energy production, geographical constraints, economic growth, uncertainty growth, cost of investments in provided assets (CAPEX), outside policies, lifetime of equipment, possible adjustability of plan if prediction changes, trade-off between CAPEX and OPEX. The output of the software is web-visualized for better convenience.

Acknowledgments

I would like to acknowledge Michael Chertkov and all his research team for their support and supervision of the project. His advice and guidance have helped a lot with many encountered difficulties. I am grateful to Russel Bent, Scott Backhaus, Janusz Bialek, and David Pozo for their criticism, comments, and suggestions. I am grateful to Line Roald for collaboration and for aiming to find and resolve challenging and practical problems. I would like to acknowledge Skoltech and all Skoltech team for the organization, management and for providing this great opportunity to learn, perform research and work with great people.

Contents

List of acronyms and abbreviations	10
List of figures	12
List of tables	18
1 Introduction	19
1.1 Background	19
1.2 Introduction to the project	23
1.3 Contributions	29
1.4 Thesis layout	31
1.5 List of publications	34
I Stochastic Programming Approach to Operational and Uncertainty Aware Planning Using a Set of Deterministic Operational Scenarios	36
2 Placement and Sizing of Series Compensation (SC) and Static Var Compensation (SVC) Devices in Transmission Grids: The Case of AC Power Flows	38
2.1 Optimization model	39
2.2 Problem statement	41
2.3 Optimization algorithm	42
2.4 Solver validation	44
2.4.1 Comparison of the solutions for 9-bus system	44
2.4.2 Comparison of the solutions for 30-bus system	47
2.5 Single scenario optimization	51
2.5.1 OPF feasible operation	51
2.5.2 OPF infeasible operation	57
2.6 Multiple scenarios optimization	59
2.6.1 All OPF feasible scenarios	60
2.6.2 General case	62
2.7 Summary	65

3	Operations and Uncertainty Aware Installation of FACTS Devices in a Large Transmission System	66
3.1	Optimization framework for finding optimal location of FACTS devices	67
3.2	The Algorithm	71
3.2.1	Linearization	71
3.2.2	Solving the QP problem	72
3.2.3	Resolving AC PF	72
3.3	Generation of scenarios for long-term planning	72
3.3.1	Scenario sampling for each segment	74
3.3.2	Congestion analysis correction	74
3.3.3	Defining initial generation profile	75
3.4	Methodology and installation justification	75
3.4.1	IEEE 30-bus model	75
3.4.2	2736-bus Polish model	78
3.5	Multiple-scenario-aware long-term planning	80
3.5.1	IEEE 30-bus model	80
3.5.2	2736-bus Polish model	80
3.6	Summary	81
4	Methodology for Multi-stage, Operations and Uncertainty Aware Placement and Sizing of FACTS in a Large Power Transmission System	83
4.1	Optimization model	84
4.2	Problem statement	87
4.3	Solution algorithm	89
4.3.1	QP/LP implementation	89
4.3.2	AC-PF feasibility	90
4.4	Approach analysis	90
4.4.1	Algorithm validation	90
4.4.2	Scalability analysis	90
4.5	Gradual investments to resolve congestion	93
4.6	Summary	97
II	Planning with Probabilistic Representation of Uncertain Operational Conditions	98
5	Cloud-AC-OPF: Model Reduction Technique for Multi-Scenario Optimal Power Flow via Chance-Constrained Optimization	100
5.1	Multi-scenario AC-OPF	101

5.2	Uncertainty modelling	102
5.3	Reduced linear response modeling of the controllable resources	103
5.4	Cloud-AC-OPF	104
5.5	Cloud-AC-OPF: analytic reformulation	104
5.6	Analytic averaging of objective function	106
5.7	Implementation and solution approach	106
5.8	The case study analysis	107
5.8.1	MS-AC-OPF and three flavours of Cloud-AC-OPF	107
5.8.2	Scalability analysis	107
5.9	Reduction analysis	108
5.9.1	Comparison by the value of optimal objective	108
5.9.2	Comparison of the Cloud-AC-OPF and MS-AC-OPF optimal dispatches	109
5.10	Summary	111
6	Multi-Cluster-AC-OPF: Model Reduction for Multi-Stage, Multi-Scenario Optimal Power Flows	112
6.1	Requirement for the model reduction	113
6.1.1	Multi-Stage Multi-Scenario AC-OPF	113
6.1.2	Concept of the model reduction	115
6.2	Multi-Cluster-AC-OPF	115
6.2.1	Clustering of the operational conditions	116
6.2.2	Cluster modelling	116
6.2.3	Reduced linear response modeling of the controllable resources	117
6.2.4	Multi-Cluster-AC-OPF formulation	118
6.2.5	Multi-Cluster-AC-OPF: analytic reformulation	119
6.3	Implementation and solution approach	121
6.4	Case study analysis	122
6.4.1	Clustering approaches	123
6.4.2	Ground truth solution	124
6.4.3	MC-AC-OPF solution analysis	125
6.5	Summary	126
7	Summary, Conclusions and Recommendations for Future Research	127
7.1	Summary	127
7.2	Conclusions	128
7.3	Recommendations for future research	130

8	Appendix	132
8.1	Power system modelling	132
8.2	Power Flow (PF) and Optimal Power Flow (OPF) problems	135
8.3	FACTS devices	137
8.4	Equations for general optimization problem of FACTS placement and sizing	142
8.5	Equations for linearized optimization problem	143
8.6	Multiple-scenarios optimization generalization (deterministic)	147
8.7	Chance-Constrained Optimal Power Flow (CC-OPF)	148
8.7.1	Problem statement and analytic reformulation	148
8.7.2	Generalized Chance-Constrained OPF	150
8.7.3	Definition of uncertainty margins ($\lambda(x, \alpha)$)	152
8.7.4	Analytic averaging of cost over uncertainty set	154
	Bibliography	156

List of Acronyms and Abbreviations

- TSO - Transmission System Operator
- PST - Phase Shifting Transformer
- ESS - Energy Storage System
- HVDC - High Voltage Direct Current (line)
- CAPEX - Capital Expenditure
- OPEX - Operational Expenditure
- AC - Alternating Current
- DC - Direct Current
- AC-PF - Alternating Current Power Flow formulation
- AC-OPF - AC Optimal Power Flow problem, engaging AC PF model
- AC-CC-OPF - Alternating Current Chance Constraints Optimal Power Flow problem
- FACTS - Flexible Alternating Current Transmission System
- CC-OPF - Chance Constrained Optimal Power Flow
- MS-AC-OPF - Multi-Scenario AC-OPF, combination of a number of AC-OPF problems, accounted together
- MS-MS-AC-OPF - Multi-stage Multi-scenario AC OPF
- Cloud-AC-OPF - "cloud" reduction model for MS-AC-OPF. "Cloud" term here is not relevant to cloud computing, it represents a set of power system operational scenarios, which together form a probabilistic "cloud".
- MC-AC-OPF - multi-cluster-AC-OPF reduction model for MS-MS-AC-OPF

- RTC-GMLC - reliability test system - grid modernization lab consortium - power system model used for simulations
- SC - Series Compensator
- SVC - Static Var Compensator
- TCSC - Thyristor Controlled SC
- QP - Quadratic programming
- LP - Linear programming
- EV - Electric Vehicles
- CPLEX - advanced solver for optimization with linear constraints
- DC approximation - in the context of power system modelling, approximation of AC-PF formulation, used for transmission systems
- DC-OPF - corresponding OPF formulation accounting for DC-PF model
- SLP - Sequential Linear Programming
- Cutting plane - approach for constraints management in the optimisation problem
- Matpower - Matlab toolbox for power system modelling
- MINLP - Mixed Integer Non-linear Programming
- MILP - Mixed Integer Linear Programming
- IPOPT - Interior Point Optimiszer
- LD curve - Load Duration curve
- JUMP - domain-specific modelling language for mathematical optimisation embedded in Julia
- PU - per units - a way to measure system parameters in term of nominal value
- LMP - Locational Marginal Price
- FTR - Financial Transmission Rights

List of Figures

1.1	Global electricity consumption with years.	20
1.2	Net yearly electricity generation in EU-27.	21
1.3	Net early electricity generation in the USA.	21
1.4	Europe electricity production by fuels.	22
1.5	US electricity production by fuels.	23
2.1	Flowchart of an iterative algorithm.	43
2.2	Schematic representation of an iterative loop for 3-node system (single operational scenario is considered).	43
2.3	OPF solution of 9-bus system. Generators are blue, slack bus is white and loads are marked in green. Numbers next to each bus are id, voltage and phase for the given bus.	45
2.4	Solver solution for the same 9-bus system and the same scenario. Initially overloaded line marked in red.	45
2.5	Dependence of number of overloaded lines on iteration number.	46
2.6	Dependence of the total overload value for all overloaded lines on iteration number.	46
2.7	Active power generation dispatch comparison. Blue bars - initial dispatch on the 1st iteration of algorithm, orange bars - final solution, purple - OPF dispatch.	47
2.8	Reactive power generation dispatch comparison. Blue bars - initial dispatch on the 1st iteration of algorithm, orange bars - final solution, purple - OPF dispatch.	47
2.9	Dependence of number of overloaded lines on iterations. There is no convergence.	48
2.10	Dependence of reactive power output for each generator on iteration number.	48
2.11	Solver solution for the 30-bus system and the same scenario. Initially overloaded line marked in red. Generators represented by squares and loads by circles, the color of the node represents voltage level (white - low, yellow - high). Generators are numbered in the same way as in the Figs. 2.12- 2.13.	49
2.12	Active power generation dispatch comparison. Blue bars - initial dispatch on the 1st iteration of algorithm, orange bars - final solution, purple - OPF dispatch.	50
2.13	Reactive power generation dispatch comparison. Blue bars - initial dispatch on the 1st iteration of algorithm, orange bars - final solution, purple - OPF dispatch.	50
2.14	Dependence of SCs capital cost on iteration number.	51

2.15	Dependence of SVCs capital cost on iteration number.	51
2.16	Active power generation dispatch comparison for OPF feasible scenario and 1 hour service period. Blue bars - initial dispatch on the 1st iteration of algorithm, orange bars - final solution, purple - OPF dispatch.	52
2.17	Optimal solution for the 30-bus system for 15 years service period and base load level (uniform load scaling factor is 1). Initially overloaded line marked in red. Generators represented by squares and loads by large circles, the color of the node represents voltage level (white - low, yellow - high). Generators are enumerated. SVC compensated load is shown by a small circle, SVC installed capacity is given - for one scenario installed capacity is equal to actual compensation setting.	53
2.18	Convergence of the SVC capital investment cost for 15 years service period and $\alpha = 1$ (uniform load scaling factor).	54
2.19	Active power dispatch comparison for 15 years service period and $\alpha = 1$. Blue bars - initial dispatch on the 1st iteration of algorithm, orange bars - final solution, purple - OPF dispatch.	54
2.20	Optimal solution for the 30-bus system for 30 years service period and $\alpha = 1.03$ (uniform load scaling factor is 1.03). Initially overloaded line marked in red. Generators represented by squares and loads by large circles, the color of the node represents voltage level (white - low, yellow - high). Generators are enumerated. SVC compensated load is shown by a small circle, SVC installed capacity is given - for one scenario installed capacity is equal to actual compensation setting.	55
2.21	Active power dispatch comparison for 30 years service period and $\alpha = 1.03$. Blue bars - initial dispatch on the 1st iteration of algorithm, orange bars - final solution, purple - OPF dispatch.	56
2.22	Reactive power dispatch comparison for 30 years service period and $\alpha = 1.03$. Blue bars - initial dispatch on the 1st iteration of algorithm, orange bars - final solution, purple - OPF dispatch.	57
2.23	Active power dispatch comparison for four solutions of OPF infeasible scenario with $\alpha = 1.07$ and service period in the range from 1 hour to 30 years. Blue bars - initial dispatch on the 1st iteration of algorithm, orange bars - final solution, purple - OPF dispatch.	58

2.24	Visualization of the solver output. Circles and squares mark consumers and generators, respectively. Voltage profile is shown in color (transitioning from yellow for maximum voltage to white for the minimal voltage). Line marked blue was initially overloaded and it was also selected by the solver for SC correction/placement. Number, shown next to the blue line, shows correction (in percentage). Node which was chosen for the (only) SVC correction is shown as a white dot. Bold numbers which appear next to the dot show level of the voltage and corrected/installed reactive power provided at the optimal solution.	59
2.25	SVCs cost convergence for multiple scenarios solver, 10 different load configurations are used for simulation.	60
2.26	Average over 10 load configurations generation cost convergence with iterations. . .	61
2.27	Convergence of each of 10 operational costs corresponding to the generated scenarios.	61
2.28	Progress of overloading management, solver relieves line congestion for each operational case.	61
2.29	Illustration of the algorithm dynamics: we show dependence of line overloads in MVA (lines numbered on the right) and dependence of the total cost in M\$/years (blue dotted line shadowed from above) on the number of iterations.	63
2.30	Visualization of the final states for two scenarios (out of 10 considered). Marking and color-coding (yellow-to-white) is the same as given in the captions of Fig. 2.24. Additionally we show "actual setting of the device"/"capacity of the device". Initially overloaded and compensated line is marked blue, initially overloaded line which was relieved without placement of a SC device on it is shown red, and line which is chosen for compensation even though it was not overloaded prior to the correction is shown green.	64
3.1	Piecewise-constant approximation of the LD curve.	73
3.2	Computational time comparison for 30-bus model.	78
3.3	Computational time vs the number of scenarios for the Polish model.	79
3.4	Optimal solution for 10 years of planning in the case of the 30-bus model. Loads = yellow circles; gens = squares; blue dashed line = line with installed SC that was overloaded initially for some scenarios; green dot = node where an SVC is installed. Voltage levels are shown in PU; capacities of SVCs and SCs are shown in MVar and in % of initial line inductance.	81
3.5	Optimal solution for 10 years of planning in the case of the Polish model. Red dashed lines = lines that were initially overloaded for some scenarios. Two built SCs are shown by green lines. The big green dot illustrates an SVC device. SVC: 3.3 MVar, SCs: 14.4%, 70.4% (left to right).	82

4.1	Illustration of the relation between the number of scenarios, $M(t)$ (each defined in the time interval, t) and the number of time intervals, T . $N = \sum_{t=1}^T M(t)$ is the total number of constraints imposed (per line or per node) within our optimization formulation. (See text for additional explanations.)	86
4.2	Computational time of IPOPT (orange), of our main algorithm (red) and of our algorithm sped up with the cutting plane (dark blue) are shown as functions of the number of time intervals, T , for the 30 bus model. In all the tests shown the number of scenarios (per time interval) was 10. Loading level is unity initially and it increases (imitating economic growth) by the factor 0.005 per time step. Scenarios are generated with the deviation factor 0.01. (See Section 3.3 for details.) Budget constraint (of \$110,000 per time step) is applied. Our algorithms (with and without cutting plane sped up) are limited to 20 iterations.	92
4.3	Computational time of IPOPT (orange), of our main algorithm (red) and of our algorithm sped up with the cutting plane (dark blue) are shown as functions of the number of samples in the case of a single time interval for the 30 bus model. Loading level is set to 1.05. Scenarios are generated with the deviation factor 0.01. (See Section 3.3 for details.) No budget constraints are applied. Our algorithms (with and without cutting plane sped up) are limited to 20 iterations.	92
4.4	Computational time of our main algorithm reinforced by the cutting plane shown vs the number of time intervals for the 2736 bus-large Polish model in the case of a single scenario (per time interval). The optimization cost is linear (according to the base case documented in Mathpower) and thus LP is used at each iteration step of our reinforced algorithm solved in 15 iterations. In this case the loading level is set to unity in each time frame. Budget constraint of \$50,000 per time step is applied.	93
4.5	Snapshot of the final solution (after all the investments are made). Red marks lines from the active set of cutting plane. Thin green marks lines with installed SCs which are not overloaded (initially). Dashed blue marks lines which are both in the active set (overloaded) and chosen for SC installation.	95
4.6	Dependence of the optimal cost on time (blue bars) provided by our reinforced algorithm for the Polish model in the case of a single scenario (the same for different time intervals) and the year-long horizon split in 12 periods (months). Orange line shows initial ACOPF cost (without investments). Red line shows ACOPF cost with thermal limits ignored. Yellow line corresponds to the optimal solution found in the case when the entire horizon is treated as a single time-interval.	96

4.7	Installed capacity of the SC devices at corresponding lines shown in percentage of the initial line inductances. This is the case of a single scenario therefore operational values coincide with respective capacities. For example, inductance of line #50 is reduced to 0.	96
5.1	Computational complexity reduction scheme	102
5.2	Obj. function comparison for low loading regime (MS-AC-OPF vs Cloud-AC-OPF-a). Probability of the chance constraints violation is $\epsilon = 1\%$	108
5.3	Obj. function comparison in the regime of high load (MS-AC-OPF vs Cloud-AC-OPF-a) shown as a function of the uncertainty level and ϵ	109
5.4	Obj. function comparison at high loading regime for different versions of the Cloud-AC-OPF-k. $\epsilon = 1\%$ for each model.	110
5.5	Illustration of the Cloud-AC-OPF solution quality in terms of the generation response to perturbations in the regime of low loading.	110
5.6	Illustration of the Cloud-AC-OPF solution quality in terms of the generation response to perturbations in the regime of high loading.	111
6.1	Illustration of the relation between number of scenarios, $M(t)$ (each associated with the time interval, t) and the number of time intervals, T . $N = \sum_{t=1}^T M(t)$ is the total number of constraints imposed (per line or per node) within the investment planning framework.	114
6.2	Schematic illustration of the complexity reduction offered by the Multi-Cluster-AC-OPF.	115
6.3	Schematic illustration of the relation between time series samples (a) and their phase-space clustering (b). We emphasize here (on the illustrative example of two clusters) that neighboring temporal samples are not necessarily close to each other in the phase-space metric used to identify clusters.	116
6.4	Analytic reformulation process from the original MC-AC-OPF with probabilistic constraints to the tractable model with deterministic constraints.	120
6.5	Base case peak loading conditions for the RTS-GMLC 73 bus system. Squares are generators, circles are loads, the direction of power flows is shown by the arrows. Voltage level is shown and also color coded (low - white, high - yellow). Stressed lines are marked in orange with the percentage showing loading level.	122
6.6	State space schematic illustration in terms of area loading. 105408 samples of operational conditions are totally provided and shown.	123
6.7	State space clustering of state vectors using K-means algorithm (24 clusters) and its' illustration on Areas loading diagram for 1 and 2 Areas.	124
6.8	State space clustering of state vectors by 24 hours of the day and its' illustration on Areas loading diagram for 1 and 2 Areas.	124

6.9	Ground truth solution - ACOPF computed individually for each sample. Left: generation cost depending on power generation, right: histogram showing number of samples with power generation from the given interval. Total computational time - 29665 sec (8.24 hours).	125
8.1	Branch model illustration from [1].	133
8.2	TCSC for stable transmission of surplus power from Eastern to Western India from [2].	138
8.3	SVC system enable and support remote variable generation from [3].	139
8.4	The impact of SC on a) voltage and b) angular stability [4].	141

List of Tables

- 3.1 Implementation of the LD curve scheme 74
- 3.2 Monetary advantage of considering operational variables, illustrated on the IEEE 30-bus model. 76
- 3.3 Monetary advantages of adding the operational cost to the optimization objective for the IEEE 30-bus model. 77
- 3.4 Comparison of the proposed heuristics with the brute-force IPOPT solution of the exact problem Eq.(3.1.1) for the IEEE 30-bus model. 77
- 3.5 Monetary advantage of considering operational variables for the 2736-bus Polish model. 79

- 4.1 Comparison of our heuristic algorithm against the (brute-force) IPOPT algorithm for the IEEE 30-bus model. 91

- 5.1 Computational time comparison for the introduced models 107

- 6.1 Complexity comparison of the MS-MS-AC-OPF and MC-AC-OPF 121
- 6.2 Features of the MS-AC-OPF solutions (20 clusters) 126

Chapter 1

Introduction

1.1 Background

The subject of the thesis research is power system, and we are going to start highlighting important special features of the power systems. Any other infrastructures where a commodity is transported from supply to demand (for example, food chain, crude oil, or natural gas systems) are characterized by the ability to store the commodity. However, the power systems are different - storage, even though available in theory and increasing capacity during the last decade, is still expensive and not widespread. Thus imposing a significant feasibility requirement to maintain in operations an almost real-time balance of supply and demand.

Schematically, power system components are generation facilities, transmission grid, and power consumers. Transmission System Operator (TSO) is the entity responsible for keeping the lights on. It makes sure that the power is delivered reliably at the specified frequency and the voltages stay sufficiently close to their nominal values. At the same time system operator is set to operate the system in a way that none of the components are overloaded and in a cost-efficient manner.

Power systems across the globe undergo tremendous changes during the last 10-15 years. On the generation side, it is the introduction of renewable sources of energy. From an economical and ecological point of view, renewables are desirable. However, renewables also create complications related to their inherited uncertainty and the necessity to control related fluctuations by some other means. Also, they are usually situated at remote locations, specified by the availability of solar radiation/wind, thus require additional transmission capacity to use generated power.

On the consumption side, the gradual growth of the demand pushed many transmission grids close to the operational limits. Also, the uncertainty of demand at the transmission level is increased as well due to the installation of the distributed generation facilities. Overall, both loading level and operational uncertainty are growing. The combination of a highly loaded system and significant uncertainty increases operational risk.

Loading growth and installation of renewable power capacity are illustrated in the examples of the

USA and Europe. In the Fig. 1.1 global electricity consumption is illustrated [5]. The steady growth of electricity consumption is observed globally. It is worth noting that during the last 5-10 years, power generation in Europe (Fig. 1.2) and the USA (Fig. 1.3) remains stable [5, 6], which means that in this regions consumption is not growing as well. Main recent consumption growth occurs in Asia.

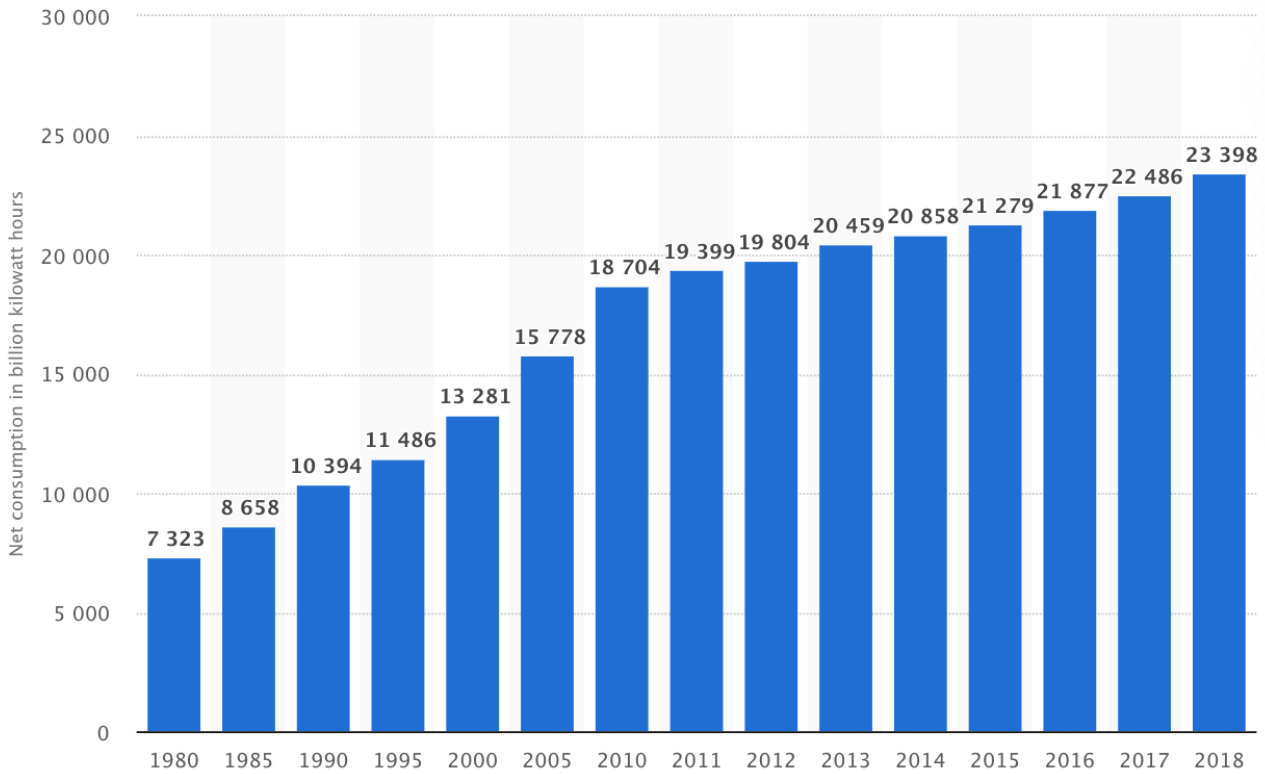


Figure 1.1: Global electricity consumption with years.

During the last years, relatively constant power consumption in Europe and the USA may indicate that transmission capacity/throughput problems are less important, but it is not exactly true. First, the introduction of renewables at remote locations highly influences power flows structure, meaning that when closer power generation is substituted for remote renewable, more transmission capacity is required. Second, renewable power generation usually requires additional reactive power support, which is not always local. Third, there is a new emerging challenge for the power systems which already operate close to the limits. Shift from traditional cars to Electric Vehicles (EVs) will request a lot of additional power generation and transmission capacity as well. For example in the USA yearly gasoline consumption is about $5 \cdot 10^{11} l/year$ [7]. This corresponds to about $170 \cdot 10^{17} J/year$ of energy consumed from fuel. Accounting for 30% efficiency of the combustion engine and 70% efficiency of the EV system, an additional $70 \cdot 10^{17} J/year$ of electricity is required for all US cars to be EV, which is about half of current USA electricity consumption.

During the last decade, a lot of renewable power sources were introduced both in Europe and

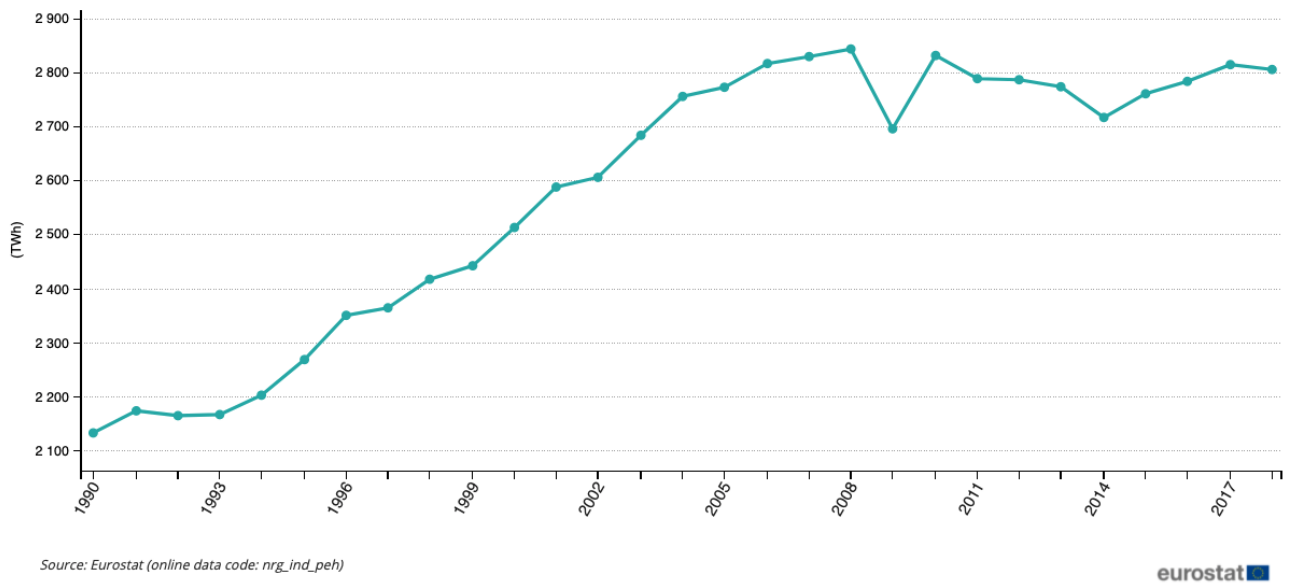


Figure 1.2: Net yearly electricity generation in EU-27.

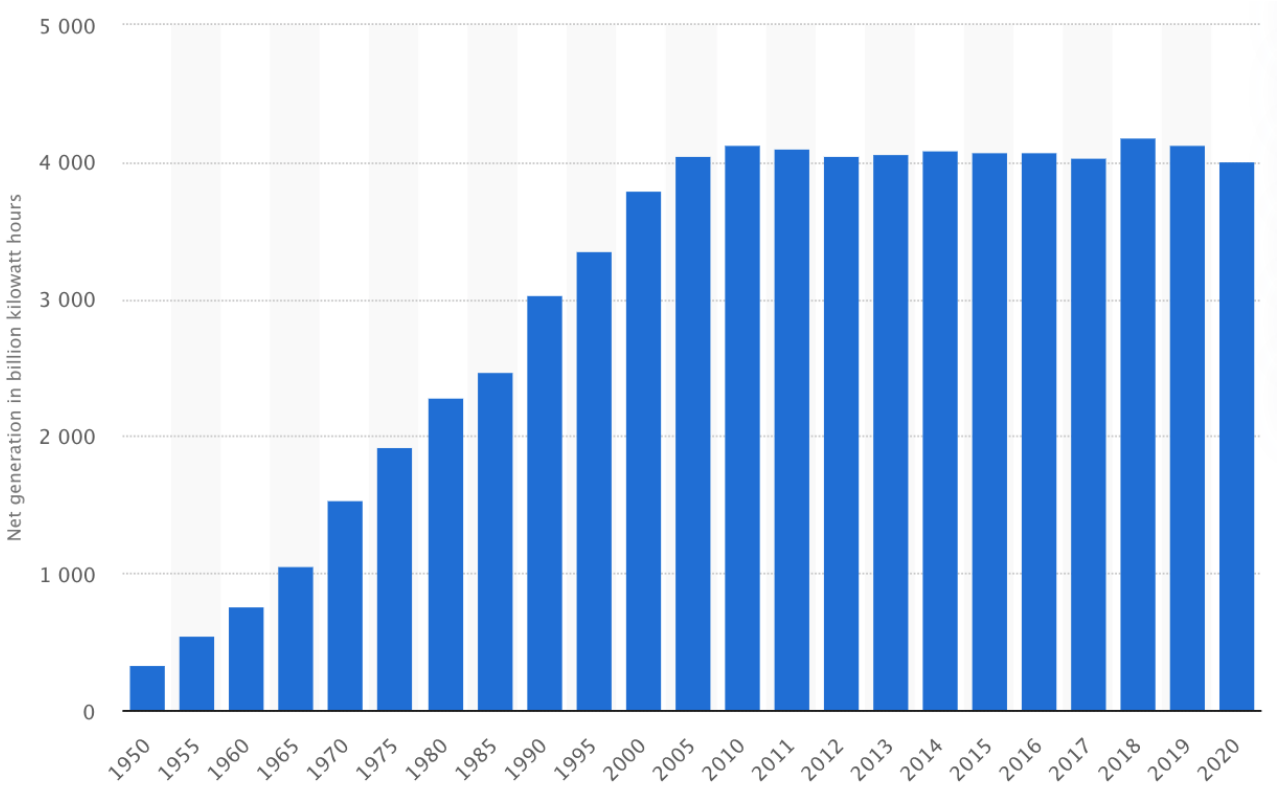


Figure 1.3: Net early electricity generation in the USA.

the USA (see Fig. 1.4 and Fig. 1.5) [8]. In the USA, solar and wind resources help to retire dirty coal generation. In Europe, both solid fossil fuels and natural gas resources are substituted by renewable energies. And currently, about 20% of electricity in Europe is produced by renewables. This is great progress towards clean and sustainable electricity generation. But, accounting for the appearing

EV trend, combined with expected economic growth - even more renewable power capacity will be introduced to the system, and power consumption and transmission loading will continue to grow. Uncertainty and stochastic behavior of the system will be even more significant.

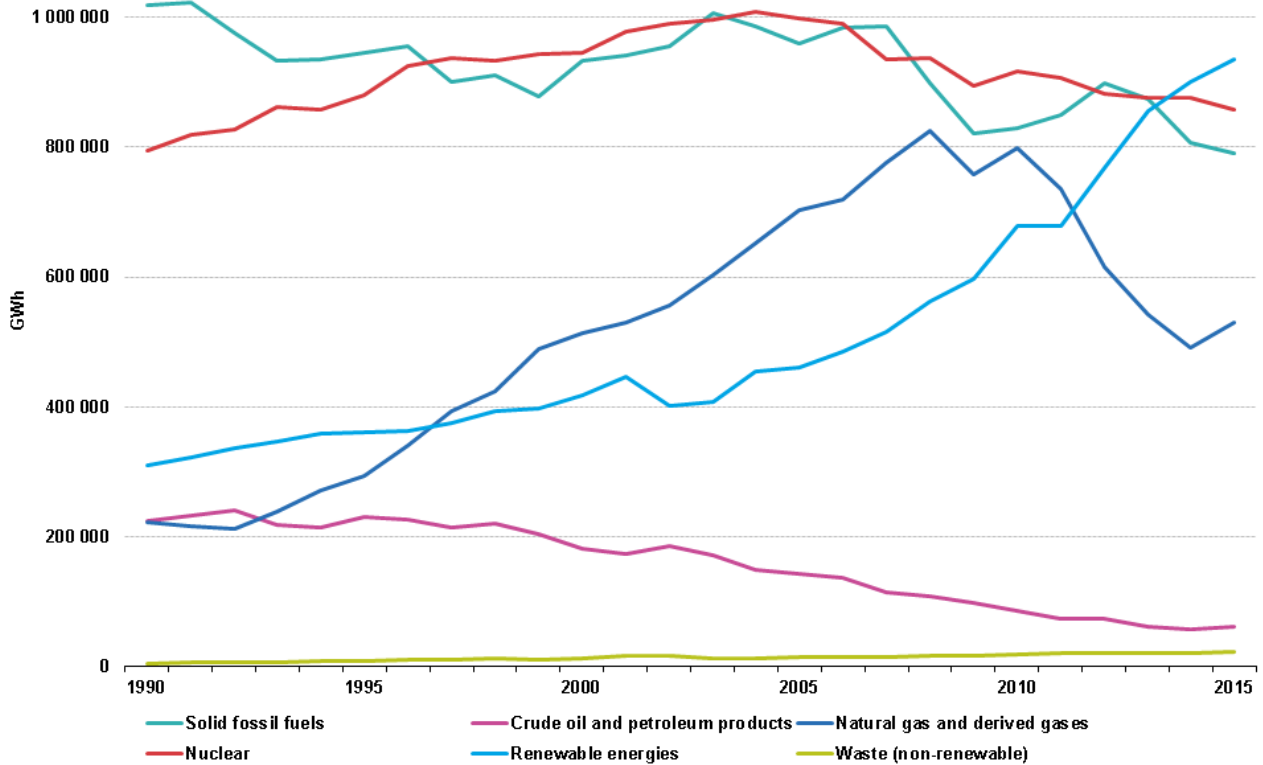


Figure 1.4: Europe electricity production by fuels.

There are two ways of dealing with this problems, and we believe both are required to maintain reliable power system operation in the future. The first is fully operational, and the second involves the installation of additional equipment to the power grid. In the first direction, the examples of the opportunities are transmission lines switching, demand-side response, renewables curtailment, and improved methods of operational control from the TSO side. Advances in optimization and control, improved forecasting methods, methods of handling uncertainty and risk at operational planning are among them. In the second direction, installation of Phase Shifting Transformers (PST), Energy Storage Systems (ESS), Flexible Alternating Current Transmission Systems (FACTS), High Voltage Direct Current (HVDC) lines are the possible opportunities that are already applied. However, installation of the new equipment to the grid or upgrade of the retired equipment requires advantages in the planning methodologies accounting for the recent operational planning models. The focus of the thesis is a combination of power system upgrade computed by an advanced optimization and state of the art operational planning models, incorporated to account for modern infrastructure behavior.

The aims of this thesis is:

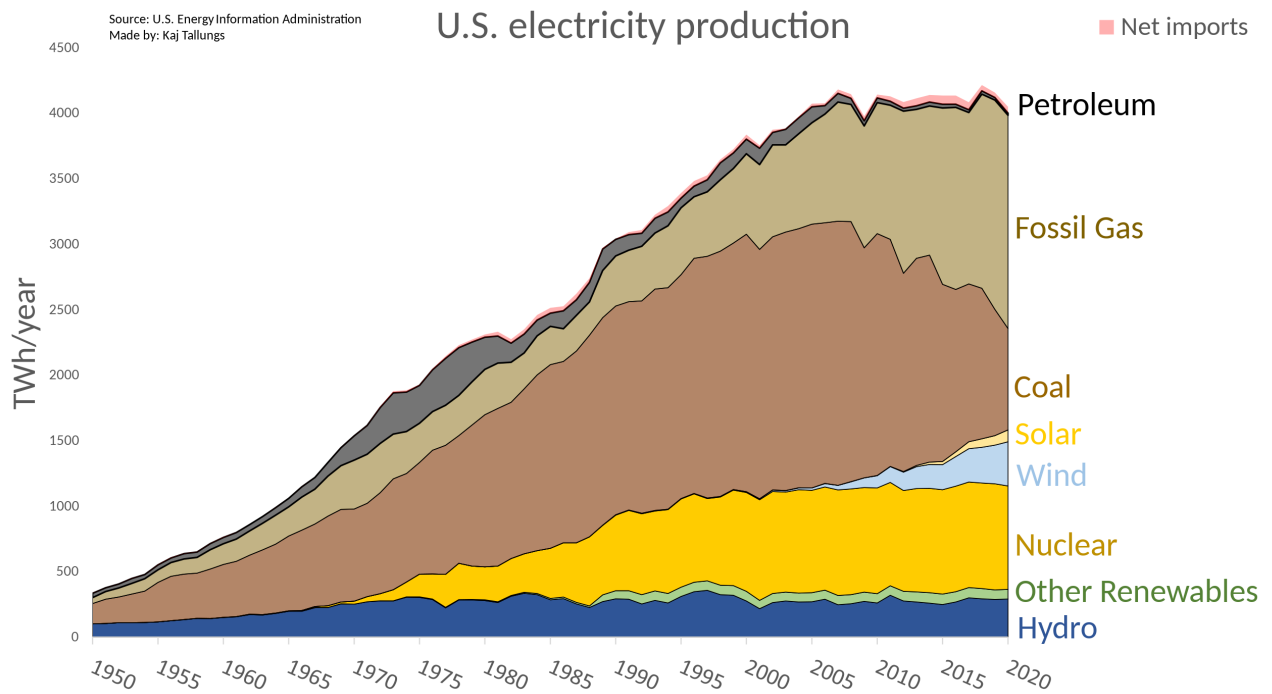


Figure 1.5: US electricity production by fuels.

- to contribute to the development of operational and uncertainty aware planning methodologies for the installation of the new equipment to the power system. That allows addressing current challenges regarding transmission capacity and operational risk/feasibility without expansion of the transmission system (practically too long, expensive, or even prohibited). The goal is to handle such planning based on the Optimal Power Flow (OPF) problem which is a main integral problem of operations and operational planning. And also account for the diverse set of future operational conditions, the uncertainty of the future forecasts, stochastic behavior of the system with renewables as well. The idea is that proper introduction of additional degrees of freedom used together with available control options will help to use existing transmission capacity more effectively. While the incorporation of advanced operational modeling into planning will allow making methodology more practically suitable for analysis and decision making.

- to contribute to the analysis of large-scale operational planning problems in general as they are an internal part of the planning problems. Develop probabilistic chance-constraint formulations for this type of problems. Further, this can be applied to power system planning as well.

1.2 Introduction to the project

The time frame considered in this thesis is power system mid-term to long-term planning, from a few months to a year and several years. Over a time horizon of several months, the system can be considered globally fixed in terms of available generation capacity and transmission lines. And by the

beginning of such time interval, an installation of the capacity of new equipment is possible, which is then used inside the time interval. The bigger time frames from a year to several years can be split into periods of several months, where the structure is virtually fixed, accounting for the existing plan of installation of generation capacity, transmission lines, maintenance scheduling, and installation of other equipment. The discretization of operational regimes inside each time interval corresponds to the generation dispatch time horizon. In that sense, each operational setting can be performed individually, i.e., we do not account for ramping activities between operational points inside the planning time frame.

We use exact AC-OPF model generalization to account for operations at the planning stage. The OPF is an optimization problem that minimizes the total cost of electricity while enforcing physical constraints such as limits on transmission capacity, voltage levels, power flow constraints, and generation capacity. OPF model generalization is used for planning methodology as it directly relates the developed methodology to practical system operation under market conditions. Equipment, which is discovered to be installed by the methodology, then again can be controlled by generalized OPF or special independent optimization (but accounting for other degrees of freedom should be explored).

There are two types of market conditions: central-dispatch (Russia, USA) and self-dispatch (Europe). The concise description is taken from [9].

”In central-dispatch markets, electricity markets are cleared by the TSO under consideration of the physical limits of the transmission grid. The market is typically cleared in several stages, including unit commitment to determine which generation units are online, day-ahead market clearing to obtain hourly generation schedules, and real-time markets to make adjustments in intra-day operation. Each stage typically involves solving some version of the OPF problem. The OPF problems used for market clearing purposes in the US are often based on the DC approximation of the power flow problem. The resulting optimization problem is linear and has well defined Lagrangian multipliers, which are used to determine electricity prices, the so-called Locational Marginal Prices (LMPs).” [9]

”In self-dispatch markets, electricity markets are cleared without consideration of the transmission grid, or with some limited information such as import/export constraints. This is the most common method for market clearing in Europe. In this set-up, the TSO has no direct influence on the outcome of the market clearing, but are provided with the planned generation schedules in the day-ahead. The TSO uses available control actions to make the market-based schedule comply with the physical grid limitations. Common control actions include transmission switching and set-point changes for PST or HVDC, generation redispatch or curtailment of renewable energy. The TSO is typically required to take the actions that have lowest cost and interfere the least with the market outcome. The TSO in a self-dispatch market hence also benefit from solving an OPF to determine the least cost, optimal changes to the system for the given a market outcome.” [9]

Overall, the OPF problem is suitable for operational planning for any power system, independent of the market type. And we use an exact AC-OPF version of that for planning purposes accounting

for both active and reactive power flows in the system. And also generalize for accounting for additional degrees of freedom and installation cost of the equipment searching for a good balance between installation and operations, which makes the developed methodology relevant for practical problems.

In this thesis, we first consider mid-term to long-term transmission system upgrade planning when new equipment is added to the system. The illustration is performed on the FACTS placement and sizing. A short description of the devices and impact provided by FACTS is provided in Section 8.3. FACTS are installed in Europe for various reasons, mostly for local support. It is worth mention that modification of the transmission capacity of power corridor by the installation will influence LMPs and price of FTRs. When installation is accounted by OPF procedure, LMPs are automatically considered. In this thesis we explore more theoretical global effect of FACTS placement. A review of the research on installation is provided in the current section below. Now, let us introduce the difference between traditional planning and possible planning problems, which can be considered.

Traditional planning of the development of the power system is local. If there is a lack of power generation at a bus, generation capacity can be increased, or a new line to the bus can be built. The transmission system is expanded if there is a lack of transmission capacity. Again the options are to build a new line or reinforce the existing one. The local and worst-case planning approach is quite simple computationally but cannot be effective if the power system operates in the constrained regimes close to the operational limits. Highly loaded operational conditions, together with increased variability in power flows due to increased level of uncertainty and fluctuations, require multiple local investments for the system upgrade and reinforcement. Therefore, local worst-case scenario planning is very expensive or can even be impossible. Furthermore, high renewables integration requires additional reactive power support, which again would be expensive if implemented in a dense large-scale manner. Additionally, Direct Current (DC) approximation is usually used for system development planning. However, a natural, exact AC operational model is required when the system operates close to feasibility limits (accounting for both active and reactive power flows). Also, AC model is the only option for reactive power support consideration. Traditional planning usually not accounting for existing operational degrees of freedom, which can provide additional flexibility for making decisions. Such improvement seems even more beneficial for mid-term placement and sizing problems (e.g., FACTS installation, storage placement, and sizing) when additional flexibility is introduced to the system. This option is motivated by the severely limited transmission expansion opportunity in Europe combined with increased uncertainty and congestion. Installation of FACTS does not require the construction of new power lines and can be performed much faster in comparison with transmission expansion. Serial Compensation (SC) and Static VAR Compensation (SVC) can be considered as simultaneous upgrade options. The main effect of an SC device consists in "rerouting" active power, while an SVC device injects or consumes reactive power locally. It is more reasonable to use such devices in transmission grids because they usually have loops, and power has more than one way to go to consumers. The effect is non-local, and when combined with generation redispatch, it may

lead to significant modification of the state. The second flexibility option is storage placement and sizing. Properly placed storage systems allow to mitigate power imbalance, help during consumption/generation peak conditions. Storage systems are a promising upgrade targeted by multiple EV companies (Tesla, Lucid), available both for transmission and distribution levels.

Another important problem that can be expensive or even not feasible in a modern environment for traditional planning approaches is generation capacity upgrade, a genuine issue due to the aging of installed generators. For example, in Russia average age of generators is about 35 years [10] and up to 20 billion USD are planned to be invested in generation upgrade by 2035. Also, old generation equipment can cause pollution and can be retired in a regulated manner. Even an upgrade for renewable power sources can be computationally analyzed in a large-scale manner. Old generators should be upgraded for the capacity availability (power demand is growing), which again should be planned (any generators cannot be built at any location and construction is long), e.g., coal generators in China, and planned to be gradually retired and upgraded. Improved planning value, in this case, would be feasibility/security analysis, less investment cost, faster money payback, and increased interest rate. This will lead to less tariff growth because usually, final customers pay for the upgrade through increased tariffs. Also, proper generation upgrades will provide OPEX reduction.

Motivation to explore FACTS option in this thesis is coined in the following points. First, they represent additional degrees of freedom for both nodes and edges of the transmission grid, and hopefully, a similar approach can be used for other installations. Second, they are relatively fast to build and have really broad applications. Third, there are many publications on FACTS (review is provided further), and to the best of our knowledge, there are no scalable results providing similar to those introduced in this thesis setting.

When the system becomes constrained, the transmission capacity needs to be expanded in order to provide committed services [11]. The congestion created by modern power system trends described above combined with the difficulty of building new generation and transmission locally is contributing to a growing interest [12, 13, 14, 15, 16, 17, 18, 19, 20, 21, 22, 23, 24, 25, 26, 27, 28] in utilizing a class of transmission-grid devices known commonly as Flexible Alternating Current Transmission System (FACTS) devices [29, 30, 31, 32, 33, 34]. Although FACTS devices provide new degrees of flexibility to relieve congestion without the emissions or right-of-way issues of new generation and transmission, they are quite expensive and must be deployed in a manner that maximizes benefit to the overall system.

To fully extract the benefit of FACTS devices, one ought to build in the operations and control of FACTS devices into algorithms for optimal placement and sizing that consider the entire network, not just a small section of the network. There are two significant challenges in this approach. The first is the combination of planning and operations. This type of integration is not entirely new, see, e.g., [15, 16, 20], but a system-level approach to the problem is deemed difficult. The second is the difficulty of the system-wide approach that suffers, in general, from the “curse of dimensionality”—

the effort to exactly compute results scales exponentially with the system size and the number of possible FACTS locations.

The problem of placement and sizing is normally considered separately from the problem of operations and control problems and vice versa. Planning problems seek to place FACTS devices and determine the required operational ranges. The planning problem is a strategic decision, which takes into account multiple system conditions extending over years. On the contrary, the control problem seeks the best response to current conditions or those expected within a relatively short period of time. However different the two types of problems may seem, they may be combined in a unified principled manner, similar to an approach developed in [35] for placement of storage. In [35], planning and operations were merged in an iterated two-step process. First, grid and storage combined operations were simulated over a range of generation and load conditions (with appropriate costs on storage charging/discharging), and statistics were kept on storage utilization on a node-by-node basis. In the second step, underutilized storage nodes were pruned, leaving only highly utilized nodes. Iteration of these steps algorithmically forces a sparse storage deployment—a generally desirable result for large-scale infrastructure. However, the computational burden of this approach is rather high. Explicitly incorporating sparsity into the optimization formulation itself, e.g., by using a fixed cost for placing even a small amount of storage, turns the problem into an even more difficult mixed-integer formulation with both discrete and continuous variables. However, recent results in compressed sensing [36, 37] suggest that using the ℓ_1 -norm instead of a fixed cost may allow sparsity to be enforced implicitly while keeping the optimization variables in the preferred and computationally efficient continuous domain.

A second challenge to the optimal placement and sizing of FACTS devices is the non-local nature of power flows over transmission networks and the need to consider system-wide impacts of FACTS placement. While it is impractical to implement direct approaches which scale exponentially with the system size for large transmission systems consisting of thousands of components, some new techniques adopted from statistical physics [38, 39, 40] and optimization [41, 42, 43, 44] suggest that even seemingly difficult optimization problems can be modified into formulations which are probably polynomial (or even linear). Such simplifications are not achievable in all cases, and one often must search for computationally efficient yet empirically accurate heuristics. Two heuristic methods – linearization of constraints combined with Sequential Linear Programming [45] and cutting plane methods [46, 47] demonstrate good potential for non-linear optimization.

A number of alternative formulations for optimal placement and sizing of FACTS devices have been proposed. In particular, [48, 49, 50] were focused on minimizing the operational cost. An investment cost is minimized in [51, 52]. Reduction of the transmission losses and increase of the power system loadability was analyzed in [53, 49] and [54, 55, 56]. Reduction of the load curtailment, and improvement of voltage profile and voltage stability index were discussed in [57, 52, 58, 56]. The resulting mathematical formulations were, typically, made in the existing literature in terms of a Mixed Integer Non-Linear Programming (MINLP). Then MINLP were resolved via the sensitivity analysis

[57, 59]; relaxation and/or decomposition to Mixed Integer linear Programming (MILP) [60]; and genetic algorithms [61, 62, 63, 64]. [65, 66, 67, 68] provide a review of FACTS placement using optimization techniques, stability index based methods for placement, genetic algorithm based approach and sensitivity based methods. The sensitivity-based methods are very efficient for resolving large-scale problems containing only a few indicators aimed at identifying the lines and/or buses that most significantly affect the placement of the FACTS devices. However, such methods cannot optimize device locations, required installed capacities of the devices, and the number of devices required. Genetic algorithms are advantageous for finding globally optimal solutions but suffer from extremely slow convergence. Relaxation techniques, utilized to convert MINLP to MILP [69], suffer from the lack of approximation control, whereas decomposition techniques, which consist of substitution of the original MINLP with a sequence of MILPs, lead to impractically large hierarchies. The main problem with the aforementioned approaches lies in their poor performance in terms of their computational scaling. Methods suggested in the past are handicapped by their ability to resolve problems limited to only a relatively small number of nodes (a few hundred). Resolution of thousands of nodes large models of practical significance with multiple scenarios were not even considered. Thus a typical approach to resolving the challenge of scaling consisted in relaying on approximation techniques to simplify the modeling of the line flows [52] or substituting AC power flow modeling by DC modeling [60]. Unfortunately, these methodologies suffer from the lack of approximation quality assurance, thus making them impractical for planning and installation problems of realistic size.

One stand-alone computational approach showing a significant practical promise for resolving realistic size optimization models formulated as MINLP – Benders decomposition [54] and related scenario-based decomposition. In [54] scalability is demonstrated for the single scenario cases, but for the multiple scenarios, it is limited to models with tens of buses. The allowed number of the installed devices should be limited as well in this paper. Finally, it also worth mentioning that placement of FACTS devices requires a significant installation cost even for devices with small installed capacities; therefore motivating approaches focused on a search for a sparse placement [69, 70, 71].

However, not only transmission expansion problems are hard. Even large-scale operational planning problems can be computationally demanding and considered in the second part of the thesis, e.g., resolution of AC-OPFs for multitude of operational conditions for thousands of bus grid. Such a single-stage non-linear planning problem can be approached by the resolution of separate optimizations when the initial problem can be decomposed. Parallel computing can be used for acceleration in that case. Nevertheless, many two-stage large-scale non-linear planning problems with diverse first stage will be intractable as decomposition is not available. However, the resolution of such two-stage problems is important as they structurally correspond to the stochastic planning approach when operational diversity is represented by a set of deterministic samples. This class of problems represents one way of approaching examples presented in the previous paragraph. Thus, model reduction techniques are required for such optimizations.

Motivated by the mentioned large-scale problems, we develop a conceptually new approach to power system planning. Assuming that computational constraints are resolved (and we resolve them), we aim to gain as much knowledge and information from the planning stage as possible. We believe that an improved, reformulated planning approach can resolve many operational problems in the future and make the transmission system more reliable and efficient at less cost than before. In contrast to traditional we propose a concept of operational and uncertainty aware planning characterized by the following features:

- Operational awareness: both investment/capacity and operational degrees of freedom are considered. The investment decision is made taking into account future power system operation with new equipment installed
- Uncertainty awareness: planning is performed accounting for uncertainty and variability of future operational conditions
- CAPEX + OPEX is optimized. The trade-off between installation and operations is optimized
- Exact AC modeling of operations is incorporated, which is required in the modern environment
- Multiple future time frames consideration, required for possible adjustability of plan and introduction of constraints depending on the time period
- Future representation: multiple deterministic scenarios/samples or probabilistic clouds representing operational conditions
- Scalability of the developed approaches and algorithms to practical sizes problems

For the second part corresponding to large-scale operational planning, we propose a Cloud-AC-OPF and Multi-Cluster-AC-OPF complexity reduction models for Multi-Scenario AC-OPF (MS-AC-OPF). Mathematically they are similar to well-studied Chance-Constrained AC-OPF (CC-AC-OPF) formulation but extended and conceptually different as approach mid-term to long-term operations. We again develop tractable analytical reformulations and solution algorithm for that.

1.3 Contributions

The contributions of the project are:

Operational and uncertainty aware planning framework for mid-term and long-term problems is developed using stochastic programming approach - operational diversity is represented by a set of deterministic samples.

- Multiple operational scenario planning model is developed for FACTS placement and sizing large-scale problem. It accounts for additional flexibility provided by the potentially installed capacity at planning stage together with available degrees of freedom, uncertainty of future conditions, and optimizes trade-off between CAPEX and OPEX.
- Exact AC-PF model is incorporated to the framework allowing to explore planning decisions at congested environment, to analyze reactive power support opportunities accounting for non-local state behavior.
- Scalable solution algorithm is developed for the proposed planning framework.
- The developed solution algorithm is validated at medium size grid model against non-linear solvers. Validation is also performed for the cases when planning becomes equivalent to standard AC-OPF against popular open-source Matpower solver.
- Multiple time frames model of the planning horizon is incorporated, allowing to analyze gradual capacity installation. The solution algorithm is adopted for the generalization.
- Scenario sampling methodology is introduced for future operations and uncertainty incorporation to practical planning examples.
- Applicability of the developed methodology is demonstrated on multi-scenario large-scale examples of 2736 bus Polish grid for FACTs placement and sizing problem. We provide analysis of the obtained solutions and decision improvements received in comparison with simplified planning models.
- Web-based visualization tools are developed for framework applications.

Planning with a probabilistic representation of operational conditions is considered as an alternative approach to scenario sampling.

- Multi-Scenario-AC-OPF (MS-AC-OPF) is considered separately as a sub-problem of mid-term to long-term planning. It is an important and challenging operational planning problem itself and requires complexity reduction in two-stage optimization applications as it is non-linear and usually cannot be decomposed to individual scenarios.
- Cloud-AC-OPF model reduction is developed for MS-AC-OPF as a generalization of Chance-Constrained-AC-OPF (CC-AC-OPF) methodology by incorporation of three various parameterizations of response to the realization of uncontrollable resources inside the set of scenarios.
- Analytical tractable formulation is developed for Cloud-AC-OPF model.
- Solution algorithm is developed for analytical reformulation of Cloud-AC-OPF and validated on a synthetic set of scenarios of IEEE 30-bus test case (manually sampled).

- Single cloud model is generalized to Multi-Cluster-AC-OPF model, which accounts for a practical diverse set of operational conditions (historical conditions, for example).
- Solution algorithm is adopted for Multi-Cluster-AC-OPF, and case study analysis is performed on 73 bus RTS-GMLC model with 105408 samples of conditions representing a year of operations at 5 min interval where exact AC-OPF is computed for each scenario as ground truth. Various ways to cluster scenarios are considered and analyzed.

1.4 Thesis layout

The thesis is divided into two main parts. The first part explains the operational and uncertainty aware planning methodology applied to the placement and sizing of FACTS devices problem. Uncertainty and variability here are modeled by stochastic programming using a set of deterministic scenarios representing operational conditions. The research, first started from modeling within DC-approximation [70, 71], increased the detalization of the setting to single scenario AC case, and then to the most general long-term planning case with exact AC power system operational model, multiple scenarios, and multiple time intervals. Additionally, scalability to practical size systems is demonstrated. The second part introduces another approach for operational and uncertainty aware planning when the state space is modeled by probabilistic clouds without deterministic samples consideration. This methodology is more complicated in terms of modeling but promises a better representation of uncertainty and variability of operational conditions and more suitable to large-scale practical problems when the operational state space of the system is broad and diverse.

Part I: Stochastic Programming Approach to Operational and Uncertainty Aware Planning Using a Set of Deterministic Operational Scenarios

Chapter 2 represents the first step towards operational and uncertainty aware planning of power systems. Here we develop a planning methodology and solution algorithms which then would be applied to large-scale problems and generalized to multi-time interval long-term case. Aiming to relieve transmission grid congestion, improve or extend the feasibility domain of the operations and reduce overall energy generation cost by supporting transport of renewable energy and energy from cheap generation facilities to the demand places, we build optimization heuristics, generalizing standard AC Optimal Power Flow (OPF) procedure, for placement and sizing of Flexible Alternating Current Transmission System (FACTS) devices of the Series Compensation (SC) and Static VAR Compensation (SVC) type. We model devices that generally represent a way to compensate lines or loads, respectively, and the compensation level can be adjusted according to the installed capacity. The main effect of an SC device consists in modifying line inductance while an SVC device injects or consumes reactive power. One use of these devices is in resolving the case when the AC-OPF solution is not feasible because of congestion. Another application of interest is related to developing a long-term investment strategy for placement and sizing of the SC and SVC devices to reduce operational cost

and improve power system operation where one also takes into account multiple scenarios, e.g., various load configurations, availability of generators, and line connections. We develop the optimization framework which accounts for the most general AC case and works with multiple scenarios. It allows us to find sparse and non-local solutions such that the number of installed devices is relatively small, and problems at a particular location of the system can be better resolved by installing compensation devices in other locations. We find one optimal placement and sizing of FACTS devices for multiple scenarios and optimal device settings for each scenario simultaneously. Our solution of the non-linear and non-convex generalized AC-OPF problem consists of building a convergent sequence of convex optimizations containing only linear constraints. The approach, which scales well for large/realistic systems, is illustrated on single and multi-scenario examples of the Matpower case-30 model.

Chapter 3 investigates installation of FACTS devices on the practical example of Polish system available in Matpower. Decentralized electricity markets and integration of renewables demand expansion of the existing transmission infrastructure to accommodate inflected variabilities in power flows. However, such expansion is severely limited in many countries because of political and environmental issues. Furthermore, high renewables integration requires additional reactive power support, which forces the transmission system operators to utilize the existing grid creatively, e.g., take advantage of new technologies, such as flexible alternating current transmission system (FACTS) devices. We formulate, analyze and solve the challenging investment planning problem of installation in an existing large-scale transmission grid multiple FACTS devices of two types (series capacitors and static VAR compensators). We account for details of AC character of the power flows, probabilistic modeling of multiple-load scenarios, FACTS devices flexibility in terms of their adjustments within the capacity constraints, and long-term practical trade-offs between capital vs operational expenditures (CAPEX vs OPEX). It is demonstrated that proper installation of the devices allows doing both - extend or improve feasibility domain for the system and also decrease long-term power generation cost (make cheaper generation available). Non-linear, non-convex, and multiple-scenario-aware optimization is resolved through an efficient heuristic algorithm consisting of a sequence of quadratic programmings solved by CPLEX combined with exact AC-PF resolution for each scenario for maintaining feasible operational states during iterations. The efficiency and scalability of the approach are illustrated on the IEEE 30-bus model and the 2736-bus Polish model from Matpower.

Chapter 4 extends the previously developed methodology to the multi-time interval case representing gradual installation of capacity into the power system. The multi-stage (-time-frame) optimization aims to achieve a gradual distribution of new resources in space and time. Constraints on the investment budget, or equivalently constraint on building capacity, are introduced at each time frame. Our approach adjusts operationally not only newly installed FACTS devices but also other already existing flexible degrees of freedom. This complex optimization problem is stated using the most general AC Power Flows. Non-linear, non-convex, multiple-scenario, and multi-time-frame optimization is resolved via efficient heuristics, consisting of a sequence of alternating Linear Programmings or

Quadratic Programmings (depending on the operational cost dependence on the power injected by the generators) and AC-PF solution steps designed to maintain operational feasibility for all scenarios. Computational scalability and other benefits of the newly developed approach are illustrated on the example of the 2736-nodes large Polish system. One most important advantage of the framework is that the optimal capacity of FACTS is build up gradually at each time frame in a limited number of locations, thus allowing to prepare the system better for possible congestion due to future economic and other uncertainties.

Part II: Planning with Probabilistic Representation of Operational Conditions

The second part investigates a different approach to operational and uncertainty aware planning of power systems. Inspired by the Chance-Constraint Optimal Power Flow operational planning accounting for the uncertainty of the renewables, we basically question is it possible to achieve more than using stochastic programming with a limited number of representable scenarios. Is it possible to account for the whole state space for practical size systems at installation planning. This challenging problem appeared to be quite complicated. What is accomplished so far in that direction is represented in the following chapters.

Chapter 5 discusses aggregation of multiple AC-OPF solutions of close in the operational state-space operational points. This is an important problem as many practical planning and operational applications in power systems require (including the extension to long-term planning problems) simultaneous consideration of a large number of operating conditions or Multi-Scenario AC-Optimal Power Flow (MS-AC-OPF) solution. However, when the number of exogenously prescribed conditions is large, solving the problem as a collection of single AC-OPFs may be time-consuming or simply intractable computationally. In this chapter, we suggest a model reduction approach, coined Cloud-AC-OPF, which replaces a collection of samples by their compact representation in terms of mean and standard deviation. Instead of determining an optimal generation dispatch for each sample individually, we parametrize the generation dispatch as an affine function of the corresponding setpoint dispatch (single for the cloud) and the response to change of the uncontrolled parameters. The Cloud-AC-OPF is mathematically similar to a generalized Chance-Constrained AC-OPF (CC-AC-OPF) of the type recently discussed in the literature but conceptually different as it discusses applications to long-term planning. We further propose a tractable formulation and implementation and illustrate our construction on the example of 30-bus IEEE model.

Chapter 6 explores the application of the developed reduction at the practical RTS-GMLC case with a multitude of operational points for the system provided. Many practical planning and operational applications in power systems require resolving in parallel collections of AC-OPFs each corresponding to a scenario considered over a stage within the planning horizon. In this setting, each scenario is described in terms of an exogenously prescribed consumption/production of all uncontrolled participants of power system operations. Normally, a number of such scenarios are prohibitively large to allow resolving all of them, even on the most powerful supercomputers. We propose a model

reduction approach, Multi-Cluster-AC-OPF, which performs clustering of a large and diverse set of multi-stage operational samples and then replaces a collection of samples assigned to each cluster by their compact representation in terms of its mean and standard deviation. The essence of our approach is in substituting parallel evaluation of many generation dispatch optimizations (each per sample, per time period) by a much smaller number (correspondent to the number of clusters) chance-constrained optimizations where samples are split into clouds, and each cloud is represented by an affine function of random parameters. The resulting Multi-Cluster-AC-OPF is validated on the RTS-GMLC 73 bus case, where time series of 105408 samples of operational conditions are provided, representing a year of operations sampled every 5 mins.

Chapter 7 summarizes the information provided in the thesis, comments on the most important results and contributions. Also, it provides directions and recommendations for future research.

Chapter 8 provides the details of the power system models and demonstrate analytical derivations used in the developed methodologies. It also provides additional information on FACTS applications.

1.5 List of publications

- Vladimir Frolov, Line Roald, Michael Chertkov, “Multi-Cluster-AC-OPF: Model Reduction for Multi-Stage, Multi-Scenario Optimal Power Flows”, (on the example of RTS-GMLC model), work in progress
- Vladimir Frolov, Line Roald, Michael Chertkov, “Cloud-AC-OPF: Model Reduction Technique for Multi-Scenario Optimal Power Flow via Chance-Constrained Optimization”, The 13th IEEE PowerTech 2019
link: <https://arxiv.org/pdf/1905.10455.pdf>
- Vladimir Frolov, Priyanko Guha Thakurta, Scott Backhaus, Janusz Bialek, Michael Chertkov, “Operations- and Uncertainty-Aware Installation of FACTS Devices in a Large Transmission System”, IEEE Transactions on Control of Network Systems, Special Issue on Analysis, Control and Optimization of Energy System Networks, DOI: 10.1109/TCNS.2019.2899104, Volume: 6, Issue: 3, Sept. 2019
link: <https://arxiv.org/pdf/1608.04467.pdf>
- Vladimir Frolov, Michael Chertkov, “Methodology for Multi-stage, Operations- and Uncertainty-Aware Placement and Sizing of FACTS Devices in a Large Power Transmission System”, 10th Bulk Power Systems Dynamics and Control Symposium – IREP’2017, conference presentation and proceedings paper,
link: <http://irep2017.inesctec.pt/conference-papers/conference-papers/paper58p3r2zgjn.pdf>

- Vladimir Frolov, Scott Backhaus, Misha Chertkov, “Efficient algorithm for locating and sizing series compensation devices in large power transmission grids: II. Solutions and applications” 2014 New J. Phys. 16 105016,
doi:10.1088/1367-2630/16/10/105016
- Vladimir Frolov, Scott Backhaus, Misha Chertkov, “Efficient algorithm for locating and sizing series compensation devices in large power transmission grids: I. Model implementation” 2014 New J. Phys. 16 105015,
doi:10.1088/1367-2630/16/10/105015

Part I

Stochastic Programming Approach to Operational and Uncertainty Aware Planning Using a Set of Deterministic Operational Scenarios

The first part of the project is about the deterministic approach of modeling power system operational conditions. In this case, multiple scenarios (representing operational conditions) are required for the incorporation of variability and uncertainty of the power system behavior. First, the idea of non-local investments which improve the system by installation in the proper place is introduced in the example of Series Compensators (SCs) when DC approximation is used for simplified regimes modeling. Then full AC model with multiple scenarios is developed. Then, it is applied to large-scale investment planning problems. Finally, the methodology for solving multiple time intervals accounting for multiple scenarios is introduced and again applied to large-scale investment planning.

Chapter 2

Placement and Sizing of Series Compensation (SC) and Static Var Compensation (SVC) Devices in Transmission Grids: The Case of AC Power Flows

This chapter introduces the setting and problem statement for the installation of two types of FACTS devices using AC system modeling. It also illustrates the developed solution algorithm and functionality of the developed solvers for single scenarios and multiple scenarios. Finally, the long-term planning approach is clarified. This chapter demonstrates an approach to operational and uncertainty aware planning of power system, which is then applied in the following chapters of the 1st part of the Thesis. The methodology was first proposed in [72], and we generalize, extend and improve it in further research.

In this chapter, we generalize the previously developed optimization framework of FACTS placement [70] [71], sizing, and operational optimality to the general AC case. The approach is also adopted for handling multiple configurations of loads and generations within single optimization. Our approach consists in posing an optimization problem that extends the standard AC OPF by introducing new degrees of freedom accounting for the flexibility in line inductances and reactive power corrections provided by SC and SVC devices. In addition to discovering optimal investment strategy in FACTS devices, our optimization problem also outputs optimal settings for these devices, which are specific for every configuration/scenario (of injection consumption) included in the formulation.

The problem is stated as a network optimization problem, which is generally non-convex and nonlinear. To overcome the difficulties, we build efficient optimization heuristics which construct a convergent and carefully controlled sequence of convex optimizations with linear constraints. These convex optimizations are solved efficiently with the state-of-the-art Mosek solver [73]. Importantly, our approach is scalable, i.e., it allows the extension to a large system with polynomial growth of com-

plexity with an increase in the system size, but scalability issues are not resolved in this chapter. This aspect of our approach and developed methodology is extremely important for practical applications, which is discussed in the following chapters.

2.1 Optimization model

We begin by describing the network setting and introducing notations. As it was discussed previously, a power network is modeled as a graph defined by the set of nodes which are either loads or generators, and a set of edges which are transmission lines with some inductance x , resistance r , and charging capacitance b .

- The layout of the power transmission network, $\mathcal{G} = (\mathcal{V}, \mathcal{E})$, where \mathcal{V} and \mathcal{E} represent the set of nodes and edges of the network/graph, with line characteristics such as inductances, resistances and shunt capacitances are known.
- List of projected scenarios, i.e. different load configurations, $a = 1, \dots, N$. The scenarios may include sampled (typical) configurations and/or contingency (rare) configurations projected for different level of loading.
- Each scenario is characterized by:
 - Occurrence probability
 - State of the network – energized network is the subgraph of the complete network
 - State of generators – list of generators on-line
 - Configuration of loads

List of fixed parameters characterizing scenario a is as follows:

- $T^{(a)}$ - temporal rate (frequency) of scenario occurrence
- $\mathcal{G}^{(a)} = (\mathcal{V}^{(a)}, \mathcal{E}^{(a)}) \subseteq \mathcal{G}$ - energized subgraph of the full network, \mathcal{G}
- $x_0^{(a)} = (x_{ij}^{(a)} | \{i, j\} \in \mathcal{V}^{(a)})$ - vector of initial inductances of energized lines
- $r^{(a)} = (r_{ij}^{(a)} | \{i, j\} \in \mathcal{E}^{(a)})$ - vector of resistances of lines
- $b^{(a)} = (b_{ij}^{(a)} | \{i, j\} \in \mathcal{E}^{(a)})$ - vector of shunt capacitances of lines
- $P_{\min(\max)-gen}^{(a)} = (P_{i;\min(\max)-gen}^{(a)} | i \in \mathcal{V}_g^{(a)} \subset \mathcal{V}^{(a)})$ - vectors of minimum (maximum) active power outputs of energized generators

- $Q_{\min(\max)-gen}^{(a)} = (Q_{i;\min(\max)-gen}^{(a)} | i \in \mathcal{V}_g^{(a)})$ - vectors of minimum (maximum) reactive power outputs of energized generators
- $P_{load}^{(a)} = (P_{i;load}^{(a)} | i \in \mathcal{V}_l^{(a)} \subset \mathcal{V}^{(a)})$ - vector of active power consumptions at loads
- $V_{\min(\max)}^{(a)} = (V_{i;\min(\max)}^{(a)} | i \in \mathcal{V}^{(a)})$ - vectors of minimum (maximum) allowed voltages
- $S_{\max}^{(a)} = (S_{ij,\max}^a | \{i, j\} \in \mathcal{E}^{(a)} \subset \mathcal{E})$ - vector of the apparent power limits of energized lines

The following are scenario-indexed degrees of freedom which are optimized over:

- $x^{(a)} = (x_{ij}^{(a)} | \{i, j\} \in \mathcal{V}^{(a)})$ - vector of line inductances (modified by SC devices)
- $Q^{(a)} = (Q_i^{(a)} | i \in \mathcal{V}^{(a)})$ - vector of reactive power injection/consumption at loads and generators (modified by SVC devices)
- $P_g^{(a)} = (P_{i;g}^{(a)} | i \in \mathcal{V}_g^{(a)})$ - vector of active power injections at the generators (operational cost for each scenario is cost of active power generation)
- $V^{(a)} = (V_i^{(a)} | i \in \mathcal{V}^{(a)})$ - vector of operational voltages
- $\theta^{(a)} = (\theta_i^{(a)} | i \in \mathcal{V}^{(a)})$ - vector of operational phases

Cost of the device placement and related service period:

- C_{SC} - SC capacity placement cost (per 1 Ohm)
- C_{SVC} - SVC capacity placement cost (per 1 MVar)
- N_y - service period of the system

Finally, global (i.e. scenario independent) optimization degrees of freedom are:

- $\overline{\Delta x} = (\overline{\Delta x}_{ij} | \{i, j\} \in \mathcal{E})$ - vector of SC device capacities (positive values, allowed up and down regulated intervals are assumed equal)
- $\overline{\Delta Q} = (\overline{\Delta Q}_i | i \in \mathcal{V}_l)$ - vector of SVC device capacities (positive values, regulated up and down intervals are assumed equal)

To account for the operational flexibility of the devices, we use as optimization variables scenario independent capacities and independently actual correction values for the devices contained within the capacity limits. We utilize the standard π -model for lines, however, without tap changers and phase shifters for simplicity (they can be easily added to the model). Branch modeling is described in Section 8.1.

2.2 Problem statement

The problem is to place and size FACTS devices of SC and SVC types taking into account multiple scenarios and define actual settings of the devices in a way that the combination of the cost of the upgrade and the cost of operations (load configurations), will be minimized:

$$\min_{\overline{\Delta x}, \overline{\Delta Q}; \text{state}^{(a)}, \forall a} \text{COST}(\overline{\Delta x}, \overline{\Delta Q}; \text{state}^{(a)}) \quad (2.2.1)$$

$$\begin{aligned} \text{COST} \doteq & (C_{SC} \sum_{\{i,j\} \in \mathcal{E}} \overline{\Delta x}_{ij} + C_{SVC} \sum_{i \in \mathcal{V}_l} \overline{\Delta Q}_i \\ & + N_y \sum_{a=1..N} T_a * C_a(P^{(a)})) \end{aligned} \quad (2.2.2)$$

$$\text{state}^{(a)} \doteq (x^{(a)}, v^{(a)}, \theta^{(a)}, Q^{(a)}, P^{(a)}), \forall a$$

$$x^{(a)} = x_0^{(a)} + \Delta x^{(a)} \quad \forall a$$

$$Q_{load}^{(a)} = Q_{load-0}^{(a)} + \Delta Q_{load}^{(a)}, \forall a$$

$$-\overline{\Delta x} \leq \Delta x^{(a)} \leq \overline{\Delta x}, \forall a$$

$$-\overline{\Delta Q} \leq \Delta Q_{load}^{(a)} \leq \overline{\Delta Q}, \forall a$$

$$V_{\min}^{(a)} \leq V^{(a)} \leq V_{\max}^{(a)}, \forall a$$

$$Q_{\min-gen}^{(a)} \leq Q_{gen}^{(a)} \leq Q_{\max-gen}^{(a)}, \forall a$$

$$P_{\min-gen}^{(a)} \leq P_{gen}^{(a)} \leq P_{\max-gen}^{(a)}, \forall a$$

$$\sqrt{(P_{ij}^{(a)})^2 + (Q_{ij}^{(a)})^2} \leq S_{\max}^{(a)} \quad \forall a; \forall \{i, j\} \in \mathcal{E}^{(a)}$$

$$P_i^{(a)} + iQ_i^{(a)} = \sum_{j: \{i,j\} \in \mathcal{E}^{(a)}} (S_{ij}^{(a)}), \forall i \in \mathcal{V}^{(a)}, \forall a$$

where all the inequalities containing vectors are considered component-wise; $C_a(P^{(a)})$ stands for the function representing the cost of generation for scenario a , and $\forall a$ is a shortcut for, $\forall a = 1, \dots, N$. The objective function (2.2.2) represents capital investment cost of the installation of two types of FACTS devices (taking linear in the installation capacities and thus promoting sparseness, see [70, 71] for related discussion) plus operational cost summed over all the scenarios with their probabilities taken into account and multiplied by the number of years (service period). The optimization constraints above have the following meaning:

- state for each scenario is defined by vectors of line inductances, voltages, phases, active and reactive power injections at nodes
- actual line inductance is equal to its initial value plus SC correction adjusted to a scenario, however maintained within the installed capacity bounds
- actual reactive power demand for a load is equal to its initial value plus SVC adjusted to a

scenario, however, maintained within the installed capacity bounds

- limits for reactive power generation
- limits for active power generation
- line thermal limits
- active and reactive power balance at nodes

Thermal and power balance constraints are non-linear and non-convex. In order to resolve this complication, we develop the iterative heuristic approach to solve Eq. (2.2.1) described in the next section.

It can be seen that the formulated problem is a generalization of the AC-OPF. If we choose just one scenario for optimization and predefine capacities of the devices to be zero, we will get standard AC-OPF formulation.

2.3 Optimization algorithm

The idea of the algorithm is to proceed sequentially. At each step within the sequence, we linearize the constraints around a current state (found at the preceding step) of each operational scenario and then use a standard convex optimization solver to evaluate the resulting quadratic programming (QP) optimization (for the generation cost modeled as a quadratic function) with linear constraints. We also control each step so that the resulting correction to the current state is sufficiently small to justify the linearization. The algorithm is terminated when preset target precision/accuracy is reached. The flowchart of the algorithm is shown in Fig. 2.1. The schematic representation of the algorithm behavior is illustrated in the Fig. 2.2 for a step by step explanation of the solution for 3-node system.

First, initialization part goes. Given scenarios of operational conditions are provided to the solver. Generation dispatch is initialized for each as standard OPF with line capacity limits removed.

Then, iterative loop consisting of four steps goes:

1. Linearization of the thermal and power balance constraints of Eq. (2.2.1) around current operational point for each scenario is applied (see Appendix for the details).
2. QP with linear constraints is constructed in the form similar to Eq. (2.2.1).
3. QP is evaluated. A feasible solution of the QP optimization problem is found (if available). The solution outputs components of an optimization vector in Eq. (2.2.1) including installed capacities and operational settings for all considered scenarios simultaneously.
4. we run AC Power Flow (AC-PF) solver (in our first experiments, we use Mathpower solver, later custom solver) to update operational points - make a back projection on exact AC power balance constraints and compute updated feasible operational points.

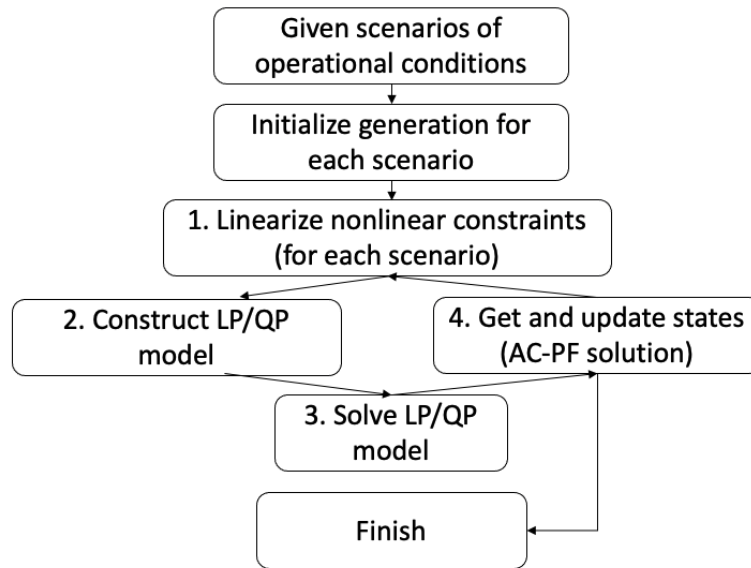


Figure 2.1: Flowchart of an iterative algorithm.

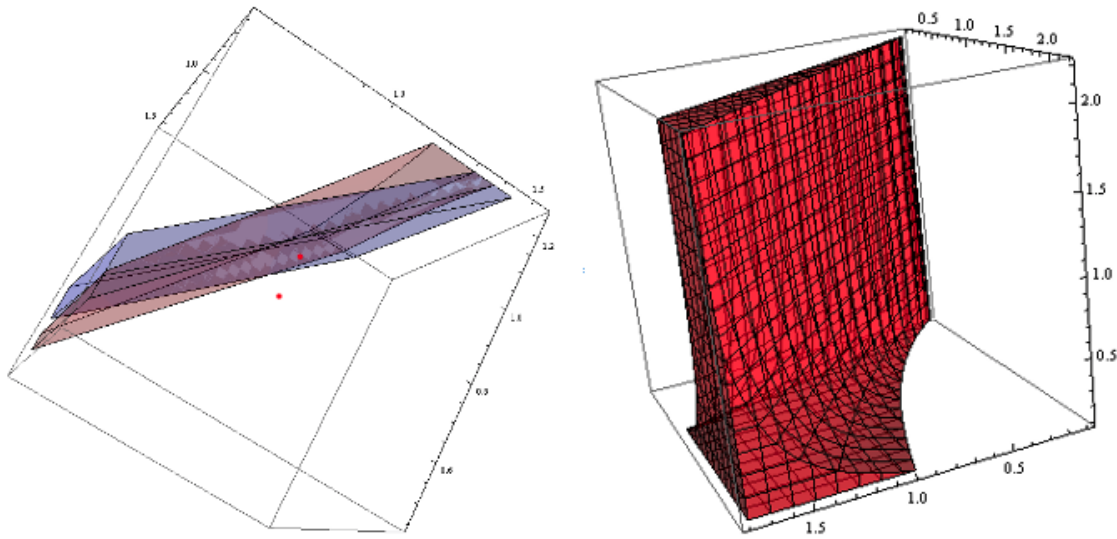


Figure 2.2: Schematic representation of an iterative loop for 3-node system (single operational scenario is considered).

Fig. 2.2 illustrates a step by step performance of algorithm on the simplest 3-node power system example. Red non-convex region on the right is a representation of the feasible space of the problem Eq. (2.2.1) for a 3-node system. If some constraints are not feasible at initialization step, then red operational point (on the left) lies outside of the enlarged exact feasible domain (red on the left). On the step 1. linearized domain is constructed (blue domain on the left). Steps 2-3 move the red operational point from outside of the red domain to the surface of blue domain. It is not necessary inside the red domain and not necessary even feasible AC-PF operational point. Step 4 allows to

update the state - basically it correspond to an updated feasibility domain of the problem (red on the right) and updated operational point (red on the left).

Note that at step 2 we artificially restrict change of reactive power injections on generators. The the restriction is caused by the empirical observation that for a system with multiple alternative loops for power flows and reactive power assumed injected/consumed at no cost; there may be multiple solutions with close costs and similar active power generation, however showing rather distinct profiles of reactive power injection/consumption.

In this scheme linearization of the constraints is detailed in Appendix. We consider apparent power squared flowing through the line $\{i, j\}$ under the scenario, a , $(P_{ij}^{(a)})^2 + (Q_{ij}^{(a)})^2$, as well as real and reactive powers injected/consumed at a node, i , under scenario, a , $P_i^{(a)}$ and $Q_i^{(a)}$, as functions of the state variables (x, v, θ) , and then linearize around the current state by computing partial derivatives over state variables explicitly as it is shown in Appendix.

We have developed two separate solvers, each supplied with its own visualization tool. Our first solver works with a single scenario. We use the solver to validate the approach and the algorithm. Then we applied the experience gained constructing the single scenario solver to build the multiple scenarios solver. In constructing the solvers, we have resolved multiple technical problems. See Appendix for details. The next section validates the solvers and then we give examples of simple problems resolutions.

2.4 Solver validation

We first develop a single scenario solver and then extend it to multiple scenarios. In order to check if the solver works correctly, we compare it against the solver included in Matpower AC-OPF package. As previously mentioned, we have built a generalized OPF type optimization problem, and if we choose the installed capacities of the devices to be zeros, we should obtain just the same OPF solution as provided by other/existing solvers/software (if it is feasible).

2.4.1 Comparison of the solutions for 9-bus system

Here we take a single configuration of 9-bus model and artificially overload one line by reducing its thermal limit. Then we run OPF to find a feasible solution which is illustrated in Fig. 2.3. Initial overload of the line means that on the 3* step of our algorithm, the resulting power flow through the line is higher than the thermal limit.

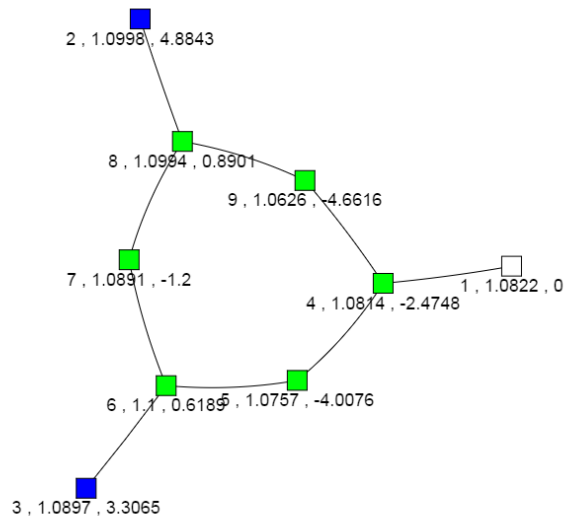


Figure 2.3: OPF solution of 9-bus system. Generators are blue, slack bus is white and loads are marked in green. Numbers next to each bus are id, voltage and phase for the given bus.

In Fig. 2.4 the solution which is obtained by the solver is shown in the same way but with voltage levels coded in colors from white to yellow. It can be seen that nodes have similar voltages to the OPF solution resulting in no observed overloads.

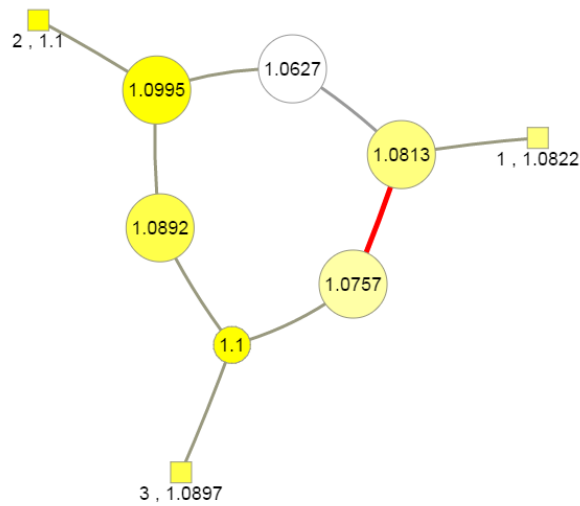


Figure 2.4: Solver solution for the same 9-bus system and the same scenario. Initially overloaded line marked in red.

Then in the Figs. 2.5- 2.6 we show how the solution progresses with iterations. In this simple case with a small initial overload about 5 iterations are needed to actually converge to a solution.

Overloaded Lines Number vs Iterations:

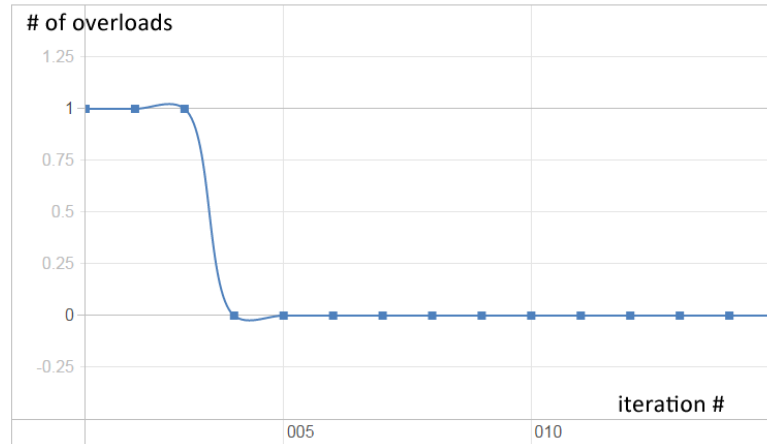


Figure 2.5: Dependence of number of overloaded lines on iteration number.

Overload Value vs Iterations:

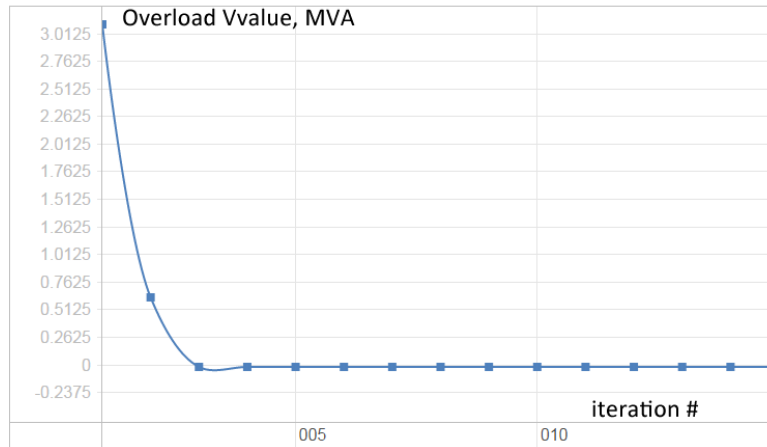


Figure 2.6: Dependence of the total overload value for all overloaded lines on iteration number.

The following Figs. 2.7- 2.8 compares initial active and reactive generation dispatch with the final one and with the solution given by the OPF procedure. It can be seen that the solver works fine and gives the same solution as the Matpower solver [74].

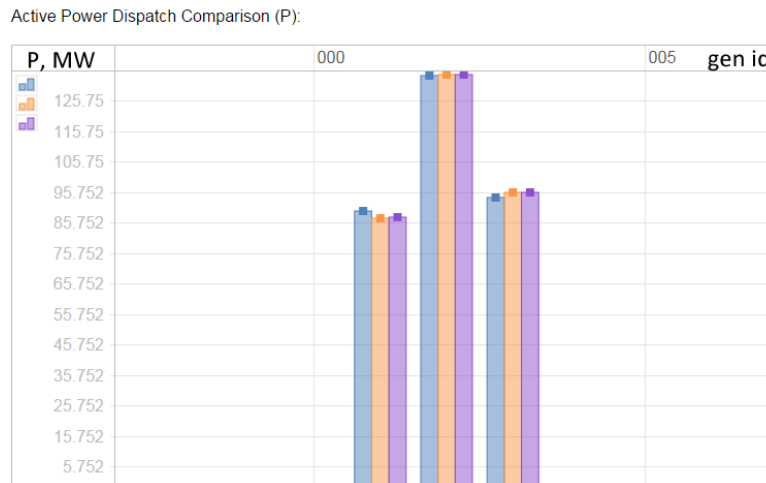


Figure 2.7: Active power generation dispatch comparison. Blue bars - initial dispatch on the 1st iteration of algorithm, orange bars - final solution, purple - OPF dispatch.

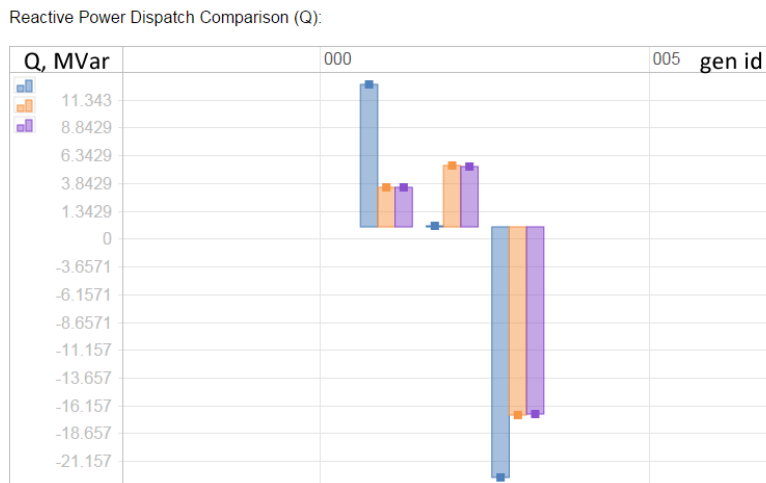


Figure 2.8: Reactive power generation dispatch comparison. Blue bars - initial dispatch on the 1st iteration of algorithm, orange bars - final solution, purple - OPF dispatch.

2.4.2 Comparison of the solutions for 30-bus system

Then we perform the same experiment for a more complicated 30-bus power system which is shown in Fig. 2.11. And surprisingly, the solver does not converge (the number of line overloads is in Fig. 2.9).

Having tried various possibilities and optimization tricks, we have finally discovered that the problem is caused by the reactive power dispatch for generators that have grid connections with loops.

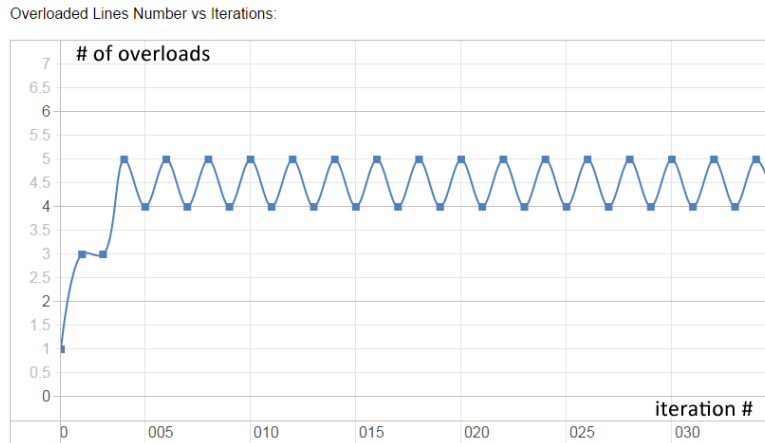


Figure 2.9: Dependence of number of overloaded lines on iterations. There is no convergence.

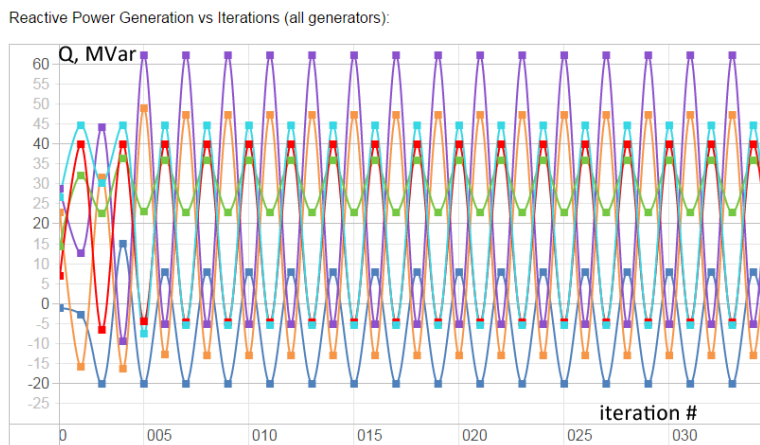


Figure 2.10: Dependence of reactive power output for each generator on iteration number.

There is no cost for reactive power, and the solution space is degenerated. For each active generation dispatch, there are many appropriate configurations of reactive power dispatch, and the solver "cannot choose" between them. It can be seen in Fig. 2.10 which illustrates the progress of reactive power outputs for each active generator with iterations. The total value of reactive power injected into the system remains approximately the same, but the dispatch always changes from one to another.

One possible solution for this problem is to limit the maximum change of reactive power output for the generator during the iteration. We also decrease this limit with iterations to obtain convergence of the solution and manage to get the same regime, shown in Fig. 2.11, as OPF procedure does.

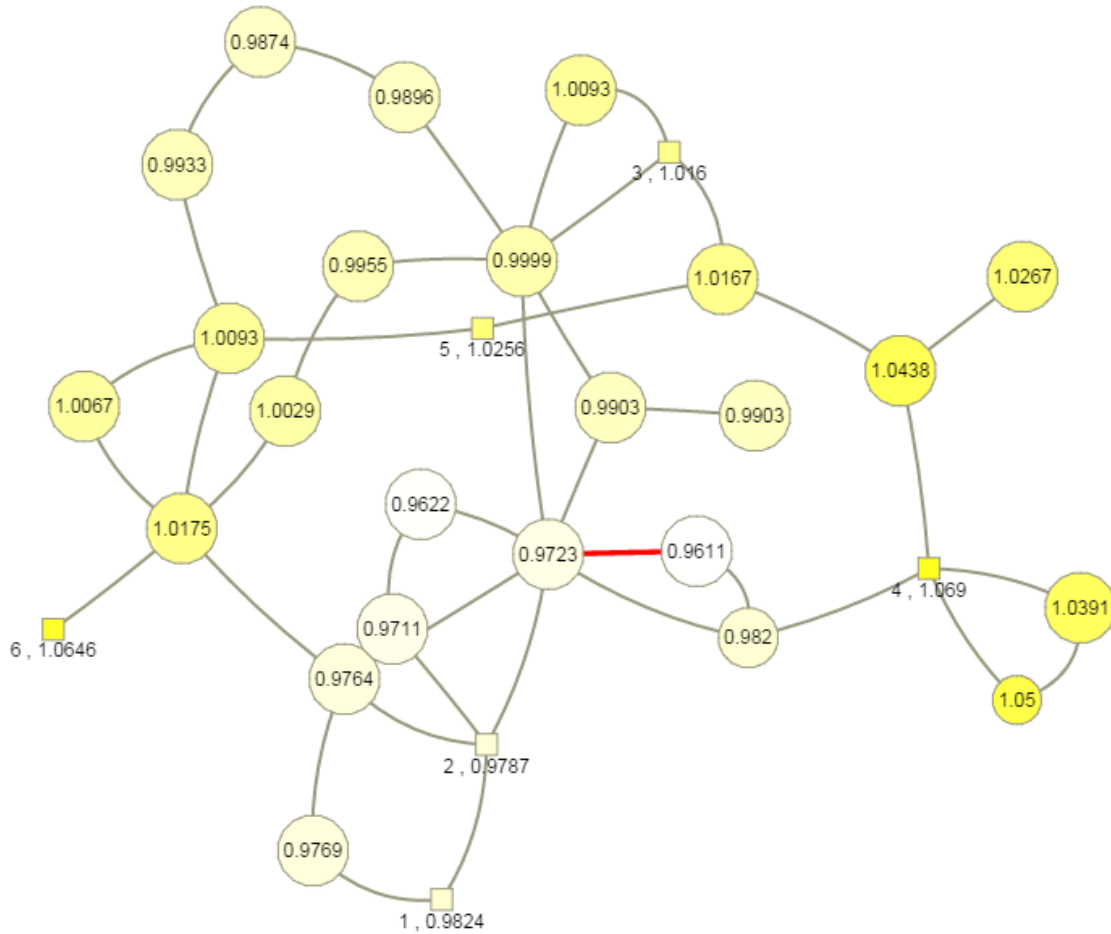


Figure 2.11: Solver solution for the 30-bus system and the same scenario. Initially overloaded line marked in red. Generators represented by squares and loads by circles, the color of the node represents voltage level (white - low, yellow - high). Generators are numbered in the same way as in the Figs. 2.12- 2.13.

Comparison of initial, final and OPF generation dispatch is given in the Figs. 2.12 - 2.13.

Active Power Dispatch Comparison (P):

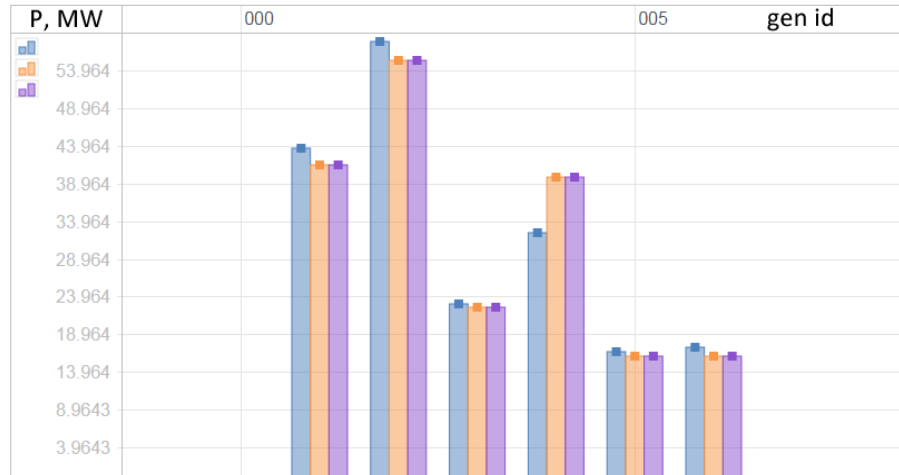


Figure 2.12: Active power generation dispatch comparison. Blue bars - initial dispatch on the 1st iteration of algorithm, orange bars - final solution, purple - OPF dispatch.

Reactive Power Dispatch Comparison (Q):

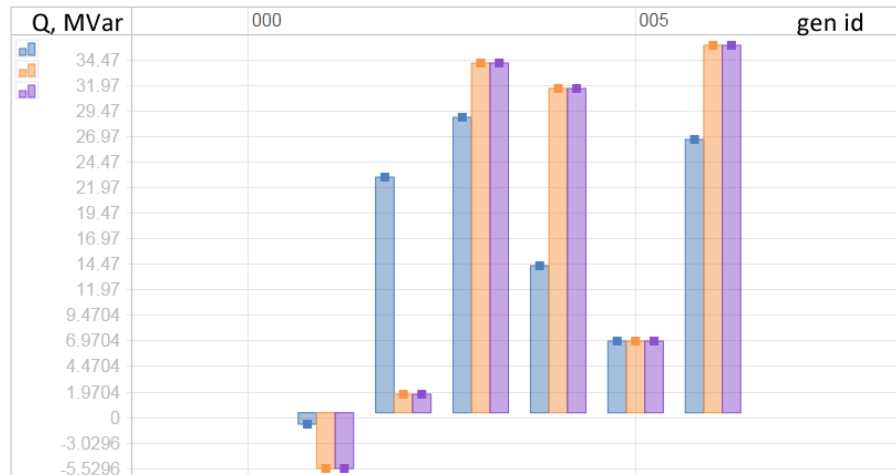


Figure 2.13: Reactive power generation dispatch comparison. Blue bars - initial dispatch on the 1st iteration of algorithm, orange bars - final solution, purple - OPF dispatch.

We conclude that our algorithm discovers right solutions for known asymptotic.

2.5 Single scenario optimization

Once the single scenario solver which shows reasonable solutions for the test cases is constructed, we use it to explore optimization of feasible and infeasible single scenarios for 30-bus model considered previously.

2.5.1 OPF feasible operation

For the first simulation, the service period is taken to be 1 hour. Figs. 2.14- 2.15 illustrates how the cost of installed SC and SVC devices depends on iteration number in this case.

SCs Cost vs Iterations (Capital Investment Cost, \$):

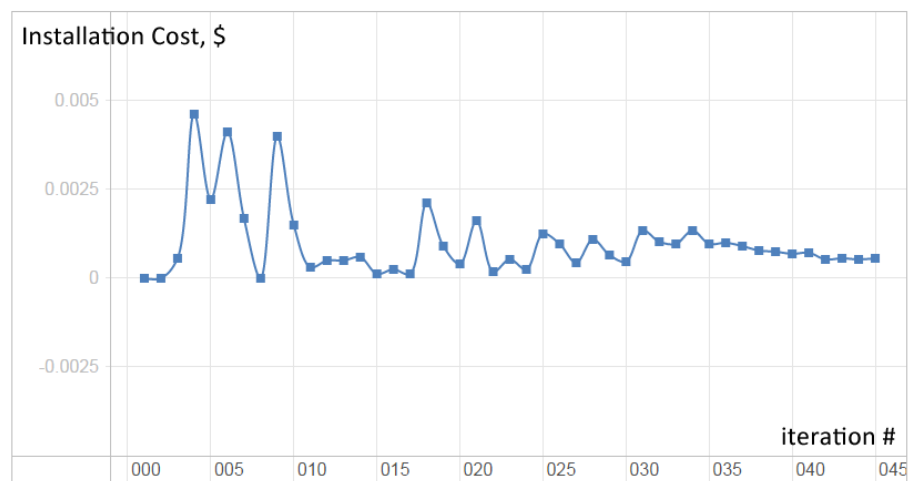


Figure 2.14: Dependence of SCs capital cost on iteration number.

SVCs Cost vs Iterations (Capital Investment Cost, \$):

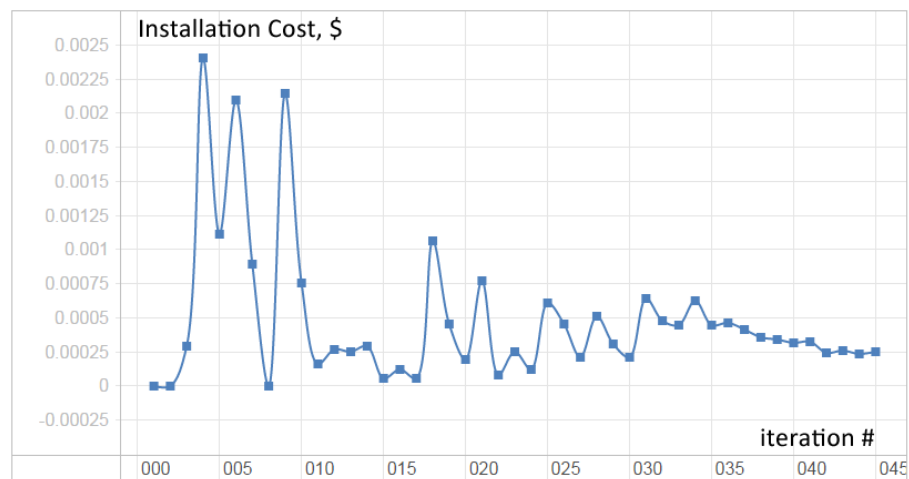


Figure 2.15: Dependence of SVCs capital cost on iteration number.

We conclude that it is not reasonable to invest money into the system for 1 hour service period, the capital investment cost is approximately zero, OPF solution is feasible in this case, and the optimal decision is to operate in OPF dispatch regime. Solver returns OPF dispatch solution in this simulation as it is shown in Fig. 2.16.

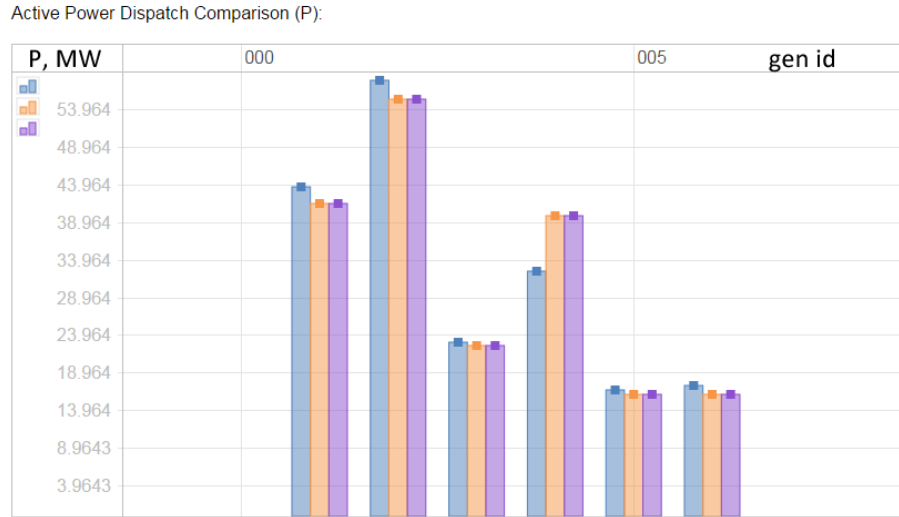


Figure 2.16: Active power generation dispatch comparison for OPF feasible scenario and 1 hour service period. Blue bars - initial dispatch on the 1st iteration of algorithm, orange bars - final solution, purple - OPF dispatch.

For the second simulation, the service period is chosen to be 15 years. One observes in Fig. 2.17 that it is optimal to place one SVC device in the system and generate reactive power locally instead of transporting it from generators. This solution helps to relieve line overload, which occurs in OPF without thermal limits regime and reduces operational cost for the system, and saves money.

The operational cost data is the following:

- OPF Cost: 576.893 \$/hour (75803800 \$ total for 15 years)
- Solver Cost: 574.549 \$/hour (75632500 \$ total cost for 15 years which is capital investment plus operational)

In this non-overloaded case, the developed approach allows finding a placement that saves about 0,3% of operational cost for this system for given conditions.

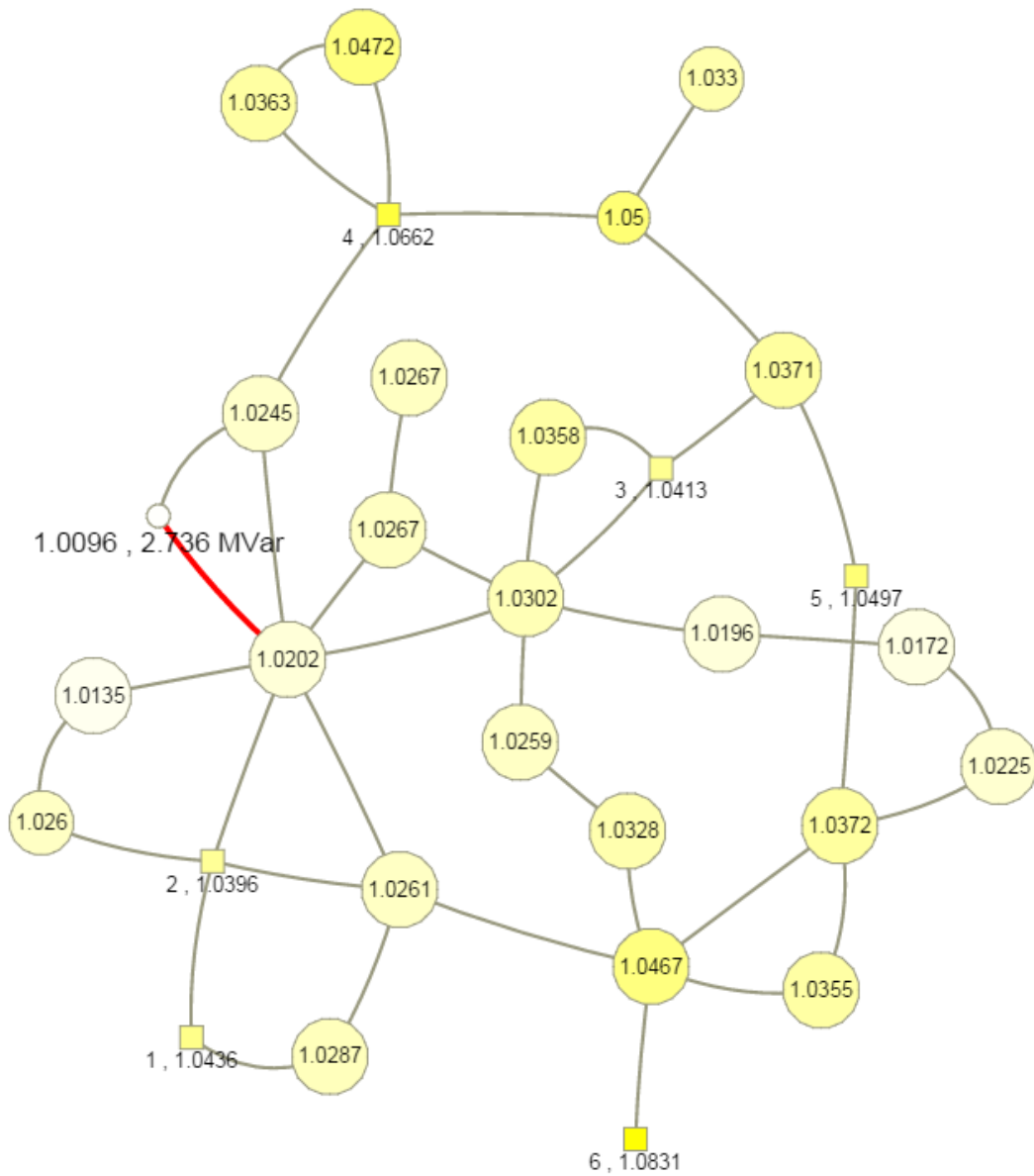


Figure 2.17: Optimal solution for the 30-bus system for 15 years service period and base load level (uniform load scaling factor is 1). Initially overloaded line marked in red. Generators represented by squares and loads by large circles, the color of the node represents voltage level (white - low, yellow - high). Generators are enumerated. SVC compensated load is shown by a small circle, SVC installed capacity is given - for one scenario installed capacity is equal to actual compensation setting.

The following Figs. 2.18- 2.19 illustrate the convergence of the algorithm and show the comparison of the initial active generation dispatch with the final one and with the solution given by the OPF procedure. It can be seen that here in comparison with 9-bus model, about 25 iterations are needed to get the solution. That is because the system is bigger, and we also limit the maximum change of reactive power generation.

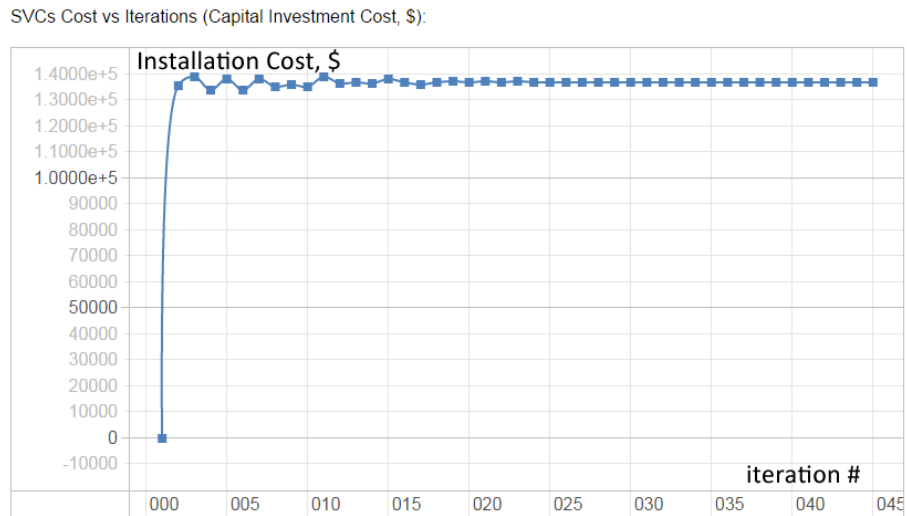


Figure 2.18: Convergence of the SVC capital investment cost for 15 years service period and $\alpha = 1$ (uniform load scaling factor).

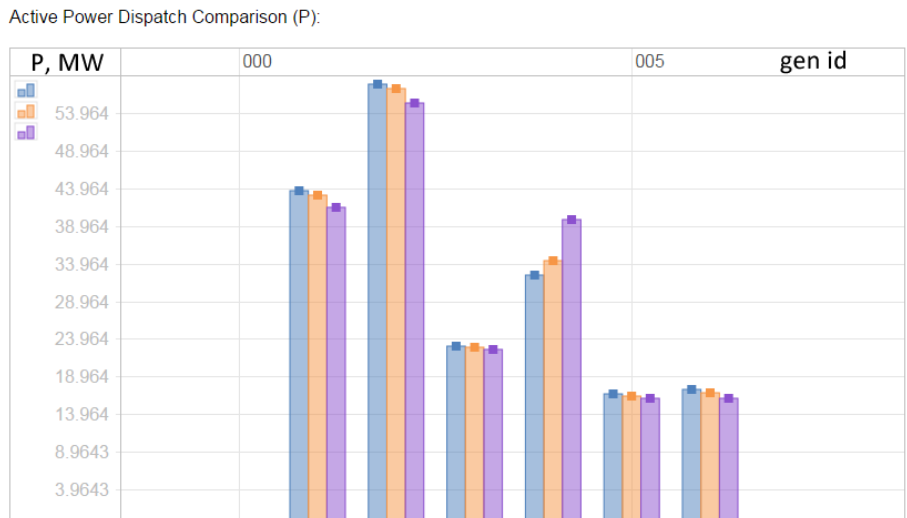


Figure 2.19: Active power dispatch comparison for 15 years service period and $\alpha = 1$. Blue bars - initial dispatch on the 1st iteration of algorithm, orange bars - final solution, purple - OPF dispatch.

For the next simulation, we will uniformly overload the system till the point when OPF is still feasible, which will take place at $\alpha = 1.03$, and then choose the service period to be 30 years. The goal of the experiment is to see how much saving one can gain by devices installation in the 30-bus system model. Load configuration should be OPF-feasible, as otherwise, we would not be able to compare the costs.

The solution is shown in the Fig. 2.20.

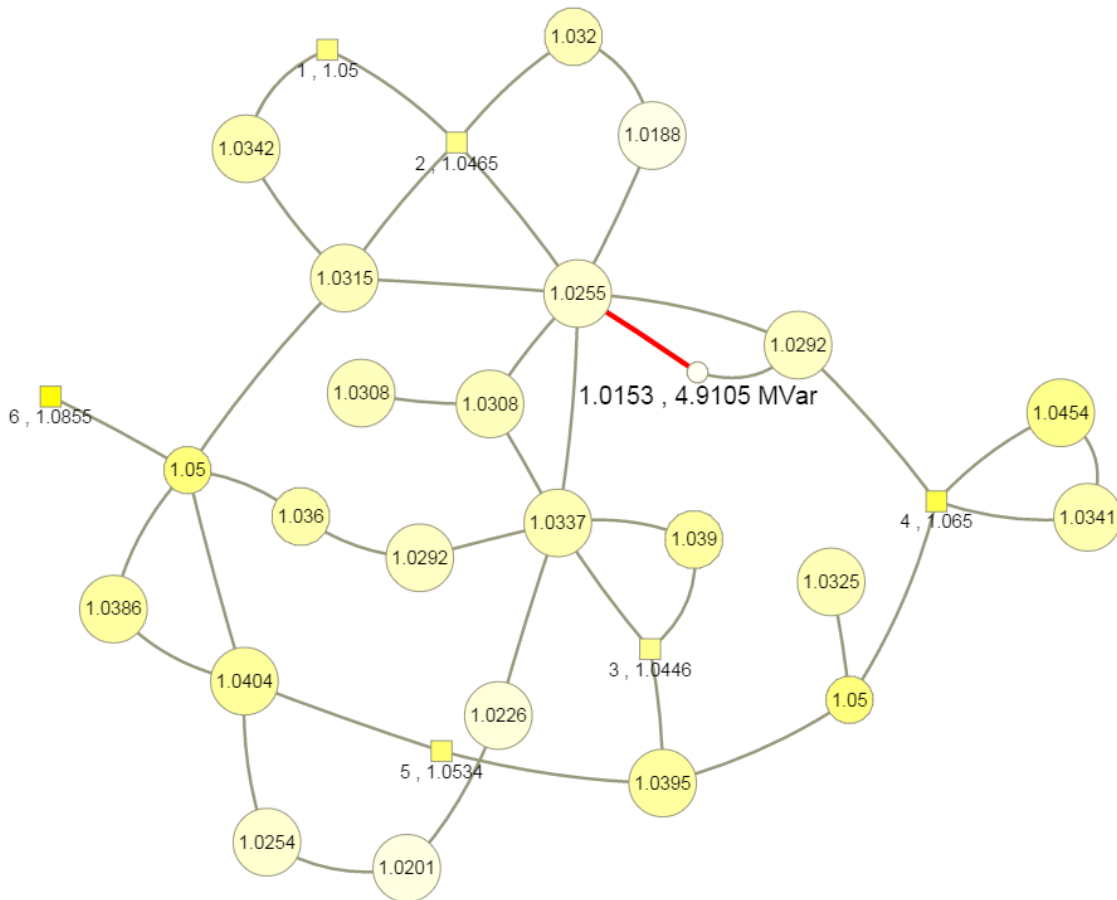


Figure 2.20: Optimal solution for the 30-bus system for 30 years service period and $\alpha = 1.03$ (uniform load scaling factor is 1.03). Initially overloaded line marked in red. Generators represented by squares and loads by large circles, the color of the node represents voltage level (white - low, yellow - high). Generators are enumerated. SVC compensated load is shown by a small circle, SVC installed capacity is given - for one scenario installed capacity is equal to actual compensation setting.

The structure of the solution is similar to the case when 15 years service period was considered. That is because the structure of the system is also similar. All initial parameters except load values are the same, and the load scaling factor is very close to 1. For multiple scenarios, we introduce an approach to generating different scenarios which describe a given load level.

- alpha: 1.03

- OPF Cost: 622.481 $\$/hour$ (163588000 \$ total for 30 years, no investments were made)
- Solver Cost: 596.598 $\$/hour$ (157032000 \$ total cost for 30 years which is capital investment plus operational)

Here the operational saving is about 4%. For real systems, this percent can translate into a very significant saving. However, let us restate the warning - these savings should be calculated based on many operational scenarios, and we will do that in the following Sections.

Next, let us analyze the structure of active and reactive power dispatch to see how exactly the congestion is relieved.

In Fig. 2.21 it can be seen that the final active power generation dispatch (which defines the generation cost) is approximately the same as the dispatch at the first iteration, which is OPF without thermal limits.

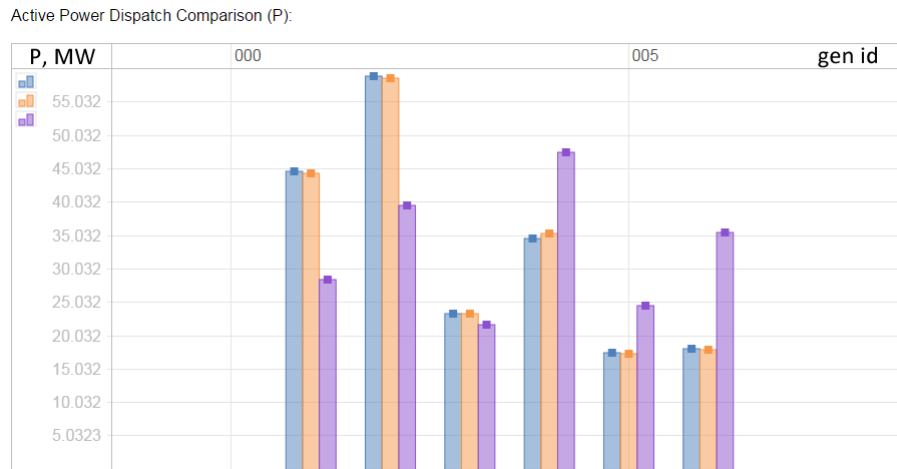


Figure 2.21: Active power dispatch comparison for 30 years service period and $\alpha = 1.03$. Blue bars - initial dispatch on the 1st iteration of algorithm, orange bars - final solution, purple - OPF dispatch.

Power flow limitations do not allow to use cheaper energy because it cannot be transported due to line congestion, and the developed approach uses the ability of FACTS devices to reroute power in order to optimally support cheap energy to go to demand places. As a result, ideally, we can get the same price for the generation which is given by non-constrained OPF, so if it is significantly less than OPF cost, it signals that the system is congested, and one can try to use FACTS devices in order to resolve that.

Final reactive power dispatch in the Fig. 2.22 is also similar to the initial one, but overall less power is produced by generators (each generator produces less reactive power than OPF without thermal limits procedure shows). In this case, SVC compensator does two things - it relieves the congestion of a line and produces reactive power at a place. Less power is transported around the network, which reduces losses.

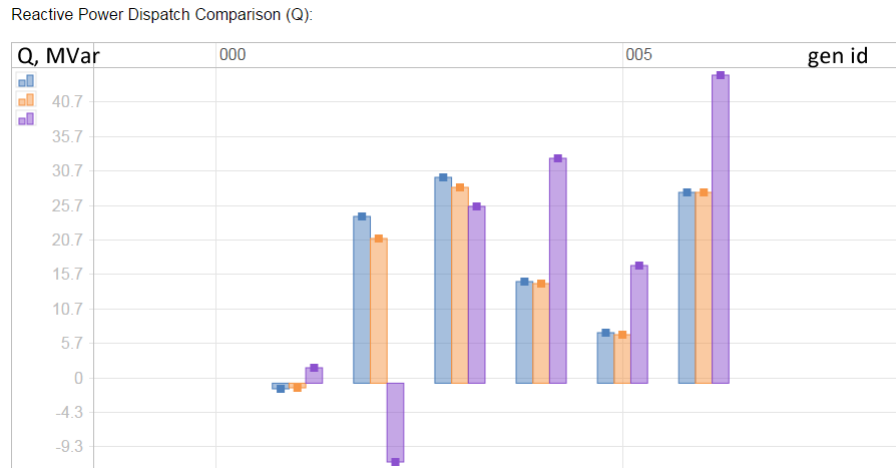


Figure 2.22: Reactive power dispatch comparison for 30 years service period and $\alpha = 1.03$. Blue bars - initial dispatch on the 1st iteration of algorithm, orange bars - final solution, purple - OPF dispatch.

2.5.2 OPF infeasible operation

If the system is uniformly overloaded by $\alpha > 1.03$ then OPF solution is not feasible, the system cannot operate for this load configurations, but we can try to optimally reinforce the system with FACTS placement in order to extend the feasibility domain and prevent lines overloading caused by increased consumption levels.

We perform 4 simulations with fixed load level and different service periods in order to see how the solution progresses. For each simulation, α is taken to be 1.07, and service periods will be 1 hour, 1 year, 15, and 30 years.

We do not show actual final states here. They are similar with one SVC placed in the same node as previously (see Fig. 2.20 for example). The installed capacities of the SVC are 2.8MVar, 4.24MVar, 6.92MVar, and 7.28MVar - each time when service period increases, we can invest more money in order to get a better economy on operational cost.

Fig. 2.23 shows the comparison of active power dispatch solutions. It can be observed that when going to 30 years service period, the dispatch becomes closer to OPF without thermal limits.

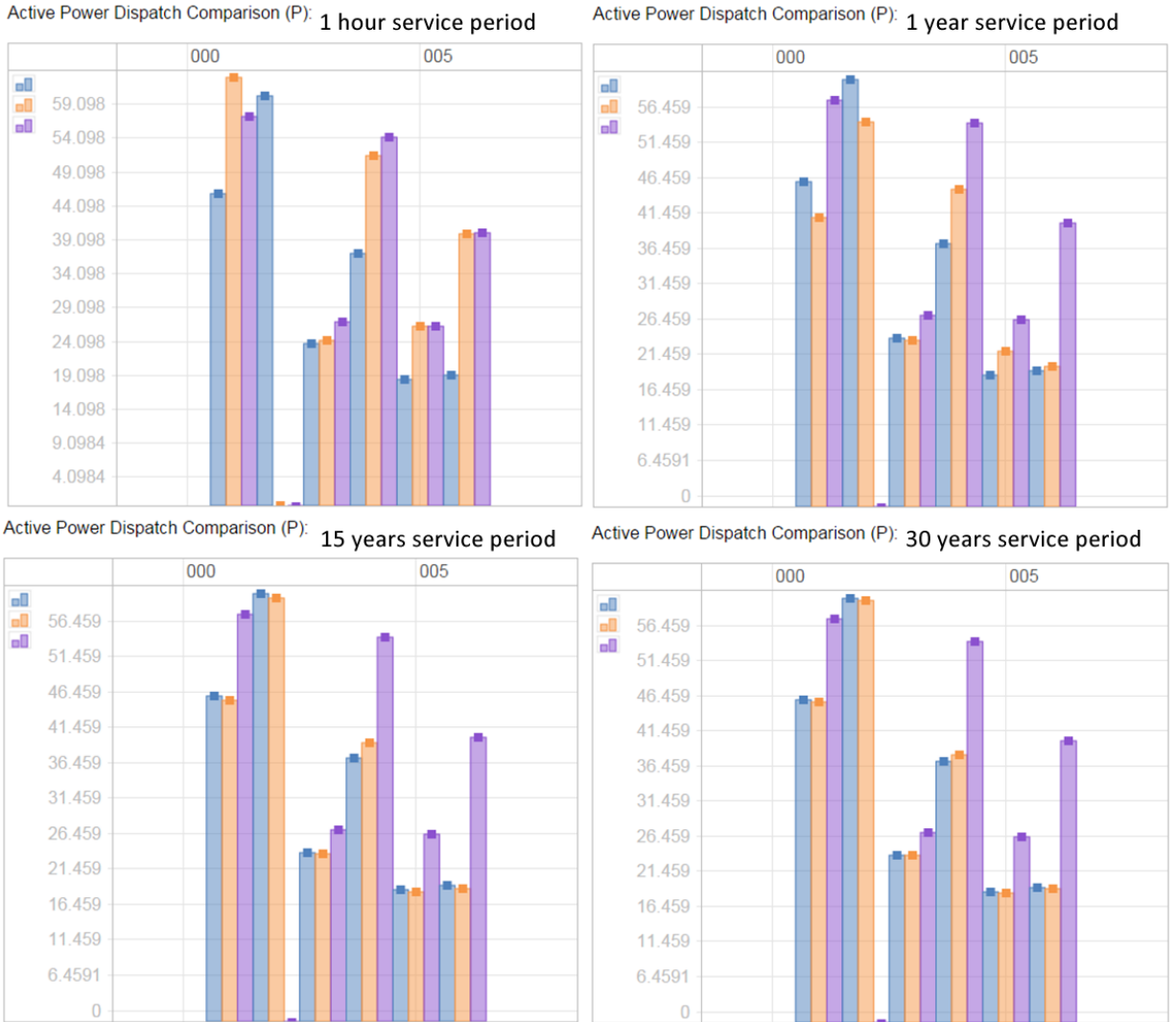


Figure 2.23: Active power dispatch comparison for four solutions of OPF infeasible scenario with $\alpha = 1.07$ and service period in the range from 1 hour to 30 years. Blue bars - initial dispatch on the 1st iteration of algorithm, orange bars - final solution, purple - OPF dispatch.

The last experiment in this section is performed for OPF-infeasible single load configuration, which was created by overloading the feasible base case of the Mathpower uniformly by 15%. We consider the single-scenario optimization over 15 years of the planning horizon. The obtained solution is shown in Fig. 2.24. We observe that the optimal correction is achieved with investment in one SC device and one SVC device, so both types of devices were used in this case.

Both devices have a similar effect on the state of the power system, but they do it in a different way by line inductance adjustment or reactive power injection. The developed approach allows finding optimal configuration, taking into account installation prices and scenario settings, and choose between the devices or find a good combination of installed FACTS.

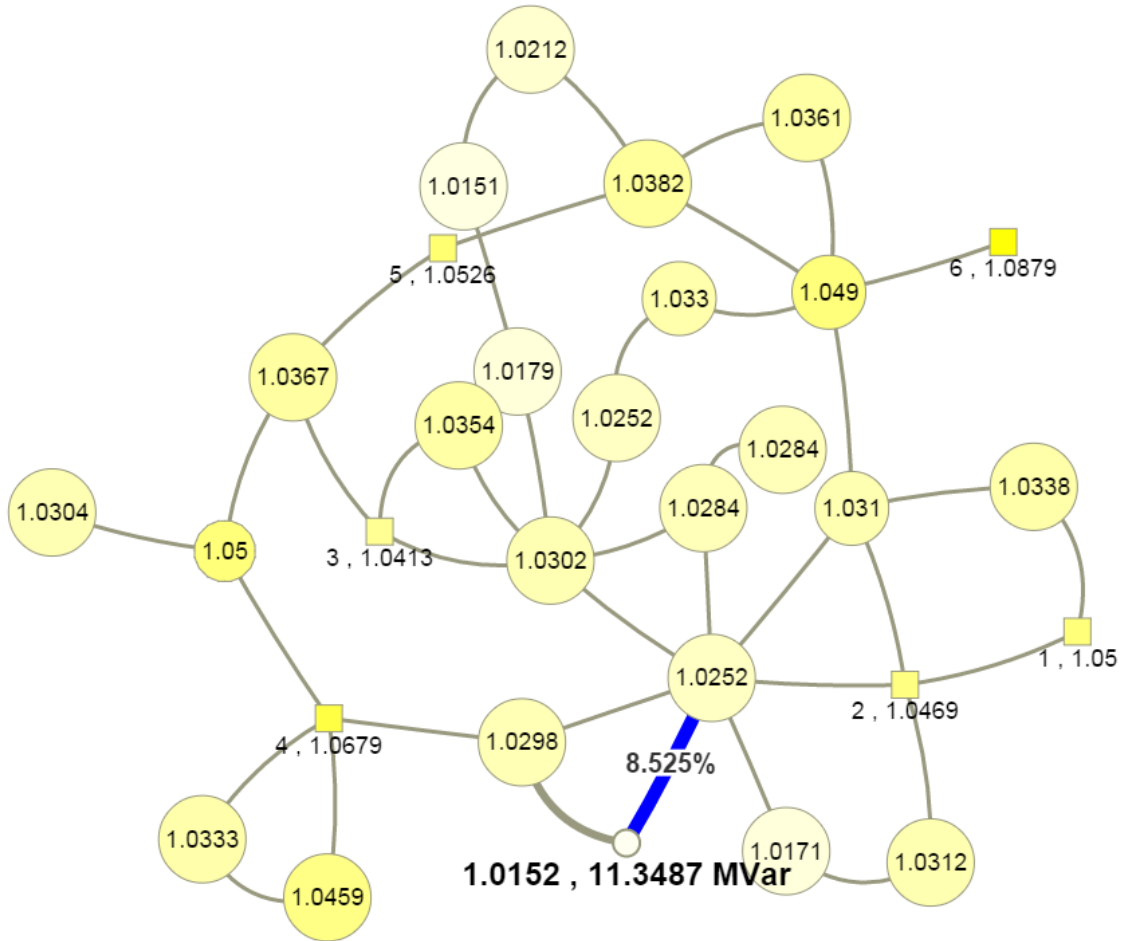


Figure 2.24: Visualization of the solver output. Circles and squares mark consumers and generators, respectively. Voltage profile is shown in color (transitioning from yellow for maximum voltage to white for the minimal voltage). Line marked blue was initially overloaded and it was also selected by the solver for SC correction/placement. Number, shown next to the blue line, shows correction (in percentage). Node which was chosen for the (only) SVC correction is shown as a white dot. Bold numbers which appear next to the dot show level of the voltage and corrected/installed reactive power provided at the optimal solution.

2.6 Multiple scenarios optimization

Based on our experience gained working on a single scenario solver, we develop a general version that finds one optimal investment for multiple scenarios and optimal settings of the installed devices for each load configuration simultaneously. In this section, we illustrate the performance of multiple scenario solver and explore the effect of FACTS devices on the system in the OPF feasible and infeasible regimes.

2.6.1 All OPF feasible scenarios

Firstly, we work with multiple all OPF feasible scenarios when it is possible to compare operational costs with OPF solutions.

10 different scenarios are considered on equal footing, i.e., each occurring with the probability of 10%. Each of the ten configurations is generated from a base feasible case of the Matpower with the subsequent addition of random correction to initial power consumption at nodes. Corrections are sampled from the Gaussian zero mean distribution with a standard deviation equal to the 3% of the load positioned at the node. That is rather small level of fluctuations. The problem is that for the given 30 bus model, due to line congestion, in many cases, we obtain OPF infeasible load configurations.

In this case, all 10 scenarios are similar from the loads distribution point of view, and the result of the optimization is to place one SVC device and use it at approximately 100% compensation level for each scenario which is similar to previous results for a single scenario solver. The reasons are the same - preference to local generation of reactive power and relieve of line contingency.

The behavior and performance of solver in this simulation is illustrated in the Figs. 2.25 - 2.28.

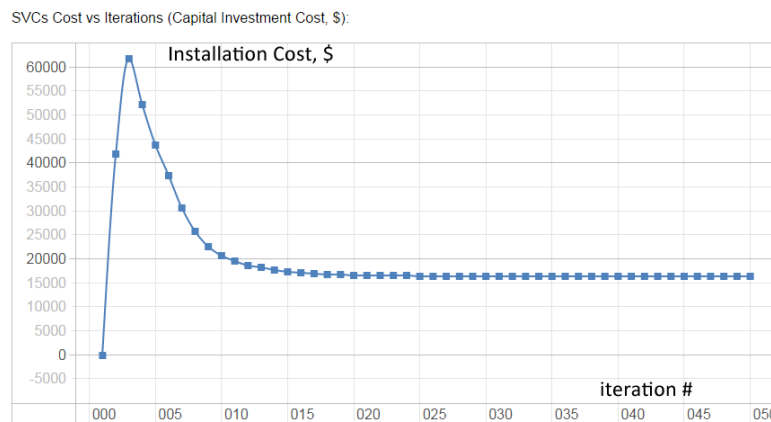


Figure 2.25: SVCs cost convergence for multiple scenarios solver, 10 different load configurations are used for simulation.

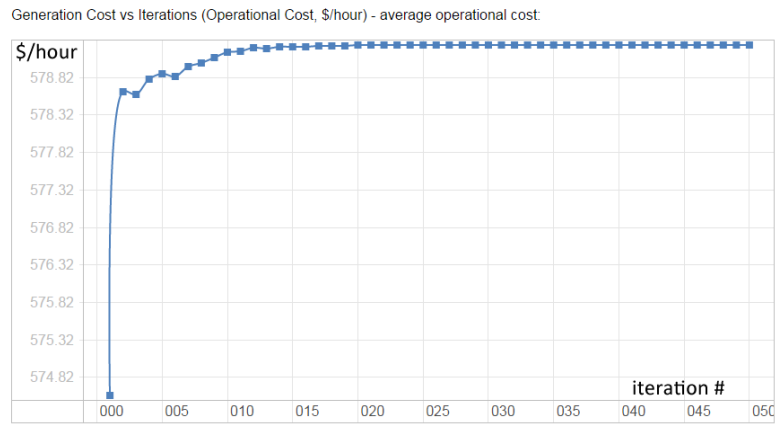


Figure 2.26: Average over 10 load configurations generation cost convergence with iterations.

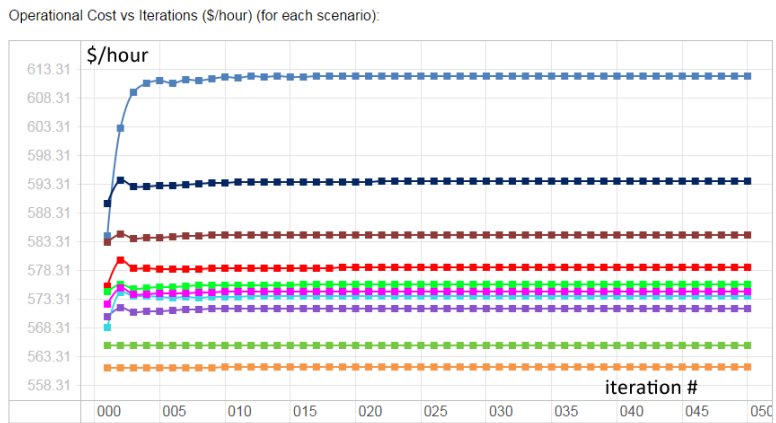


Figure 2.27: Convergence of each of 10 operational costs corresponding to the generated scenarios.

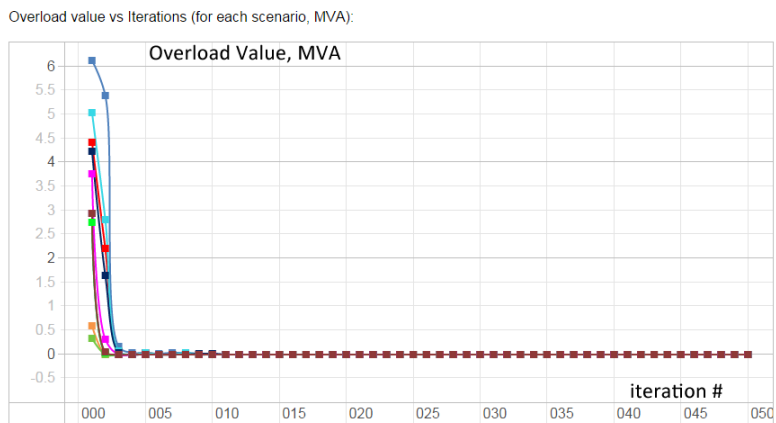


Figure 2.28: Progress of overloading management, solver relieves line congestion for each operational case.

One can observe the difference of multiple scenario optimization from a simple single scenario case. The state which represents each given loading configuration progresses independently but uses joint for all the scenarios installed capacity of FACTS devices for that. Finally, line overloads are relieved, and optimal generation dispatch is found for each operating regime. If we compare average over scenarios OPF cost with the solution when investment is made, we will observe some economy:

- Average OPF cost: 580.6 \$/hour
- Average scenarios cost: 579.3 \$/hour
- Economy percentage (avoided operational cost percentage): 0.23 %

When the scenarios are OPF feasible, the solver does not use the ability of FACTS devices to reinforce the system, there is no need for that, but when some of the cases are infeasible, and loads are distributed around the system in different ways, we observe interesting results of how actually FACTS help to improve the regimes by cost reduction and reinforce the system in the same time.

2.6.2 General case

Next, we illustrate the performance of our multiple-scenario solver with the example accounting for 10 configuration scenarios, and some of them can be OPF infeasible. Here we cannot calculate the economy in comparison to OPF solutions, but it is interesting to observe what kind of solutions do we get and how the devices are adjusted for various load configurations, and if we actually use the flexibility of the devices or not.

The scenarios are considered on equal footing, i.e., each occurring with the probability of 10%. Each of the ten configurations are generated overloading uniformly by 10% a feasible case of the Matpower with subsequent addition of random correction (sampled from the Gaussian zero mean distribution with standard deviation equal to the 10% of the load positioned at the node)

The system is optimized over the year-long time horizon. In this case, some of the scenarios are originally OPF-feasible, and others are not. Fig. 2.30 shows optimal voltage profiles and optimal settings for the installed devices over two (out of ten) exemplary scenarios. We observe that the multi-scenario algorithm discovers distinct feasible solutions for each of the scenarios. The resulting optimal placement is sparse. Moreover, once a device is installed, it is not utilized at its maximum in all the scenarios.

Progress of the algorithm is shown in Fig. 2.29.

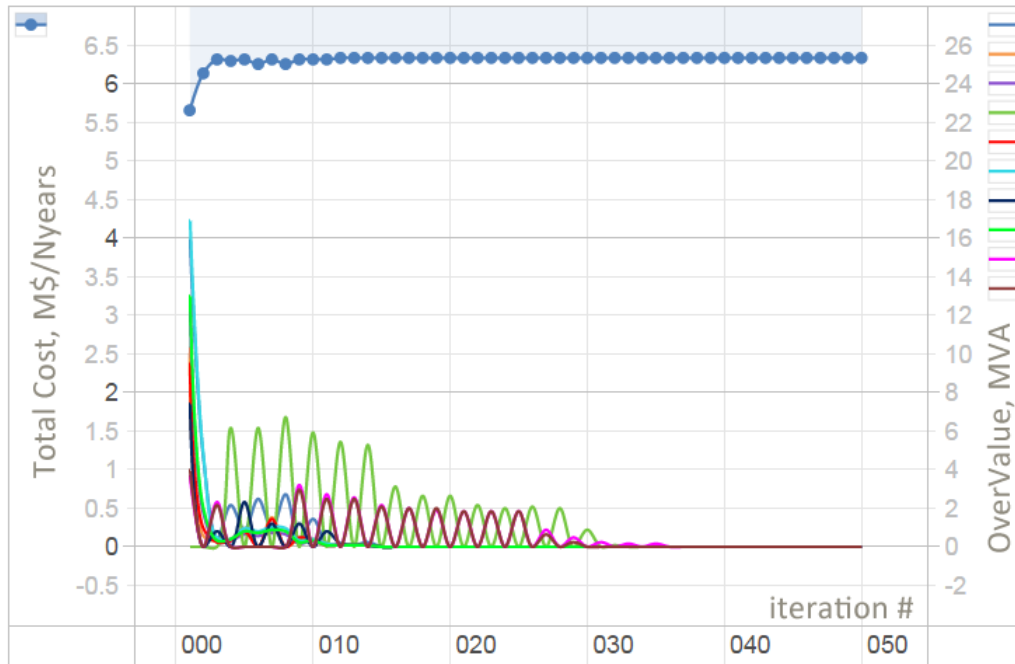


Figure 2.29: Illustration of the algorithm dynamics: we show dependence of line overloads in MVA (lines numbered on the right) and dependence of the total cost in M\$/years (blue dotted line shadowed from above) on the number of iterations.

Left y-axis of Fig. 2.29 illustrates convergence of the total cost (value of the objective function). We find that the multi-scenario solver requires approximately 30 iterations to converge. Right y-axis portion of Fig. 2.29 illustrates gradual (and generally non-monotonic) reduction of line overloads.

2.7 Summary

This chapter introduces the setting and problem statement for the installation of two types of FACTS devices using AC system modeling accounting for multiple manually created operational conditions. Solution algorithm and solvers suitable for a comparably small system of 30 bus are developed and validated on the simple examples. The next step is the extension of models to practical systems and additional work on solver's performance.

Chapter 3

Operations and Uncertainty Aware Installation of FACTS Devices in a Large Transmission System

This chapter discusses the application of the developed methodology to large-scale operational and uncertainty aware installation planning. It addresses the practical value of such installation and demonstrates the positive effect of the novel planning approach.

Inspired by the aforementioned prior studies, this chapter proposes an alternative scalable and AC-based approach to optimal placement and sizing of a sufficiently small number of FACTS devices in a transmission grid. Highlights of our approach are as follows:

1. Optimal placement is resolved by incorporating investment and operational variables into the optimization framework simultaneously. Installation of FACTS introduces additional degrees of freedom which are adjusted (along with other operational degrees of freedom) independently for each scenario within the installed capacities. In other words, placement is resolved by taking into account operational awareness.
2. Capital and operational expenditures are optimized simultaneously. The main advantage of this approach, which to the best of our knowledge has not been discussed in the literature so far, is that the resulting optimal investment leads to a greater reduction of the operational costs, thus providing additional long-term benefits.
3. Multiple loading scenarios are considered. Scenarios are generated as samples of a probability distribution associated with projected load curves representing seasonal and daily variations. This is in contrast to the existing literature approach, which accounts for a single (usually worst-case) scenario, thus resulting in installation of an expensive device with an unclear role in other cases. Our approach instead finds a single installation (locations and capacities) resolving multiple problems (e.g., overloads, congestion, voltage problems) associated with a multitude of

possible scenarios. Also, the optimal settings (within the installed capacities, distinct for different scenarios) are discovered.

4. A novel optimization heuristic algorithm accounting for the full AC model is developed. The algorithm consists of sequential evaluation until convergence (within the preset tolerance), and it includes two substeps at each step. The first substep is an analytic linearization of the basic AC formulas (nonlinear PF equations and nonlinear line constraints) resulting in a quadratic programming (QP) formulation finding investment variables and operational settings for all scenarios. The second substep consists of solving the AC PF for each scenario, thus updating states found in the first substep.
5. The algorithm resolving multiple loading scenarios scales well; it is capable of finding a solution for large realistic transmission models with thousands of nodes in a computationally acceptable time. The resulting solution produces either an optimal solution or at least a feasible upper bound solution separated from the optimal one by a relatively small gap.

The technical improvement of this chapter in comparison with the previous one is better level of model detalization - accounting for parallel lines, phase shifting transformers, areas with different voltage levels, multiple generators at a bus, etc. Generally speaking, if the previous chapter was more about the development stage, current is all about application, justification of the results and also about resolving difficulties correspondent to resolving large scale practical model.

3.1 Optimization framework for finding optimal location of FACTS devices

In this section we, first, formulate the problem of optimal placement and sizing of FACTS devices, and then explain and discuss challenges and features of the resulting nonlinear optimization. Optimization model is repeated for simpler discussion of the details. The following notations are used:

Optimization variables:

$\overline{\Delta x} \in \mathbb{R}^{N_l}$ Vector of series FACTS capacities.

$\overline{\Delta Q} \in \mathbb{R}^{N_b}$ Vector of shunt FACTS capacities.

$x \in \mathbb{R}^{N_l}$ Vector of line inductances.

$\Delta x \in \mathbb{R}^{N_l}$ Vector of series FACTS settings.

$\Delta Q \in \mathbb{R}^{N_b}$ Vector of shunt FACTS settings.

$V, \theta \in \mathbb{R}^{N_b}$ Vectors of buses' voltages and phases.

$P_G (Q_G) \in \mathbb{R}^{N_b}$ Vector of the generators' active (reactive) power injections.

Parameters:

$\bar{P}_G (\underline{P}_G) \in \mathbb{R}^{N_b}$ Vector of maximum (minimum) active power generator outputs.

$\bar{Q}_G (\underline{Q}_G) \in \mathbb{R}^{N_b}$ Vector of maximum (minimum) reactive power generator outputs.

$\bar{S} \in \mathbb{R}^{2N_l}$ Vector of the lines' apparent power limits.

$\bar{V} (\underline{V}) \in \mathbb{R}^{N_b}$ Vector of the maximum (minimum) allowed voltages.

$P_D (Q_D) \in \mathbb{R}^{N_b}$ Vector of active (reactive) power demands.

$x_0 \in \mathbb{R}^{N_l}$ Vector of initial line inductances.

a, K Index of the sampled loading scenario and total number of scenarios

$T_{(a)}$ Occurrence probability of scenario a .

N_l, N_b Number of operational power lines and buses.

$C_1 \in \mathbb{R}$ Cost per ohm of a series FACTS device.

$C_2 \in \mathbb{R}$ Cost per MVAR of a static VAR compensator (SVC) FACTS device.

$N_y \in \mathbb{R}$ Planning horizon for the system.

$C(P_G)$ Generation cost function

M Number of segments representing each load duration curve.

N_i Number of scenarios representing each segment

$\underline{\alpha} (\bar{\alpha})$ Minimum (maximum) loading level.

$\underline{\alpha}_i (\bar{\alpha}_i)$ Minimum (maximum) loading level for segment i .

$p_i = w_i$ Occurrence probability of segment i .

β (%) Yearly uniform loading growth

$l^0 \in \mathbb{R}^{2N_b}$ Vector of active and reactive loads for the base configuration.

Our multi-scenario, operations aware nonlinear and nonconvex optimization problem, allowing installation of the series compensators at any line and static var compensators at any loading nodes, is stated, in terms of continuous variables (no discrete degrees of freedom) for both installation and operational degrees of freedom as follows:

$$\min_{\Delta x, \Delta Q, y^{(a)}} C_1 \|\overline{\Delta x}\|_1 + C_2 \|\overline{\Delta Q}\|_1 + N_y \sum_{a=1}^K T_a C(P_G^{(a)}) \quad (3.1.1)$$

subject to

$$y^{(a)} = (x, V, \theta, P_G, Q_G, \Delta x, \Delta Q)^{(a)} \quad \forall a \quad (3.1.2)$$

$$x^{(a)} = x_0^{(a)} + \Delta x^{(a)} \quad \forall a \quad (3.1.3)$$

$$P_G^{(a)} = P_D^{(a)} + P_{ij}^{(a)} \quad \forall a \quad (3.1.4)$$

$$Q_G^{(a)} = Q_D^{(a)} - \Delta Q^{(a)} + Q_{ij}^{(a)} \quad \forall a \quad (3.1.5)$$

$$(P_{ij}^{(a)})_i = \sum_{j \sim i} \Re(S_{ij}^{(a)}) \quad \forall i, a \quad (3.1.6)$$

$$(Q_{ij}^{(a)})_i = \sum_{j \sim i} \Im(S_{ij}^{(a)}) \quad \forall i, a \quad (3.1.7)$$

$$\underline{P}_G^{(a)} \leq P_G^{(a)} \leq \overline{P}_G^{(a)} \quad \forall a \quad (3.1.8)$$

$$\underline{Q}_G^{(a)} \leq Q_G^{(a)} \leq \overline{Q}_G^{(a)} \quad \forall a \quad (3.1.9)$$

$$-\overline{\Delta x} \leq \Delta x^{(a)} \leq \overline{\Delta x} \quad \forall a \quad (3.1.10)$$

$$-\overline{\Delta Q} \leq \Delta Q^{(a)} \leq \overline{\Delta Q} \quad \forall a \quad (3.1.11)$$

$$\underline{V}^{(a)} \leq V^{(a)} \leq \overline{V}^{(a)} \quad \forall a \quad (3.1.12)$$

$$\begin{aligned} & [\Re(S)^{(a)}]^T [\Re(S)^{(a)}] + [\Im(S)^{(a)}]^T [\Im(S)^{(a)}] \\ & \leq (\overline{S}^{(a)})^2 \quad \forall a \end{aligned} \quad (3.1.13)$$

Variables $\overline{\Delta x}, \overline{\Delta Q}$ represent capacities of the newly installed series capacitors (SCs) and static VAR compensators (SVCs). These are an investment, i.e., 1st stage, decision variables.

$y^{(a)} = (x, V, \theta, P, Q, \Delta x, \Delta Q)^{(a)}$ represent the second-stage decision variables associated with operations under particular scenario (thus labeled by $^{(a)}$). Notice that the second-stage decision variables include scenario-specific settings of the installed FACTS devices. Operational settings (2nd stage decision variables) are constrained by the available capacities (1st stage decision variables).

The objective function in Eq. (3.1.1) consists of three terms. The first two terms express the capital investment costs of the installation of the two types of FACTS devices. Guided by the key message from the field of compressed sensing [75], the l_1 norm representation is chosen for the investment terms to promote sparsity of the FACTS device placement. The third term in the objective stands for the operational cost introducing explicit dependence on the settings of all the considered scenarios.

Here the summation is over K scenarios accounting for occurrence probabilities of the scenarios (T_a) multiplied by the number of service years considered for the planning horizon. By including multiple scenarios over the multi-year time horizon, we thus consider operational-aware planning.

It is important to emphasize the main point, and also difficulty, in solving the multi-scenario problem – the problem cannot be split into independent optimization problems, each associated with an individual scenario. The scenarios are coupled through the expected operational cost in the objective function. Obviously, there always exists at least one scenario for which scenario-dependent decision variables coincide with the respective capacity-related decision variables (otherwise optimal capacities would allow reduction to decrease the investment cost), however for the most part (majority of the scenarios) operational settings are strictly smaller than the capacity.

The constraints supplementing Eq. (3.1.1) are as follows. (3.1.2) describes the state of the system for a given operational scenario. (3.1.3) bounds actual line inductances, which are adjusted according to the operational value (per scenario) of the installed SC devices. The operational limits are set according to the respective installed capacities, represented by (3.1.10). (3.1.4) and (3.1.5) state active and reactive power balance at every bus of the network. Elements of vectors P_G (Q_G) and P_D (Q_D) are zeros for buses that contain neither generators nor loads. (3.1.6) and (3.1.7) represent the net active ($P_{ij} \in \mathbb{R}^{N_b}$) and reactive ($Q_{ij} \in \mathbb{R}^{N_b}$) power injections at the system buses. The term ΔQ stands for the scenario-dependent SVC shunt compensation constrained by the respective installed capacities in accordance with (3.1.11). Limits on active and reactive power generation are expressed by (3.1.8) and (3.1.9). (3.1.12) and (3.1.13) define the voltage and thermal line flow constraints. Here $S_{ij}^{(a)} = S_f^{(a)}$ if i is “from” end of a line and $S_{ij}^{(a)} = S_t^{(a)}$ if i is “to” end of a line. Check Appendix for the details and nomenclature of the π -line modeling used in this thesis.

Notice that nonlinearity and nonconvexity of the constraints (3.1.6), (3.1.7), and (3.1.13) constitute the main challenge for solving the optimization efficiently. Available nonlinear solvers, such as IPOPT [76], scale poorly (exponentially) with increase in the problem size, making the tool useless for optimization over realistic large transmission networks with thousands of nodes.

To complete the optimization problem formulation, one needs to describe how the representative load scenarios are defined. Each of K scenarios, indexed by a in Eqs. (3.1.1–3.1.13), should characterize different loading configurations with occurrence probability. The scenarios may include sampled (typical) configurations and/or contingency (rare) configurations representing different loading regimes. In principle, choosing scenarios appropriate for the optimization (3.1.1) of a grid model is a stand-alone task. We choose to generate scenarios from the so-called load duration (LD) curve [77]. The scenario generation procedure is explained in Section 3.3.

3.2 The Algorithm

This section describes the algorithm which we suggest to resolve the optimization problem stated in the preceding section. The algorithm consists of the following principal steps:

1. Scenarios are generated. (The scenario generation scheme based on the Load Duration curve concept is used. See Section 3.3 for details.)
2. Generation configuration is initialized (for each scenario) according to the scheme explained in Section 3.3.3.
3. If some of the constraints (3.1.3)–(3.1.13) are violated, the operational point of the system is outside of the feasible domain defined by them. The nonlinear constraints (3.1.6), (3.1.7), and (3.1.13) are linearized around the current operational point for each scenario. This allows for the construction of a current linearized version of the nonlinear optimization problem (3.1.1)–(3.1.13). The problem maintain all constraints for all considered scenarios.
4. The resulting linearized problem is solved by QP using the interior point algorithm of the CPLEX solver [78].
5. Exact AC PF is solved to update the states obtained in the previous step. This step is needed to prepare a feasible solution for the next iteration.
6. Steps 2–5 are repeated until no constraints remain violated, the target precision is reached, or the maximum allowed number of iterations is reached.

It is important to emphasize that, by design, the algorithm maintains at each iteration a feasible physical state. Also, the algorithm is a heuristic converging to a local minimum which may or may not be the global minimum. An empirical improvement, in terms of convergence to the optimal (or at least reasonable/good) solution, is achieved through experiments with the algorithm's starting point. It was found that initiating the algorithm with the solution corresponding to optimal dispatch ignoring line constraints (see Section 3.3.3) returns satisfactory results. Note that getting not optimal but reasonable solution resolving all the constraints would normally be acceptable (in practice).

The details of the main steps of the algorithm are presented below.

3.2.1 Linearization

Each scenario acts as an input to this part of the optimization heuristics. The operational state for each scenario can be represented as

$$y^{(a)} = (x, V, \theta, P, Q)^{(a)} \quad (3.2.1)$$

For each scenario, Eq. (3.1.13) is linearized using first order Taylor expansion around the current operational point y_0 :

$$F^{(a)}(y_0^{(a)}) + \nabla F^{(a)}(y_0^{(a)})(y^{(a)} - y_0^{(a)}) \leq (\bar{S}^{(a)})^2 \quad (3.2.2)$$

Where $F(y)$ is a function defining squared absolute value of the apparent power at an end of the line. Similarly, Eqs. (3.1.4)-(3.1.7) for each scenario can be linearized as

$$\nabla(P - P_{ij}(x, V, \theta, P, Q))^{(a)}(y_0^{(a)})(y^{(a)} - y_0^{(a)}) = 0 \quad (3.2.3)$$

$$\nabla(Q - Q_{ij}(x, V, \theta, P, Q))^{(a)}(y_0^{(a)})(y^{(a)} - y_0^{(a)}) = 0 \quad (3.2.4)$$

Operational variables are adjusted independently for each scenario.¹ However, the capacity limits of the devices stay the same (common) for all of the scenarios.

The fact that all controllable parameters of the system stay adjustable/flexible results in degeneracy of the linearized problem. To resolve possible degeneracy, we take advantage of the flexibility associated with redistributing controllable voltages, active powers and reactive powers. Specifically, we introduce the following soft controllable constraint for reactive power dispatch at each QP step:

$$|Q_G^{(a)} - Q_{G_0}^{(a)}| \leq \epsilon \quad (3.2.5)$$

The constraint is accounted for additionally to Eqs. (3.1.1)–(3.1.13).

3.2.2 Solving the QP problem

The standard QP solver of CPLEX is utilized to solve the linearized problem for all the considered scenarios together. Outputs of this step include values of operational variables for each scenario along with investment variables $\overline{\Delta x}$ and $\overline{\Delta Q}$.

3.2.3 Resolving AC PF

Notice that solution of the step 3.2.2 may actually violate the AC-PF balance. Hence the exact AC-PF step is added to maintain a valid/feasible power AC-PF solution at each step of the algorithm.

All together (i.e., in combination), the steps described above provide a feasible solution and resolve a system's contingencies simultaneously and gracefully.

3.3 Generation of scenarios for long-term planning

Scenario generation/sampling is used to include the uncertainty related to system load for the planning period. Power system load growth over the time horizon is modeled via modification of the Load

¹Operational values of the installed devices are assumed to be flexible (different for each considered scenario).

Duration (LD) curve for the current year. The base LD curve is illustrated in Fig. 3.1.

The base LD curve is used first to generate LD curves for consecutive years, rescaling the base LD curve by the load growth factor of 0.5% – 1.5% a year. Second, each early LD curve is split into M piecewise-constant parts. ($M = 6$ in simulations.) Finally, each piece of an LD curve is used to generate scenarios according to a random (thus called sampling) procedure described below. This scheme of scenario generation/sampling models variations in the distribution of loads, thus simulating power system behavior during an extended period of time in the future.

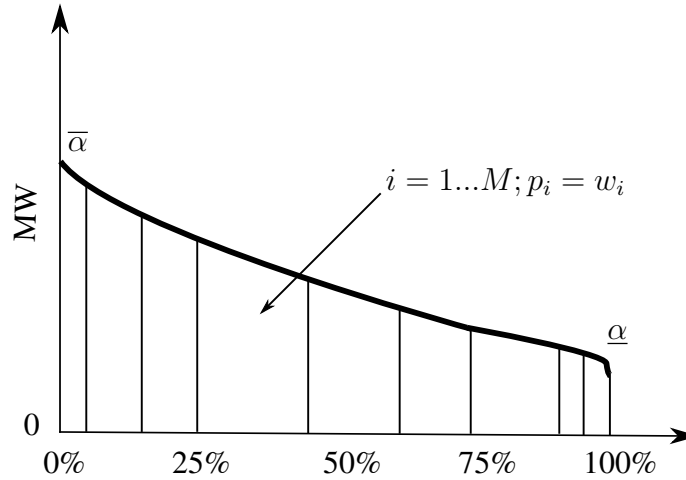


Figure 3.1: Piecewise-constant approximation of the LD curve.

It is assumed (and this assumption is confirmed in all our experimental tests) that each of the generated (sampled) load scenarios are ACOPF-feasible when the line constraints are ignored. (In other words, the setting is considered when there is enough generation capacity, even for the stressed cases.) Depending on the sampled scenario, three situations may arise.

1. ACOPF is feasible and congestion price is zero (low loading level).
2. ACOPF is feasible and congestion price is positive (higher loading level representing peak conditions).
3. ACOPF is infeasible because of congestion of lines and/or voltage constraints but the system has enough generation capacity. ACOPF without apparent power limits on lines (and without voltage constraints if infeasible) is feasible (overloaded conditions that are possible in the future).

The aim of planning installation of FACTS devices at the right locations with their corresponding capacities is to reduce generation cost for situation 2 and to improve or extend the feasibility domain of the system for situation 3. Extra years of service can hence be added to the existing grid by making it more flexible, thereby delaying investments into new lines and generators.

3.3.1 Scenario sampling for each segment

The loading level α_i for a segment i is represented by

$$\alpha_i = \frac{\bar{\alpha}_i + \alpha_i}{2} \quad (3.3.1)$$

Future loading configurations are obtained from the base case by rescaling all active and reactive loads by α_i uniformly. The resulting vector of loads for a segment is thus given by

$$l_i^0 = \alpha_i \times l^0 \quad (3.3.2)$$

Loading configurations are generated for each segment i and each $j = 1..N_i$ through modification of initial l_i^0 . This is done by adding Gaussian correction to each load with zero expected value and a respective standard deviation:

$$l_i^j = l_i^0 + \mathcal{N}(0, \sigma_{l_i^0}) \quad (3.3.3)$$

$$p_i^j = w_i/N_i \quad (\text{probability of a given scenario}) \quad (3.3.4)$$

where $\sigma_{l_i^0}$ is given by

$$\sigma_{l_i^0} = \frac{\bar{\alpha}_i - \alpha_i}{\alpha_i} \times l_i^0 \quad (3.3.5)$$

$$= \sigma \times l_i^0 \quad (3.3.6)$$

The choice of parameters used in our experimental test to sample the scenarios is described in Table 3.1.

Table 3.1: Implementation of the LD curve scheme

i	w_i	α_i	σ
1	5.50	0.940	0.064
2	19.50	0.845	0.041
3	25.00	0.775	0.045
4	25.00	0.685	0.080
5	18.80	0.590	0.068
6	6.20	0.51	0.078

3.3.2 Congestion analysis correction

If the case is considered in which, for a given load configuration, standard ACOPF outputs a solution that is not congested, i.e., a solution for which each constraint (on line flows or voltages) is satisfied

with a margin, then this scenario does not require any FACTS device installation. If the whole segment (from the procedure described in the preceding subsection) is of this “zero-congestion” type, then obviously, one does not need to generate many samples for the segment. Instead, one rescaled base scenario to represent the whole segment is picked.

3.3.3 Defining initial generation profile

The initial profile of the generation for each loading scenario has to be determined to run the algorithm. Generation capacity is assumed to be large enough for given loading levels. Two procedures are used for that: (1) solve ACOPF with the thermal limits ignored, and (2) find proportional generator response. Second, is done in the following four steps:

- Search for the smallest load rescaling factor α lowering the load and thus making the resulting case feasible.
- Solve ACOPF with this new rescaled loading.
- Proportionally increase generation and load with the value of α , which restores the initial loading of the system. Use voltages from the ACOPF solution.
- Solve ACPF to obtain generation maintaining the loading.

3.4 Methodology and installation justification

The developed approach is illustrated on examples of the IEEE 30-bus and the 2736-bus Polish models, both available through the Matpower [74] software package. The simulations are performed on a Core i7 2600K@4GHz PC with 24 GB of system memory. Both Matlab and Julia implementations, which are comparable in performance, are used. Operational cost is determined using generation cost functions from the given model. The investment cost is a value calculated according to the installation model (capacity \times installation cost). The actual installation cost of a given FACTS device configuration remains a subject for future research.

3.4.1 IEEE 30-bus model

In this section, the advantage of including operational variables and optimizing the expected value of operational cost as an objective along with the investment cost is emphasized. We also illustrate optimality and scalability of the developed heuristics by comparing our algorithm performance with the performance of the IPOPT when it is used as a state-of-the-art brute-force solver applied to the exact problem Eq.(3.1.1).

Necessity of including operational variables in determining FACTS device placement Let us, first of all, clarify the algorithm’s principal advantage of optimizing operational variables simultaneously with the investment variables. The following simulation is performed to demonstrate the actual benefit of the combined use of the capacity variables and the scenario variables. The base-case system load is increased uniformly by 5%, which leads to optimal power flow (OPF) infeasibility. Operational cost is not optimized for now ($N_y = 0$ in Eq. (3.1.1)). The initial state of the generation (needed to initialize the algorithm) is defined by the first method described in Section 3.3.3. Then the two solutions are compared. One is the actual solution of the developed algorithm with all degrees of freedom available for the optimization. The second solution is constrained by the same (fixed) generation dispatch (the initial value).

Table 3.2: Monetary advantage of considering operational variables, illustrated on the IEEE 30-bus model.

Oper. variables	SVC cap. (MVar)	SC cap. (% of init x)	Invest. cost (\$)	Oper. cost (\$/hour)
Fixed	6.936 (3 SVCs)	38 (1 SC)	415930.29	614.05
Free	1.112 (1 SVC)	0 (0 SCs)	55765.71	698.24

Table 3.2 details the comparison. The significance of accounting for additionally available degrees of freedom is obvious. We find out that although the algorithm is able to find a feasible solution in both cases, the investment cost (objective function value) is 7.5 times smaller in the adjustable generation dispatch case. The emergence of an expensive solution with a small operational cost is reported in Table 3.2. This is an indication that further experiments with tradeoffs between investment and long-term operational costs (fixed in the use cases studied) are to be explored in future studies.

Importance of including operational cost in the objective function Another important point to illustrate in the example of the IEEE 30-bus model is that combining the operational cost and the investment cost in the optimization objective is a way to make the optimization relevant to practical planning. Indeed, keeping only the investment cost produces operationally expensive solutions, whereas keeping only the operational cost results in an expensive (and not sparse) installation. Combining the effects of operations and installations in one objective allows for an efficient balance between the two.

To the best of our knowledge, only the investment cost is accounted for in the available literature devoted to the placement of FACTS devices. To mimic this standard approach (accounting for only a single worst-case operational scenario), the optimization horizon is set to zero, $N_y = 0$, in Eq. (3.1.1). Then N_y is increased to 10 years to take the effect of operations into account.

Table 3.3 illustrates the results. Two solutions found for $N_y = 1$ and $N_y = 10$ reflects sensitivity to the operational cost. Single extreme load configuration is considered (correspondent to a 5% increase of the load in the base case). When planning horizon is extended it becomes profitable to invest more into reduction of the operational cost. It is observed that an additional small investment of 200k\$ leads

Table 3.3: Monetary advantages of adding the operational cost to the optimization objective for the IEEE 30-bus model.

Plan. horizon (N_y)	Invest. cost (\$)	Oper. cost (\$/hour)	Total cost (10 years, M\$)	Difference (%)
0	55618.76	698.24	61.722	14.6
1	121838.27	616.25	55.202	2.49
10	249245.37	611.98	53.858	0.0

to a savings of 14.6% of the total cost in 10 years. Based on this example, we conclude that accounting for the operational cost in the planning problem is significant. Properly installed FACTS devices allow not only to resolve infeasibility of the loading configuration but also to reduce the generation cost, thus producing lasting long term benefits. It is important to emphasize that by accounting for multiple representable scenarios (as opposed to working with a single scenario) we achieve a much more realistic description of the whole operational space.

Optimality To verify performance of the developed heuristics, a single scenario (base case overloaded by 5%) is considered and the results are compared with the “exact” (Eq.(3.1.1)) ones produced by IPOPT (standard, brute-force, nonlinear solver that is still able to handle the 30-bus investment model).

We choose to work with IPOPT because it shows computational advantage over other nonlinear/nonconvex computational platforms applied to problems with structure similar to the one discussed here. As it is shown in [79], IPOPT is on par or it outperforms Matpower in solving classic ACOPF. An additional advantage of using IPOPT is in its availability within the JUMP/Julia computational environment we rely on. For the actual solver on QP-step (2. Solve QP) of our algorithm, the CPLEX solver is called (the solver is known to be advantageous for problems with linear constraints).

The optimization horizon is set at 1 year. Table 3.4 shows comparison of heuristics with the benchmark IPOPT. It is observed that (as expected) developed heuristics produce a very tight upper bound for the exact solution, with values of the objective function and structure of the solution that are very close to the exact values.

Table 3.4: Comparison of the proposed heuristics with the brute-force IPOPT solution of the exact problem Eq.(3.1.1) for the IEEE 30-bus model.

Solver	Bus number	Calculated cap. (MVar)	Investment cost (k\$)	Total cost (k\$)
IPOPT	8	2.436	121.80	5520.094
proposed algorithm	8	2.437	121.84	5520.159

Scalability To study how the algorithm scales with the number of scenarios, we pick the base case, increase all loads by 5%, and generate K scenarios through the Gaussian sampling procedure associated with Eqs. (3.3.3–3.3.4), where the rescaled base-case load is set to l_0 . Scaling analysis of the developed algorithm is illustrated in Fig. 3.2.

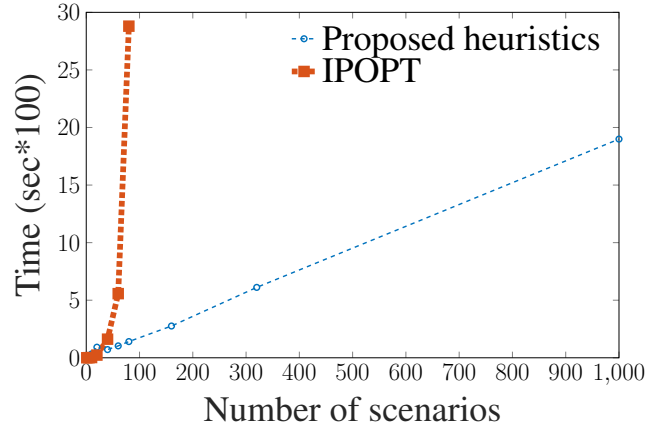


Figure 3.2: Computational time comparison for 30-bus model.

It is observed that algorithm handles an increasing number of scenarios very efficiently, solving formulations with a large number of scenarios in time that increases linearly with the number of scenarios (blue line). Performance of the brute-force IPOPT solver applied to the exact problem in Eq. 3.1.1 (shown as thick red line in Fig. 3.2) is limited.

3.4.2 2736-bus Polish model

In this section, we extend analysis of the developed algorithm to the case of the Polish grid, which is a practical-size transmission model available as a part of the Matpower package [74]. Similar approach as the one tested above on the 30-bus model is followed here.

Necessity of including operational variables in determining FACTS device placement The experimental setting stays the same as in the case of the 30-bus model. A single scenario corresponding to the normal operational state (correspondent to the base-case example from [74]) with all the loads homogeneously increased by 5% is considered for resolution. Generation dispatch is defined by the second procedure from Section 3.3.3. Table 3.5 illustrates the results. (See Section 3.4.1 for a detailed discussion of the experimental setting, related terminology, and nomenclature.) The results confirm the conclusions drawn above for the case of the 30-bus model—operational variables should be taken into account because ignoring them leads to a significant increase in the investment cost, or even worse, the infeasibility of a highly loaded configuration.

Table 3.5: Monetary advantage of considering operational variables for the 2736-bus Polish model.

Oper. variables	Investment cost (\$)	Operational cost (\$/hour)
Fixed	916616.1	1884214.9
Free	187869.6	1950027.2

Importance of including operational cost in the objective function The normal operation base-case is taken with all loads re-scaled up by 5%, and the resulting optimizations are compared (including and not including the operational cost in the objective). The comparison is made for the total cost accumulated in 10 years. It is observed that the difference between the 0-year case (where the operational cost is ignored) and the 10-year case is 2.6%, which results in 4330 M\$ of total cost savings; the additional investment (installation) cost is only 550k\$. The numbers clearly support the main hypothesis: installation is advantageous and including the operation cost in the objective is mandatory for practical grid extension planning. This is possible because congestion in the system shows a decrease, in addition to the restoration of the feasible solution.

Scalability Fig. 3.3 shows how the computational time of the algorithm scales with the number of the scenarios.

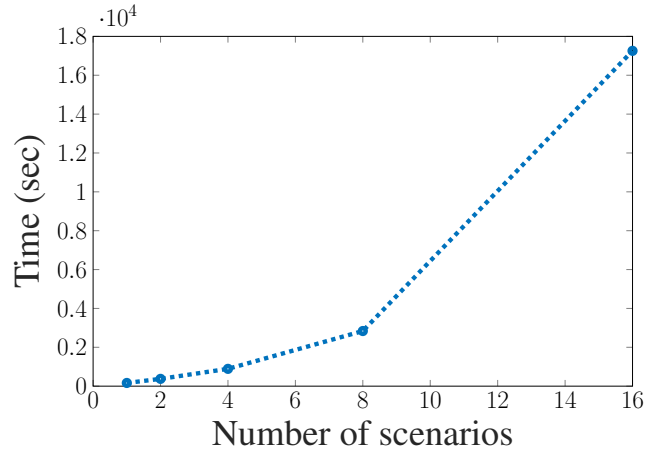


Figure 3.3: Computational time vs the number of scenarios for the Polish model.

A number of cases ranging from a single scenario to 16 scenarios are tested. The brute-force IPOPT fails to solve the Polish model case even with a single scenario (an exact problem in Eq. 3.1.1). The proposed algorithm solves the most challenging case of 16 scenarios in 17500 sec. It is deduced from Fig. 3.3 that the computational time grows polynomially as $O(K^3)$, suggesting that the proposed algorithm is practical/scalable for planning problem when computational time is not a significant constraint.

Note that the $O(K^3)$ scaling is still slower (with the K increase) than the linear-scaling behavior observed in the 30-bus model. Our suggestion is that the better performance observed in the 30-bus

model may be related to the fact that the Polish model is denser, thus requiring linearization of more PF equations. It may also be due to worse scaling of the QP solver performance in the case of the Polish model. We plan to perform a more detailed analysis in the future.

3.5 Multiple-scenario-aware long-term planning

In this section, developed methodology and algorithm, discussed in the preceding sections, are applied to the analysis of the comprehensive multiple-scenario-aware long-term planning setting. To generate the scenarios and initialize the algorithm, methods discussed in Section 3.3 and Section 3.3.3 are utilized. In all experiments discussed below the planning horizon is chosen to be 10 years.

3.5.1 IEEE 30-bus model

Sixteen scenarios per yearly LD curve are generated (160 total). The annual increase factor, β , is set to 1.5% a year. The resulting optimal solution is shown in Fig. 3.4. It is observed that proposed algorithm installs FACTS devices efficiently and sparsely, thus resolving successfully the otherwise imminent (observed for a significant portion of the 160 scenarios) AC-OPF infeasibility. The optimal solution consists of the installation of an SVC device at bus 8 with the capacity of 5.78 MVar and installation of an SC device at the line between buses 6 and 8 with a capacity increase of 1%. The proposed investment is 30k\$, resulting in an average savings of 1.8\$ per hour.²

3.5.2 2736-bus Polish model

This experiment is done with 16 sampled scenarios (2 of 16 are AC-OPF infeasible) for the 10-year horizon and with assumed yearly loading growth (factor β) of 0.5%. The resulting optimal investment is shown in Fig. 3.5 (coding of loads and gens is the same). The algorithm outputs a solution resulting in the installation of two SC devices and one SVC device to resolve the infeasibility of some of the samples. The average congestion cost of the sampled scenarios is 5738\$/hour, and the average generation cost savings is 3369\$/hour. The solution is sparse and nonlocal (new FACTS devices are installed sufficiently far away from nodes and lines where the initial congestion was observed). SVC installation is relatively small in that case because congestion was much more significant for sampled scenarios than infeasibility, basically sampled two AC-OPF infeasible conditions are still close to the feasibility region.

²All the actual values are model dependent. Costs are values of the objective function - determined according to a pre-defined cost of investment for a unit of capacity.

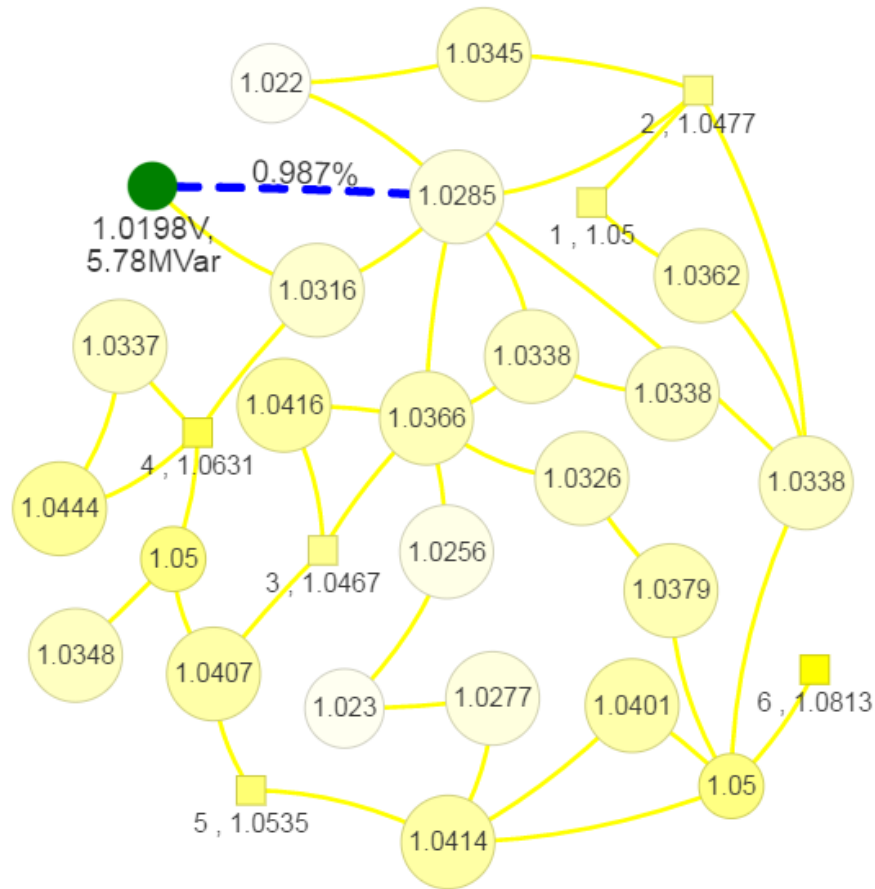


Figure 3.4: Optimal solution for 10 years of planning in the case of the 30-bus model. Loads = yellow circles; gens = squares; blue dashed line = line with installed SC that was overloaded initially for some scenarios; green dot = node where an SVC is installed. Voltage levels are shown in PU; capacities of SVCs and SCs are shown in MVar and in % of initial line inductance.

3.6 Summary

This chapter demonstrates application of the developed operational and uncertainty aware FACTS placement and sizing methodology to the cases of 30-bus system and 2736-bus Polish system models accounting for a range of operational conditions representing LD curves for the future years of operation. Special analysis is performed to demonstrate benefits, provided by introduction of the additional flexibility to the system, combined with available degrees of freedom. Which is provided by our planning approach. Solution algorithm performance is compared with state of the art IPOPT solution. The next step is to account for multiple time intervals inside the planning horizon. At a current setting only one installation of the capacity is possible.

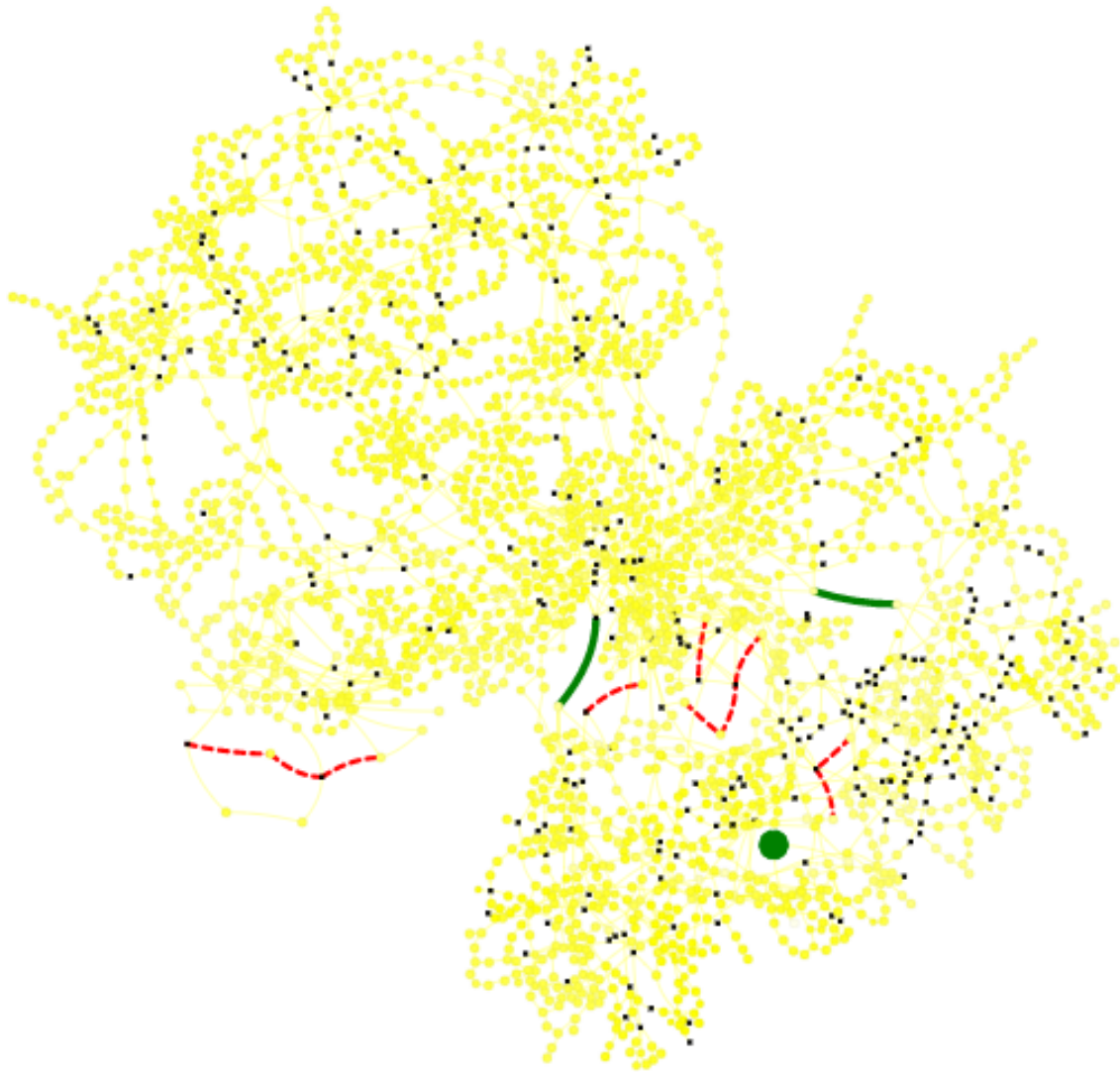


Figure 3.5: Optimal solution for 10 years of planning in the case of the Polish model. Red dashed lines = lines that were initially overloaded for some scenarios. Two built SVCs are shown by green lines. The big green dot illustrates an SVC device. SVC: 3.3 MVar, SCs: 14.4%, 70.4% (left to right).

Chapter 4

Methodology for Multi-stage, Operations and Uncertainty Aware Placement and Sizing of FACTS in a Large Power Transmission System

This chapter introduces generalization of the previous model to multiple time interval investments - when investment is done gradually in the future (i.e. additional capacity is introduced each year).

In this chapter, the last remaining issue in the optimal multiple-scenario aware, AC-based and sparse placement and sizing of the FACTS devices in a large transmission system is resolved. Here, we choose to represent the future not in one time step but in multiple time steps. In other words, here we complete the development of the stochastic approach to operational and uncertainty aware planning when operational conditions are represented by a set of deterministic samples. We propose a comprehensive resolution for finding optimal locations of FACTS devices in a large transmission system by preparing the system for future loading gradually through multi-stage, properly paced investments. The main highlights of our comprehensive approach are as follows:

1. The planning horizon is represented by multiple decision points (multiple time frames). At each new time frame, a set of new FACTS devices can be installed, and they are assumed available for operations immediately such that respective operational values do not exceed the installed capacities. Therefore, the installation of FACTS devices can be paced. We work with a finite number, T , of the time-horizon sub-intervals.
2. Future operational conditions are represented through multiple loading scenarios and associated probabilities broken into time frames. Our framework is set in the way that the scenarios are stated as an exogenous input, which allows us to separate the problem of scenario generation from the intrinsic optimization details. Given the exogenously prescribed scenarios, optimal

installation of FACTS is resolved within the optimization framework by accounting for both investment and operational variables, characterizing installation decisions and operational implementations (per scenario), respectively. It is important to stress that optimal constraints (i.e., feasible) all the scenarios. (This is in contrast with the worst case planning approach.)

3. Both capital and operational expenditures are optimized simultaneously. To the best of our knowledge, no prior works have considered optimizing them at the same time. But for practical planning horizons, operational cost is much bigger than the cost of FACTS installation. Thus relatively small additional investment allows saving a significant amount of money by reducing congestion additionally to resolving infeasibility of particular load scenarios.
4. A novel optimization iterative heuristics is developed, which is a combination of analytic linearization of non-linear constraints, a solution of Quadratic Programming (QP) or Linear Programming (LP) (depending on generation cost) problem for a finding of investment variables and operational settings for all scenarios and Alternating Current (AC) Power Flow (PF) resolution (for each scenario) to update previously found states.
5. The developed heuristics for finding optimal locations of FACTS devices considering multiple loading scenarios and multiple time frames can be applied to large power systems. In other words, the developed approach is scalable. To the best of our knowledge, the system considered in the literature addressing optimal locations of FACTS placement consists of a maximum of 1228 buses [54]. The results of the proposed methodology are demonstrated on the 2736-bus Polish system, thereby proving its scalability. Moreover, the algorithm provides upper bound solutions of the objective function with the gap of less than 0.1%

4.1 Optimization model

The following notations are used in this chapter:

Parameters:

N_l Number of power lines in operation

N_b Number of buses in the system

M Number of loading scenarios representing given time frame

N Number of scenarios representing planning horizon

T Number of time frames representing horizon

$t = 1..T$ Index of a decision point

$a = 1..M$ Index of a scenario at time frame t

$Pr_{t,a}$ Occurrence probability of a scenario a at time frame t

$x_0 \in \mathbb{R}^{N_l}$ Vector of initial line inductances

$\bar{P}_G (\underline{P}_G) \in \mathbb{R}^{N_b}$ Vector of maximum (minimum) active power generator outputs

$\bar{Q}_G (\underline{Q}_G) \in \mathbb{R}^{N_b}$ Vector of maximum (minimum) reactive power generator outputs

$P_{D_0} (Q_{D_0}) \in \mathbb{R}^{N_b}$ Vector of active (reactive) power demands

$\bar{S} \in \mathbb{R}^{2N_l}$ Vector of line apparent power limits

$\bar{V} (\underline{V}) \in \mathbb{R}^{N_b}$ Vector of maximum (minimum) allowed voltages

$C_{SC} \in \mathbb{R}$ Cost per Ohm of a series FACTS device

$C_{SVC} \in \mathbb{R}$ Cost per MVar of a shunt FACTS device

$N_{years} \in \mathbb{R}$ Planning horizon

Optimization variables (operational, scenario dependent):

$V \in \mathbb{R}^{N_b}$ Vector of bus voltage magnitudes

$\theta \in \mathbb{R}^{N_b}$ Vector of bus voltage angles

$P_G \in \mathbb{R}^{N_b}$ Vector of generator active power injections

$Q_G \in \mathbb{R}^{N_b}$ Vector of generator reactive power injections

$x \in \mathbb{R}^{N_l}$ Vector of line inductances modified by SC devices

$\Delta x \in \mathbb{R}^{N_l}$ Vector of series FACTS settings

$\Delta Q \in \mathbb{R}^{N_b}$ Vector of shunt FACTS settings

Optimization variables (investment, scenario independent):

$\overline{\Delta x}^t \in \mathbb{R}^{N_l}$ Vector of series FACTS capacities built at decision point t

$\overline{\Delta Q}^t \in \mathbb{R}^{N_b}$ Vector of shunt FACTS capacities built at decision point t

This section describes our optimization framework for operations-aware installation of FACTS devices taking into account multiple future decision points (or multiple time intervals).

Assume that the planning time horizon is N_{years} , T is the number of time intervals, M is a number of given loading configurations (scenarios) per each time frame (the number of scenarios per time frame may also vary with the time frame). In this setting, we aim to place and size the Series Compensation (SC) and Static Var Compensation (SVC) devices, where an SC device, installed at a line, modifies inductance of the line (thus allowing to reroute apparent power), while an SVC device, installed at a node, injects or consumes reactive power at the node thus helping to balance the voltage locally.

Fig. 4.1 illustrates the setting. Since scenarios are generated within each time interval independently, the total number of paths accounted for within our optimization formulation is $\prod_{t=1}^T M(t)$, where a path is a sequence of T scenarios (each per time interval). Notice that even though the number of paths is exponential in T , the total number of the operational constraints in the optimization formulation, $N = \sum_{t=1}^T M(t)$, scales linearly in T .

The overall problem is to minimize a combination of the sum (over the time intervals) of the investment cost and the sum of operational costs over all the scenarios taking into account (a) operational constraints for every scenario (per time interval) and (b) investment constraints requiring that the operational variables (for every scenario per time interval) do not exceed the respective installed capacities. **Operational settings can be different for different scenarios, but installed capacities of the devices are the same for all the scenarios representing given time interval.**

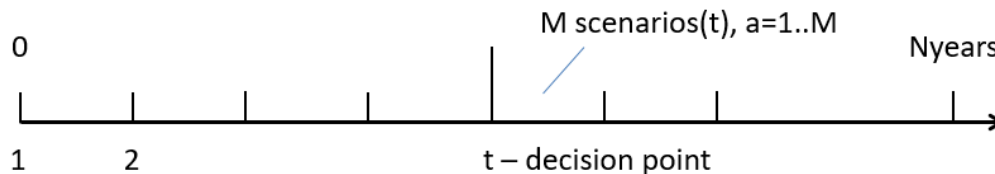


Figure 4.1: Illustration of the relation between the number of scenarios, $M(t)$ (each defined in the time interval, t) and the number of time intervals, T . $N = \sum_{t=1}^T M(t)$ is the total number of constraints imposed (per line or per node) within our optimization formulation. (See text for additional explanations.)

4.2 Problem statement

Mathematically the optimization problem is stated as follows:

$$\begin{aligned} \min_{\overline{\Delta x}, \overline{\Delta Q}, y_t^{(a)}} C_{SC} \sum_{t=1}^T \sum_{\{i,j\} \in \mathcal{E}} \overline{\Delta x}_{ij}^t + C_{SVC} \sum_{t=1}^T \sum_{i \in \mathcal{V}_t} \overline{\Delta Q}_i^t \\ + 8760 N_{years} \sum_{t=1}^T \sum_{a=1..M} Pr_{t,a} * C_{t,a}(P^{(t,a)}) \end{aligned} \quad (4.2.1)$$

subject to:

$$y^{(t,a)} = (x, V, \theta, P, Q)^{(t,a)} \quad \forall a, \forall t \quad (4.2.2)$$

$$\overline{\Delta x}_{total}^t = \sum_{h=1}^t \overline{\Delta x}^h \quad \forall t \quad (4.2.3)$$

$$\overline{\Delta Q}_{total}^t = \sum_{h=1}^t \overline{\Delta Q}^h \quad \forall t \quad (4.2.4)$$

$$\overline{\Delta x}^t \geq 0 \quad \forall t \quad (4.2.5)$$

$$\overline{\Delta Q}^t \geq 0 \quad \forall t \quad (4.2.6)$$

$$x^{(t,a)} = x_0^{(t,a)} + \Delta x^{(t,a)} \quad \forall a, \forall t \quad (4.2.7)$$

$$P_G^{(t,a)} = P_{D_0}^{(t,a)} + P^{(t,a)} \quad \forall a, \forall t \quad (4.2.8)$$

$$Q_G^{(t,a)} = Q_{D_0}^{(t,a)} + Q^{(t,a)} + \Delta Q^{(t,a)} \quad \forall a, \forall t \quad (4.2.9)$$

$$P_i^{(t,a)} = \sum_{j \sim i} \Re(S_{ij}^{(t,a)}) \quad \forall i, a, t \quad (4.2.10)$$

$$Q_i^{(t,a)} = \sum_{j \sim i} \Im(S_{ij}^{(t,a)}) \quad \forall i, a, t \quad (4.2.11)$$

$$\underline{P}_G^{(t,a)} \leq P_G^{(t,a)} \leq \overline{P}_G^{(t,a)} \quad \forall a, \forall t \quad (4.2.12)$$

$$\underline{Q}_G^{(t,a)} \leq Q_G^{(t,a)} \leq \overline{Q}_G^{(t,a)} \quad \forall a, \forall t \quad (4.2.13)$$

$$-\overline{\Delta x}_{total}^t \leq \Delta x^{(t,a)} \leq \overline{\Delta x}_{total}^t \quad \forall a, \forall t \quad (4.2.14)$$

$$-\overline{\Delta Q}_{total}^t \leq \Delta Q^{(t,a)} \leq \overline{\Delta Q}_{total}^t \quad \forall a, \forall t \quad (4.2.15)$$

$$\underline{V}^{(t,a)} \leq V^{(t,a)} \leq \overline{V}^{(t,a)} \quad \forall a, \forall t \quad (4.2.16)$$

$$\begin{aligned} & [\Re(S)^{(t,a)}]^T [\Re(S)^{(t,a)}] + [\Im(S)^{(t,a)}]^T [\Im(S)^{(t,a)}] \\ & \leq (\bar{S}^{(t,a)})^2 \end{aligned} \quad \forall a, \forall t \quad (4.2.17)$$

$$C_{SC} \sum_{\{i,j\} \in \mathcal{E}} \bar{\Delta x}_{ij}^t + C_{SVC} \sum_{i \in \mathcal{V}_l} \bar{\Delta Q}_i^t \leq MaxB^t \quad \forall t \quad (4.2.18)$$

$$\bar{\Delta x}_{ij}^t \leq \bar{\Delta x}_{ij}^{t-max}; \bar{\Delta Q}_i^t \leq \bar{\Delta Q}_i^{t-max} \quad \forall t \quad (4.2.19)$$

where $a = 1, \dots, M$ labels the scenarios; upper index t labels the time intervals, $t = 1, \dots, T$; \mathcal{V} and \mathcal{E} denotes the set of nodes and the set of (undirected) edges, of the grid-graph, where a node can be of the load type, $i \in \mathcal{V}_l$, or of the generator type, $i \in \mathcal{V}_g$.

The objective function in (4.2.1) consists of three terms. The first two, sparsity promoting terms [70, 71], express the capital investment costs of the installation of the two types of FACTS devices (investment can be performed at each decision point t). The third term stands for the operational cost in which the summation is over all the scenarios for each time frame and over the time frames ($\forall a$ is a shortcut for, $\forall a = 1, \dots, N$) accounting for respective occurrence probability multiplied by the number of years (service period). Therefore, the optimization (4.2.1) is nothing but an operational aware planning.

Each scenario in (4.2.1) is stated in terms of the set of operational variables. Description of the optimization constraints in (4.2.1) is as follows. (4.2.3) and (4.2.4) represent total available capacity at the decision moment t . (4.2.5) and (4.2.6) ensures that the already installed capacities are inherited in the future time frames. (4.2.7) bounds actual line inductances, which are adjusted according to the operational value of the installed series compensation for each scenario, within their respective installed capacities (represented by (4.2.19)). (4.2.8) and (4.2.9) represent active and reactive power balances at each bus of the network. Components of the vectors P_G (Q_G) and P_{D_0} (Q_{D_0}) are assumed equal to zero at the buses containing, respectively, no generators or loads. (4.2.10) and (4.2.11) represent the net active ($P \in \mathbb{R}^{N_b}$) and reactive ($Q \in \mathbb{R}^{N_b}$) power injections at the system buses. The term ΔQ expresses shunt compensation by SVC adjusted to a scenario bounded by the respective installed capacities (represented by (4.2.15)). Active and reactive power generation limits are set by (4.2.12) and (4.2.13). Voltage and thermal line flow constraints are represented by (4.2.16) and (4.2.17). $S_{ij}^{(a)} = S_f^{(a)}$ and $S_{ij}^{(a)} = S_t^{(a)}$ stand, respectively, for the apparent power flows from i to j and to j from i along the line $\{i, j\}$. One also accounts for the budget constraint per time step, (4.2.18), and/or for the maximum built capacity constraint per time step, (4.2.19).

The main challenge in resolving the optimization is related to the nonlinearity of the Power Flow relations (4.2.10), (4.2.11) and also to the nonlinearity of the line thermal limits (4.2.17). Available nonlinear solvers, such as IPOPT, are not effective in resolving the nonlinearities for large systems efficiently. This has motivated us to develop a heuristic algorithm consisting of the sequential linearization of the nonlinear constraints discussed in the following section.

4.3 Solution algorithm

This section describes the algorithm which allows us to resolve efficiently (and in spite of its complexity) the optimization problem just stated. Our algorithm consists of the following steps:

1. Scenarios are generated for each time frame according to the methodology suggested and described in details in [80]. Briefly, one picks the base case, re-scale it for different time frame (taking into account the economic growth), and then introduce fluctuations around the re-scaled solutions to represent the forecasted load uncertainty. The fluctuations are chosen to be Gaussian with the standard deviation proportional to the mean.
2. Generation is initialized (for each load scenario) according to scheme explained in Section 3.3.3.
3. If some of the constraints (4.2.7)-(4.2.17) are violated the initial state of the system is outside of the feasible domain defined by them. The non-linear constraints (4.2.10), (4.2.11) and (4.2.17) are linearized around the current state. This allows to construct current linearized version of the non-linear optimization problem (4.2.1)-(4.2.17).
4. The resulting linearized problem is solved by QP (or LP, depends on generation cost functions) using one of the available algorithms of the CPLEX solver [78].
5. AC power flow (AC-PF) is solved to update the state obtained at the previous step. This step is needed to prepare a feasible solution for the next iteration.
6. Steps 2-5 are repeated till either no constraints remain violated or the target precision is reached or the maximum allowed number of iterations is reached.

It is important to emphasize that, by construction, the algorithm maintains a feasible physical states at each iteration of its main loop including linearization, solution of the current QP optimization and back projection to the non-linear PF equations (achieved through the AC PF step).

To speed up the QP/LP computations, one uses a cutting plane (constraint management) procedure. We split the whole set of constraints (4.2.17) into “active” and “inactive” sets, including the constraints which were overloaded and, respectively, not overloaded, at the current state (of the previous iteration) or at any of the preceding steps. Only active constraints are explicitly accounted for in the optimization, while the validity of the inactive constraints is verified post-factum, and the active/passive split is updated at every LP/QP step.

4.3.1 QP/LP implementation

Standard CPLEX solver is called at each QP/LP step which outputs operational variables for each scenario along with investment variables for each time frame, $\overline{\Delta x}^t$ and $\overline{\Delta Q}^t$.

4.3.2 AC-PF feasibility

The QP/LP step is followed by the AC-PF step, which is needed to maintain the AC PF feasibility destroyed by the linearization. Overall, a combination of the QP/LP and AC-PF steps allows to maintain the solution and resolve contingencies of the system simultaneously and gracefully.

4.4 Approach analysis

The AC PF and optimization algorithms are implemented in Julia/JuMP. (See [81] and reference therein.) QP/LP optimizations (called at internal steps of our algorithm) are resolved by CPLEX [78]. When possible, we utilize IPOPT [76], called from JuMP, to solve the optimization problem (in its original, nonlinear formulation). The (brute-force) IPOPT solution is computationally expensive, and it is used as ground truth (to validate our heuristic algorithm). The computational performance of the algorithms is analyzed on a Macbook Pro laptop (Core i7 3.3 GHz (2 Cores), 16 Gb of RAM). The QP/LP step is followed by the AC-PF step, which is needed to maintain the AC PF feasibility destroyed by the linearization. Overall, a combination of the QP/LP and AC-PF steps allows to maintain the solution and resolve contingencies of the system simultaneously and gracefully.

4.4.1 Algorithm validation

The algorithm is validated by comparison with the IPOPT solution. Since IPOPT is not able to resolve the 2376 bus-large Polish model (even with a single scenario) we perform the initial validation study on the 30 bus IEEE model. (Both the Polish model and the IEEE 30 bus model are available within the MathPower package [74].) Table 4.1 presents results of the (IPOPT vs our heuristics) comparison, where the planning horizon is taken to be 1 year, $T = 5$, and $M = 10$ for each time interval. Budget constraint per time interval is set to \$200,000.

IPOPT objective is $6.029377e6$. Main algorithm objective is $6.029505e6$. Our main algorithm gives upper bounds solutions of the objective function with the gap less than 0.1%. As the algorithm always discovers an exactly feasible solution (in comparison with relaxation approaches), it could be an upper bound or infeasibility (if not solved).

4.4.2 Scalability analysis

Our next step (after completion of the aforementioned validation study) was to perform a comparative analysis of the algorithms' (computational) scalability.

First, we fix the number of scenarios (10 per time interval) and study dependence on the number of time intervals. The results are shown in Fig. 4.2. Then, we consider one time interval and study dependence on the number of scenarios. These results are shown in Fig. 4.3. Both tests are still done on the 30 bus model with the quadratic generation cost (de-fault in the Mathpower package). In both

Table 4.1: Comparison of our heuristic algorithm against the (brute-force) IPOPT algorithm for the IEEE 30-bus model.

t. int.:	1	2	3	4	5
# sc.:	10	10	10	10	10
alpha:	1.02	1.04	1.06	1.08	1.15
dev.:	0.001	0.003	0.005	0.01	0.02
IPOPT					
SVC (bus 8), MVAR:	4.00006	7.99995	10.5666	10.5666	10.5666
SC (line 10), %:	0	0	1.661575	1.661618	1.661625
main					
SVC (bus 8), MVAR:	4.0	8.0	10.5241	10.5241	10.5241
SC (line 10), %:	0	0	2,321978	2,321978	2,321978

cases, we compare the performance of the brute-force IPOPT solver with performance of our main algorithm and of the main algorithm reinforced by the cutting plane.

Comparing the performance of the IPOPT in the two settings, one observes a drastic difference. In the case of Fig. 4.2 IPOPT shows a surprisingly good performance, outperforming in speed both of our algorithms. (We relate this good performance of the IPOPT to using the primal simplex option within the IPOPT.) However, the situation is reversed in the case of Fig. 4.3 where, moreover, the performance of the IPOPT degrades exponentially with the number of scenarios. Our main algorithm and the reinforced (by cutting plane) algorithm show similar scaling performance in both cases (with the reinforced algorithm performing slightly better). Notice that juxtaposing here our algorithms against each other has a sense because of the comparable number of constraints contributing to the two optimization settings.

Moving to the scaling analysis of the Polish model, one first of all notes that in this case, the IPOPT fails to converge. To illustrate the performance of our reinforced algorithm, we focus on analyzing

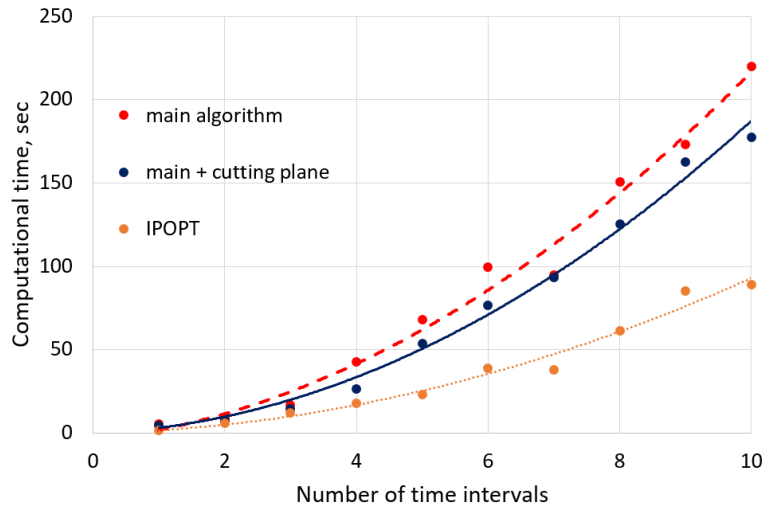


Figure 4.2: Computational time of IPOPT (orange), of our main algorithm (red) and of our algorithm sped up with the cutting plane (dark blue) are shown as functions of the number of time intervals, T , for the 30 bus model. In all the tests shown the number of scenarios (per time interval) was 10. Loading level is unity initially and it increases (imitating economic growth) by the factor 0.005 per time step. Scenarios are generated with the deviation factor 0.01. (See Section 3.3 for details.) Budget constraint (of \$110,000 per time step) is applied. Our algorithms (with and without cutting plane sped up) are limited to 20 iterations.

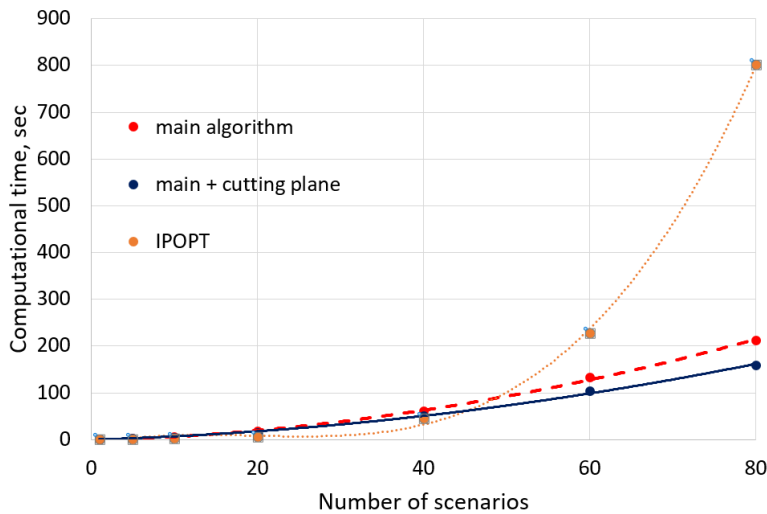


Figure 4.3: Computational time of IPOPT (orange), of our main algorithm (red) and of our algorithm sped up with the cutting plane (dark blue) are shown as functions of the number of samples in the case of a single time interval for the 30 bus model. Loading level is set to 1.05. Scenarios are generated with the deviation factor 0.01. (See Section 3.3 for details.) No budget constraints are applied. Our algorithms (with and without cutting plane sped up) are limited to 20 iterations.

dependence on the number of time intervals. The results of our scaling experiments with the Polish model are shown in Fig. 4.4, where the dashed line shows a (rather satisfactory) quadratic match (for the dependence of the overall computational time on the number of intervals.) In this case, we use the

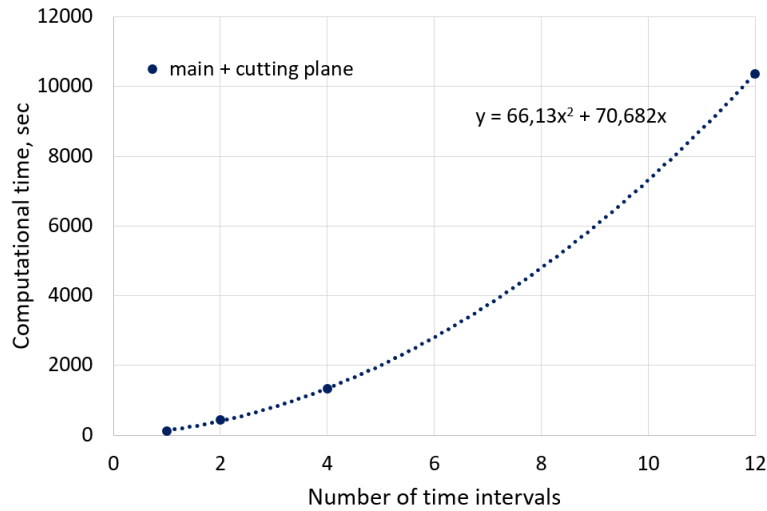


Figure 4.4: Computational time of our main algorithm reinforced by the cutting plane shown vs the number of time intervals for the 2736 bus-large Polish model in the case of a single scenario (per time interval). The optimization cost is linear (according to the base case documented in Mathpower) and thus LP is used at each iteration step of our reinforced algorithm solved in 15 iterations. In this case the loading level is set to unity in each time frame. Budget constraint of \$50,000 per time step is applied.

Primal Simplex CPLEX solver at each LP step of our algorithm. (This is LP and not QP, as in the 30 bus model, because the de-fault generation cost is linear in the Polish model of Mathpower.)

We conclude this section with a number of preliminary, and not yet fully conclusive but calling for further investigation, remarks. First of all, we have observed that developing an efficient computational strategy for our linearization algorithm/heuristics became the task that is rather sensitive to the functional form of the generation cost and the choice of variables. If the cost is linear (in generated power), introducing auxiliary (line flow) variables and using the Primal Simplex solver is the winning strategy. However, the same approach in the case of quadratic cost (QP step replacing LP step) leads to slower convergence for the Primal Simplex algorithm while the barrier algorithm fails to converge at all.

4.5 Gradual investments to resolve congestion

We apply our newly developed algorithm to study effect of the gradual investment, available only within the multi-time period framework, on the overall cost. We study the Polish model in the case of a single scenario with the optimization horizon of one year broken into 12 periods. The (single) loading scenario, chosen to be stressed but still feasible (it is only 3% away from the boundary of the AC OPF infeasibility - see Section 3.3 for details), stays the same over time. The congestion cost of the initial loading scenario (yet no investments in FACTS) is 17000 \$/hour. The investment budget is limited to \$50,000 per (one month) time interval. The results of optimal investment generated by

our reinforced algorithm are illustrated in Figs. 4.5,4.6,4.7. We observe that only SC devices were installed at 5 lines, of which only two would be overloaded (if the line limits are, first, ignored while solving AC OPF and then checked for the overload). (Lines which are both overloaded, and thus contained in the active set of our cutting plane algorithm, and which are also selected for optimal SC installation are shown blue in Fig. 4.5. Lines that are shown green were not overloaded but chosen for SC installation. Lines that are shown red were overloaded but were not chosen for SC installation.)

We observe that the optimal installation is gradual. Moreover, all (constrained) available money is spent at each (time interval) decision. Fig. 4.6 shows how the congestion reduces with time, thus leading to a reduction of the operational cost (blue bars) as time progresses. The orange line marks the result of the AC OPF before investments start. Red line marks result for the (initial, i.e., before investments) AC OPF with the thermal limits ignored.

Fig. 4.7 shows that the distribution of investments over lines and time period is nontrivial, therefore utilizing the newly available SC-capacities with other operational degrees of freedom.

We also show in Fig. 4.6 and Fig. 4.7 the result of optimal investment when the entire year (time horizon) is considered as one time interval. We observe that in the latter case, the entire installation budget is used immediately such that the final solutions in case one and 12 intervals are the same and equal to the available budget. Notice, however, that making one investment upfront for the entire year, as opposed to breaking it into 12, periods is preferable because the overall (integrated over the year) cost of generation is reduced.

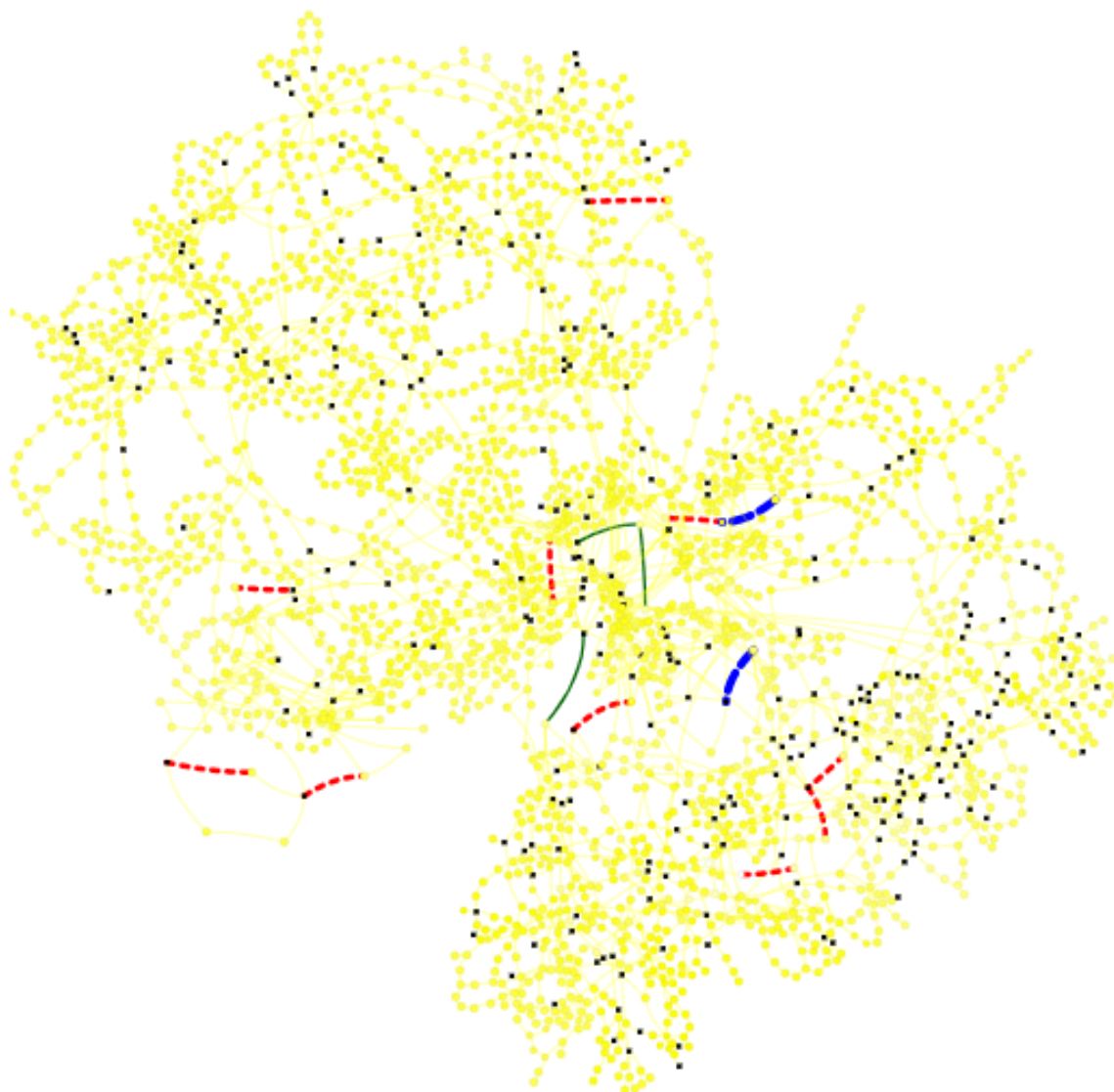


Figure 4.5: Snapshot of the final solution (after all the investments are made). Red marks lines from the active set of cutting plane. Thin green marks lines with installed SCs which are not overloaded (initially). Dashed blue marks lines which are both in the active set (overloaded) and chosen for SC installation.

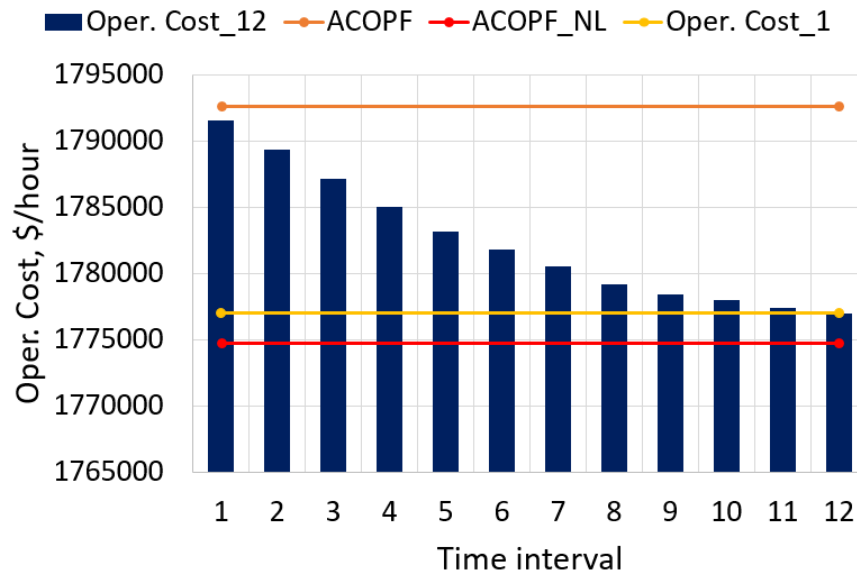


Figure 4.6: Dependence of the optimal cost on time (blue bars) provided by our reinforced algorithm for the Polish model in the case of a single scenario (the same for different time intervals) and the year-long horizon split in 12 periods (months). Orange line shows initial ACOPF cost (without investments). Red line shows ACOPF cost with thermal limits ignored. Yellow line corresponds to the optimal solution found in the case when the entire horizon is treated as a single time-interval.

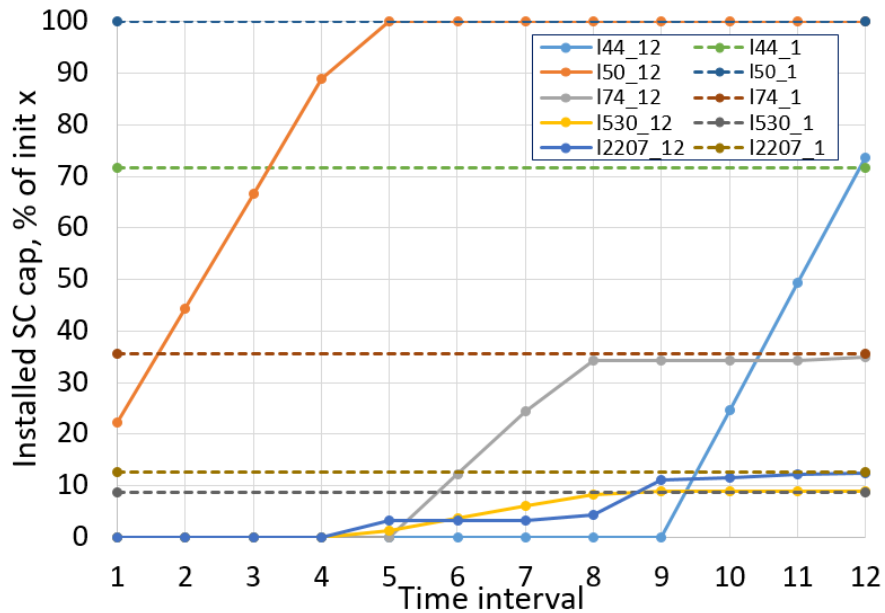


Figure 4.7: Installed capacity of the SC devices at corresponding lines shown in percentage of the initial line inductances. This is the case of a single scenario therefore operational values coincide with respective capacities. For example, inductance of line #50 is reduced to 0.

4.6 Summary

Overall, this chapter indicates a current level of the development of the methodology for operational and uncertainty planning with operational conditions represented by a set of deterministic scenarios/samples. Main technical achievement reported in this chapter is the development of an efficient heuristics for solving the non-linear, non-convex and multi-time-interval optimization. The developed algorithm builds a convergent sequence of convex optimizations with linear constraints. Each constraint is represented explicitly through exact analytical linearization of the original nonlinear constraints (e.g. representing power flows and apparent power line limits) over all the degrees of freedom (including FACTS corrections) around the current operational point for particular loading scenario over particular time interval. In order to represent uncertainty in the projected growth of the system (loads) a custom scenario sampling split over multiple time intervals is introduced. Practicality of our approach for resolving the problem of investment (new installation) planning is illustrated on the IEEE 30-bus model and 2736-bus Polish model. It is evident from the experimental results that the approach is capable of both improving the system's economy (reduce congestion price and generation cost) and also of resolving feasibility issues by introducing additional degrees of freedom (associated with the newly installed FACTS devices). It is time to move forward to the second part. Stochastic programming approach is working but it still has limitations on the uncertainty/fluctuations modeling and problem size. In the following part we explore probabilistic setting for operational planning problems in order to improve our methods of planning installations as well.

Part II

Planning with Probabilistic Representation of Uncertain Operational Conditions

The second part of the project is about the probabilistic approach of modeling power system operational conditions. In this case, variability and uncertainty of the power system behavior are represented directly through probability distributions which mathematically leads to so-called chance-constraint models. Inspired by the uncertainty aware operational planning methodology called Chance Constrained Optimal Power Flow (CC-OPF) which accounts for uncertain power sources well, we generalize it to longer time intervals and develop a way to account for operational variability and uncertainty in general (not at short-term only). First, we develop a Cloud-AC-OPF model for accounting for a set of close AC-OPFs simultaneously. Second, we generalize it and apply to practical RTS-GMLC case with multiple operational samples provided. This is still a work in progress, but we believe such tools will allow extending the applicability of operational and uncertainty aware planning for broad power system development analysis and will allow implementing important tools, e.g., account for security constraints together with long-term operations and uncertainty.

Chapter 5

Cloud-AC-OPF: Model Reduction Technique for Multi-Scenario Optimal Power Flow via Chance-Constrained Optimization

In this chapter, we focus on a problem that represents one piece of a bigger problem that we aim to address - long-term investment planning in transmission level of power system taking into account uncertainty of future operational conditions. The main difficulty in addressing this bigger problem is related to the significant variability and uncertainty of future operating conditions. One approach for taking this variability into account consists of modeling all possible operational conditions and incorporating these into the planning problem. This results in a two-stage optimization problem where the first stage optimizes over capacity/investment decisions, and the second stage optimizes the operational decisions (one set per scenario) subject to constraints given by the first stage [82, 83]. This can be computationally not tractable even using advanced solution approaches/algorithms. Overall, the size of operational samples set accounted together is limited. Another approach is to consider multiple scenarios as a multiple or single probabilistic cloud depending on its size. Here we introduce a methodology for a single cloud model. And it is not the only one application.

A variety of problems in power systems require consideration of a large number of operating conditions, corresponding to uncertain or time-varying renewable generation and load, different weather conditions, or different economic situations. Each operating condition is usually well represented by a combination of the AC power flow equations to model the power flow physics, decision variables to model controllable variables such as the generation dispatch, and a set of parameters to model a particular operating condition such as the realization of the load or renewable energy generation. Each operating condition hence gives rise to a unique instance of the AC Optimal Power Flow (AC-OPF) problem and considering all operating conditions together results in what we will refer to as the Multi-Scenario AC-OPF (MS-AC-OPF).

While significant efforts have been invested into designing and implementing solution methods

[84] and solvers [74, 85] for the AC-OPF problem, solving the MS-AC-OPF can be a challenging and time-consuming task. Even if the operating conditions, and thus decisions, are separable so that the optimization results in solving collection of single AC-OPF problems (one per-sample). For example, representing a year by 35,000 independent scenarios, each corresponding to a 15 min interval (with no uncertainty), will take about 10^5 sec, which is more than a day of computing (assuming that each problem is solved in 3 sec). An even more relevant case is the situation of a two-stage program, where we make decisions on the first stage (such as investment decisions) such that many operational situations contributing the MS-AC-OPF on the second stage are *simultaneously* feasible [86, 82, 83, 87]. In particular, as penetration of renewable technology grows, also resulting in an increase of uncertainty in generation and power flows, it becomes important to consider carefully how to identify the scenarios to represent and develop tractable methods to solve the resulting problems.

Instead of considering a large number of samples to represent time-varying loads and renewable generation, we aggregate the samples into so-called *scenario clouds*. For each cloud, we define a mean and covariance for the time-varying parameters. We then parametrize the generation dispatch as an affine function of the random parameters, which is a conservative (sub-optimal), but a feasible choice for generation control. We use this to formulate what we refer to as the Cloud-AC-OPF, which is a mathematically similar (but generalized and harder to solve) but conceptually different variant of a chance-constrained AC-OPF (CC-AC-OPF) [88, 89, 90, 91] with a prescribed robustness level. Hence, if we establish that the Cloud-AC-OPF is a good approximation of the MS-AC-OPF, we get algorithms that are capable of solving efficiently complex problems where the MS-AC-OPF represent the second (inner) stage, such as the decomposition methods developed to handle contingencies in the chance-constrained unit commitment in [92].

First, we propose the model reduction of the full MS-AC-OPF to the Cloud-AC-OPF. Second, we provide an efficient solution algorithm to solve the Cloud-AC-OPF. Third, we investigate how well the Cloud-AC-OPF approximates the true cost of the MS-AC-OPF. To keep our analysis clear and concise, we consider the case with limited variability corresponding to a single cloud and test the Cloud-AC-OPF performance against the MS-AC-OPF solved independently for each scenario. The analysis includes different parametrizations of the generation dispatch and different system loading levels.

5.1 Multi-scenario AC-OPF

We consider only the second (operational) stage of this future formulation. A typical formulation of this problem is the MS-AC-OPF, which can be stated (schematically) as follows:

$$\text{MS-AC-OPF}(x_u^{(a)}|\forall a) = \min_{x_c^{(a)}} \text{Cost}(x_c^{(a)}) \quad (5.1.1a)$$

$$\text{s.t. } \forall a : \quad \text{AC-PF}(x_c^{(a)}, x_u^{(a)}) = 0 \quad (5.1.1b)$$

$$\text{Constr}(x_c^{(a)}, x_u^{(a)}) \leq 0 \quad (5.1.1c)$$

Here, $x_c^{(a)}, x_u^{(a)}$ are controlled and, respectively, uncontrolled state variables. Values of the traditional generator dispatches are standard controlled variables. The output of renewable generators, as well as the consumption of many (aggregated) loads, are examples of the uncontrolled variables that are given input parameters to the problem. Some state variables, such as voltages and phases at all buses of the system (except for the slack bus), can be considered controlled but are uniquely determined by the AC-PF equations defined by (5.1.1b). In (5.1.1), a indexes a sample, $a = 1, \dots, M$; the objective (5.1.1a) accounts for the cost of the traditional generation; the inequalities in the conditions of (5.1.1c) express the constraints on line flows, voltages, etc, which are introduced to enforce safe operations.

In many cases of practical interest, the number of samples, M , can be too large to allow for sufficient accuracy (when approached in a brute-force fashion). A way to bypass this difficulty is in using the probabilistic methodology to describe the uncertainty set and also in representing system response to the uncertainty in a reduced, low-parametric way. The high-level logic of the reduction scheme employed in this thesis is illustrated in Fig.5.1.

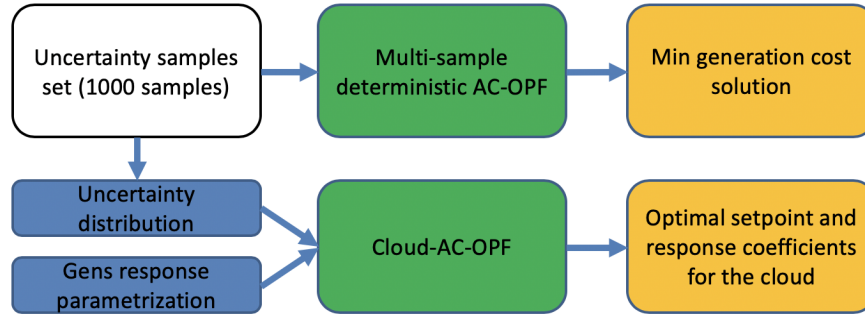


Figure 5.1: Computational complexity reduction scheme

5.2 Uncertainty modelling

The key idea of our model reduction approach is to represent a group of similar samples by a single cloud. For example, a cloud can be formed by summer off-peak or peak operational conditions on hourly basis. Time correlation between uncertain variables is not considered. Mathematically cloud can be defined using clustering of historical multidimensional state vectors on the given time basis.

Then each sample $x_u^{(a)}$ represents an uncontrolled configuration assigned to the cloud. Given all

samples in the cloud $x_u^{(a)}$ for $a = 1, \dots, M$, we can calculate the mean \bar{x}_u and the standard deviation σ_u of the cloud for each uncertain bus according to:

$$\bar{x}_u = 1/M \sum_{a=1..M} x_u^{(a)}, \quad \sigma_u = \sqrt{1/M \sum_{a=1..M} (x_u^{(a)} - \bar{x}_u)^2}$$

5.3 Reduced linear response modeling of the controllable resources

The main idea of the proposed complexity reduction approach is to parameterize the response of the controlled resources, x_c , which are primary generators, Pg , to the fluctuating component of the uncertainty characteristic, $w \doteq x_u - \bar{x}_u$. We will be using x_c to represent all controlled variables and Pg to represent a subset of control degrees of freedom associated with generator dispatch of active power. We consider the following (three) response policies/parametrizations, similar to the policies in [93]:

- a) Response with a fixed (predefined) participation factor α of the controlled generators

$$\begin{aligned} Pg_i(w) &= \overline{Pg}_i + \alpha_i \cdot \Omega & i = PV, \\ Pg_i(w) &= \overline{Pg}_i + \alpha_i \cdot \Omega + \delta p(w) & i = \theta V, \\ \Omega &= \sum_{i \in N} w_i, \quad \sum_{i \in N} \alpha_i = 1. \end{aligned}$$

Here PV and θV represent, respectively, a set of buses where active power+voltage, and phase+voltage are kept fixed (the latter applies to the system's slack bus).

- b) A version of case a) where the linear response vector, α , is not fixed, but is treated as an optimization variable.
- c) In the last, more general version, the linear response is parameterized by a matrix, α , such that each generator Pg responds separately to each component of w ,

$$\begin{aligned} Pg_i(w) &= \overline{Pg}_i + \sum_{j \in N} \alpha_{ij} \cdot \omega_j & i = PV \\ Pg_i(w) &= \overline{Pg}_i + \sum_{j \in N} \alpha_{ij} \cdot \omega_j + \delta p(w) & i = \theta V \\ \sum_{i \in N} \alpha_{ij} &= 1 & \forall j \in N \end{aligned}$$

Here, α is an optimization variable. The response is still an affine but allows for more general response patterns.

We refer to the three policies in the following uniform form:

$$Pg(w, \alpha) = Resp^k(w, \alpha) \quad k = a, b, c, \forall w$$

5.4 Cloud-AC-OPF

We are now in the position to formulate the reduced model:

$$\begin{aligned} \text{Cloud-AC-OPF}(\bar{x}_u, \sigma_u) &= \min_{\bar{x}_c, \alpha} \mathbb{E}_w[\text{Cost}(\bar{x}_c + Resp^k(w, \alpha))] \\ \text{s.t. AC-PF}(\bar{x}_c, \bar{x}_u) &= 0 \\ \text{Prob}_w [\text{Constr}(\bar{x}_c + \phi_c + Resp^k, \bar{x}_u + w) \geq 0] &\leq \varepsilon \end{aligned} \quad (5.4.1)$$

where the expectation and the probabilistic expressions are given with respect to the uncertain/uncontrolled variable w . The functions $\phi_c = \phi_c(x_c, \bar{x}_u, w)$ describe variations of the controlled variables (other than $Pg(w, \alpha)$) as a function of the realization of w .

It is important to emphasize that although the formulation (5.4.1) is similar to the CC-AC-OPF in, e.g., [88, 89], the relation between the Cloud-AC-OPF and the CC-AC-OPF is only formal. As explained above, Cloud-AC-OPF represents a reduced model, where the linear response coefficient(s) α in (5.4.1) can be understood as a (conservative) approximation of the generators ability to react to uncertainty. On the contrary, the corresponding linear coefficients in CC-AC-OPF, see e.g. [88, 89], represent the actual automatic generation response to short-term fluctuations.

In the following, we test how the three tractable reduction schemes, parameterized by $Resp^k(w, \alpha)$ with $k = a, b, c$ in Cloud-AC-OPF, approximate the MS-AC-OPF.

If the historical data is provided in the form of normal distributions with given properties, then Cloud-AC-OPF can be directly applied.

5.5 Cloud-AC-OPF: analytic reformulation

When the exogenously introduced cloud of samples, representing fluctuations of the uncontrolled sources, w , around the center of the cloud, \bar{x}_u , is sufficiently small (or just moderate in size relative to the mean - fluctuations are small), we can linearize the non-linear AC power flow equations and still expect a reasonably accurate representation of the response to the fluctuations ϕ_c . To obtain a tractable deterministic reformulation of the chance constraint in (5.4.1), we use a moment-based reformulation dependent only on the mean and standard deviation \bar{x}_u, σ_u . In fact, this reduction (tracking only two first moments) provides probabilistic guarantees for a much wider range of distributions with finite

mean and variance [94], and can more generally be understood as a robust optimization with feasibility guarantees for uncertainty realizations [95], which still requires fixing safety level parameters.

With the assumptions of linearized AC power flow equations and a moment-based chance constraint reformulation, we arrive at the following version of (5.4.1)

$$\begin{aligned} & \min_{\bar{x}_c, \alpha} Cost_1(\bar{x}_c) + \mathbb{E}_w [Cost_2(w, \alpha)] & (5.5.1) \\ & \text{s.t. AC-PF}(\bar{x}_c, \bar{x}_u) = 0 \\ & \text{Prob}_w [\text{Constr}(\bar{x}_c + G_w w + Resp^k(w, \alpha)) \geq 0] \leq \varepsilon \end{aligned}$$

where the adjustment of the controlled variables ϕ_c is defined using sensitivity matrix G_w , describing linear response of the controlled variables to variations in the exogenous/uncontrolled variables:

$$\phi_c = \left. \frac{\partial x_c}{\partial w} \right|_{\substack{x_c = \bar{x}_c \\ x_u = \bar{x}_u}} w \doteq G_w(\bar{x}_c, \bar{x}_u, \alpha)w.$$

If AC-PF system equations are feasible in the center of the cloud (at $w = 0$), then the sensitivity matrix and ϕ_c exists and differentiable. Here in (5.5.1) explicit expression for G_w , as a function of $\bar{x}_c, \bar{x}_u, \alpha$, is skipped due to space limitations; the objective function is split in two parts, correspondent to mean and fluctuations, respectively.

Following the approach of [88, 89, 90], we are able to evaluate the expectation and the probabilities in (5.5.1) analytically. Moreover, the analytic evaluation returns explicit dependencies on \bar{x}_c and α , therefore stating the Cloud-AC-OPF (5.5.1) as the following tractable deterministic optimization formulation:

$$\begin{aligned} & \min_{\bar{x}_c, \alpha} Cost_1(\bar{x}_c) + \mathbb{E}_w [Cost_2(w, \alpha)] & (5.5.2) \\ & \text{s.t. AC-PF}(\bar{x}_c, \bar{x}_u) = 0 \\ & \text{Constr}(\bar{x}_c, \bar{x}_u) \leq -\lambda(\bar{x}_c, \bar{x}_u, \alpha, \Sigma_w), \end{aligned}$$

where the dependence of the correction to the cost on α, \bar{x}_c and samples is detailed below. Uncertainty margins, $\lambda(\bar{x}_c, \bar{x}_u, \alpha, \Sigma_w)$, are computed for each type of variables (γ) and each type of bus/line (μ : PQ, PV, θV , line) as:

$$\begin{aligned} \lambda_{\gamma:\mu} &= 0, V:\theta V, V:PV, P:PQ, Q:PQ \\ \lambda_{P:PV/\theta V}^i &= \Phi^{-1}(1 - \epsilon_\gamma) \times \|(G_w^{\gamma:\mu} + \alpha_{(i,:)})\Sigma_w^{1/2}\|_2 \\ \lambda_{\gamma:\mu}^i &= \Phi^{-1}(1 - \epsilon_\gamma) \times \|(G_w^{\gamma:\mu})\Sigma_w^{1/2}\|_2, V:PQ, Q:PV/\theta V, F:line \end{aligned}$$

where Φ^{-1} stands for the inverse cumulative distribution function of the standard normal distribution.

Σ_w is the calculated covariance matrix for uncontrolled sources for the cloud. F is squared apparent power at from/to side of a line. The resulting deterministic optimization (5.5.2) over \bar{x}_c and α does not have any nice structure (e.g. it is not convex). The detailed information about the computation of uncertainty margins and sensitivity matrices is provided in Appendix.

5.6 Analytic averaging of objective function

In the case of quadratic dependence of the objective on the generation dispatch, the fluctuating part of the cost becomes

$$\begin{aligned} i-PV:\mathbb{E}_w [Cost_2^i(w, \alpha)] &= a \sum_{j=1..N} \alpha_{ij}^2 v(w_j) \\ i-\theta V:\mathbb{E}_w [Cost_2^i(w, \alpha)] &= a \sum_{j=1..N} (\alpha_{ij} + (G_w^{P:\theta V})_{1j})^2 v(w_j) \end{aligned}$$

where formal expectation over ω is stated in terms of variances of the uncertainty, $v(w_j)$, at the j -th uncertainty site, evaluated directly from (available) samples; and $G_w^{P:\theta V}$ is 1-row submatrix of G_w corresponding to sensitivity of active power at slack bus to w .

5.7 Implementation and solution approach

We solve (5.5.2) via the iterative algorithm implemented in Julia using JUMP [96], thus taking advantage of the modularity and automatic differentiation features of the software. The idea of the algorithm is to specify (current) $x \doteq (\bar{x}_c, \alpha)$ at each iteration step. Then the sensitivity matrices G_w are evaluated at \bar{x}_c with analytical dependence only on α then provided as an input to the optimization model. This dependence also applies to the uncertainty margins, λ .

Schematic description of the algorithm is as follows:

1. Initialization. Set uncertainty margins $\lambda_P^0 = \lambda_Q^0 = \lambda_V^0 = \lambda_F^0 = 0$. Solve classical AC-OPF, and set its argmin as \bar{x}_c^0 . Set iteration number to $k = 1$.
2. Evaluate starting point for optimization variables. α^{start} - defined as the equal participation of each generator evaluated for each component of the uncertainty vector. $\lambda_P^{start}, \lambda_Q^{start}, \lambda_V^{start}, \lambda_F^{start}$ are computed using sensitivity matrices at \bar{x}_c^{k-1} and α^{start} . \bar{x}_c^{start} and auxiliary variables - take $k - 1$ solution.
3. Define non-linear optimization model (5.5.2). Model variables are $\bar{x}_c = \bar{V}_c, \bar{\theta}_c, \bar{P}g_c, \bar{Q}g_c; \alpha; \lambda_P^{var}; \lambda_Q^{var}; \lambda_V^{var};$ and $\bar{p}fr_c; \bar{p}to_c; \bar{q}fr_c; \bar{q}to_c$ - the auxiliary variables. Define constraints according to (5.5.2). Effectively model is similar to AC-OPF but with corrected by the uncertainty margins constraints, additional variables and modified objective - averaged over the cloud.

4. Solve the model. Update $k = k + 1$. Go to step 2.

5.8 The case study analysis

We test our approach on the IEEE 30 bus system available within the Matpower package [74]. We set the base configuration, \bar{x}_u , of the uncontrolled degrees of freedom and draw samples for active power consumption/production at the uncertain node from a Gaussian distribution with prescribed covariances (standard deviations) around the base case. Components of the vector of standard deviations is defined according to a prescribed ratio of the base case loading (for example, 5% of initial active demand). Reactive power is set constant (base case). Uncertainty set size of 1000 samples was defined experimentally to provide stable MS-AC-OPF cost for different sample sets at given base case and level of uncertainty. We solve the MS-AC-OPF directly for all the samples, therefore setting up ground-truth standards for the following comparisons. Then we solve a different version of the Cloud-AC-OPF model and compare the solutions with the ground truth set by the MS-AC-OPF solution.

According to the introduced response model, voltage set-points on generators are fixed for different samples. Fixed reactive power does not reduce the generality of the approach; if Q is uncertain, it would be taken into account by similar sensitivity/uncertainty margin means.

5.8.1 MS-AC-OPF and three flavours of Cloud-AC-OPF

We experiment with the three flavours of the Cloud-AC-OPF model described in Section 5.3. In the following, we refer to the MS-AC-OPF with 1000 samples as MS-AC-OPF, and models (a-c) introduced in Section 5.3 as Cloud-AC-OPF-k (k=a,b,c).

5.8.2 Scalability analysis

Computations are done on a 3.3 GHz core i7 laptop CPU. The results are summarized in the Table 5.1:

Table 5.1: Computational time comparison for the introduced models

Model	Description	# Iterations	Time (sec)
MS-AC-OPF	1000 samples	1	70
Cloud-AC-OPF-a	given α	5	2.8
Cloud-AC-OPF-b	α -vector	5	41.6
Cloud-AC-OPF-c	α -matrix	5	41.4

All the Cloud-AC-OPF cases are solved faster than the bare MS-AC-OPF. We expect to see this acceleration effect be even more pronounced in the case of the aforementioned two-stage planning

models. Also, MS-AC-OPF computational time grows linearly with a number of samples, while Cloud-AC-OPF time depends only on the system size.

5.9 Reduction analysis

In this section, we discuss the quality of the Cloud-AC-OPF solutions as they are compared to the benchmark provided by the MS-AC-OPF. We choose the optimal objective function and the optimal active generation dispatch as benchmarks for comparison.

The following two operational regimes are considered:

1. Low loading - in this case all line, voltage and power injection conditions are safely within the feasible operational limits (not saturated).
2. High loading - this is a heavily congested case with a number of constraints being either saturated or close to be saturated.

5.9.1 Comparison by the value of optimal objective

Consider, first, the low-loading regime - the base case loading is set to 0.8, and the probability of a constraint violation is set to 1% (for all the constraints). The results are shown in Fig. 5.2. In this case, even the least accurate Cloud-AC-OPF-a shows a satisfactory performance. We observe a good approximation quality up to 10% of the uncertainty level when assessed by the objective function value.

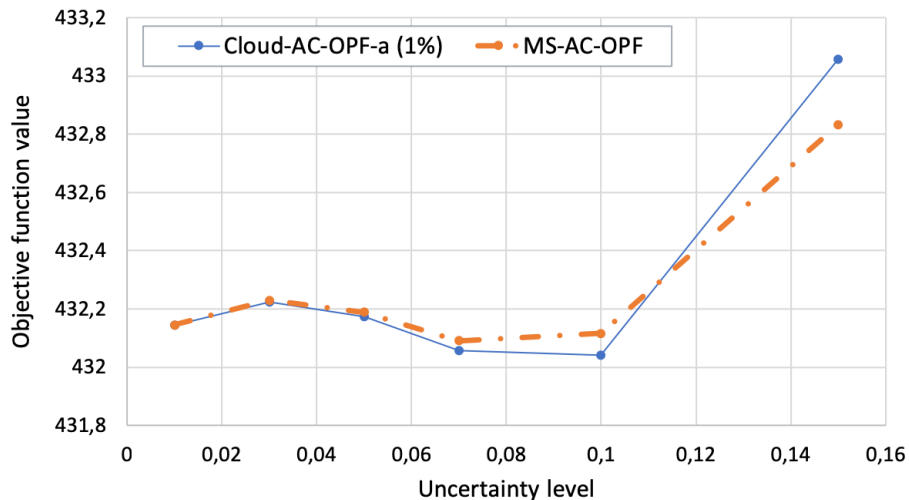


Figure 5.2: Obj. function comparison for low loading regime (MS-AC-OPF vs Cloud-AC-OPF-a). Probability of the chance constraints violation is $\epsilon = 1\%$

In the high loading regime, when the base case loading is set to 0.95 (the loading level 1.03 would be already AC-OPF infeasible), a gap in performance between the MS-AC-OPF and the Cloud-AC-

OPF appears. The gap increases with the uncertainty (variance of fluctuations). Fig. 5.3 illustrates this effect for the Cloud-AC-PF-a evaluated with the probability of constraints violation from 1% to 5%.

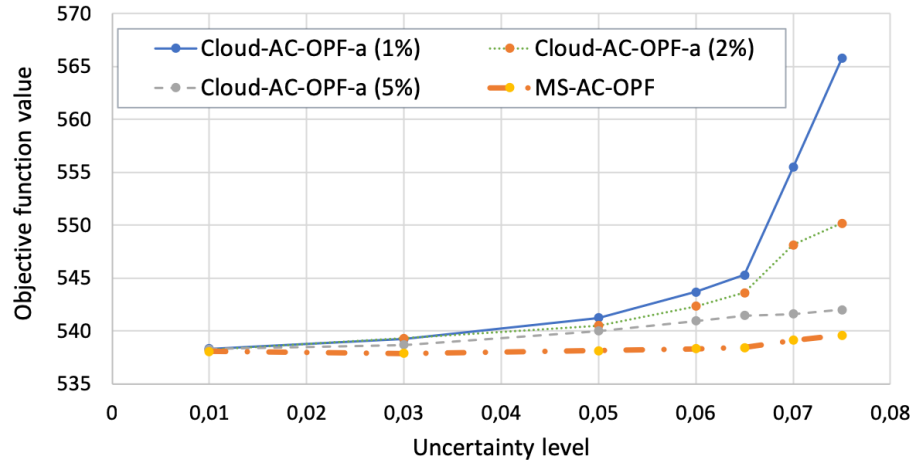


Figure 5.3: Obj. function comparison in the regime of high load (MS-AC-OPF vs Cloud-AC-OPF-a) shown as a function of the uncertainty level and ϵ .

It is also observed that the Cloud-AC-OPF models highly sensitive to variations of ϵ (probability of the chance constraints violation) in the high loading and high uncertainty regimes. This would be important when we will work with historical data. Uncertainty distribution is not necessary Gaussian in that case. It would be approximated by Gaussian with computed mean and variance. And ϵ should be carefully chosen (e.g., by doing out-of-sample analysis of the solution).

Fig. 5.4 compares the objective function value of the Cloud-AC-OPF-k with the MS-AC-OPF, depending on the generators' response parametrization model. The probability of constraints violations is set to 1%. It can be observed that Cloud-AC-OPF-b/c demonstrate better performance than the simplest model and that the most sophisticated matrix version Cloud-AC-OPF-c is advantageous in the high loading and high uncertainty regimes.

Configurational (generation dispatch) comparison is performed in the following subsection.

5.9.2 Comparison of the Cloud-AC-OPF and MS-AC-OPF optimal dispatches

Comparison of optimal dispatches in the original MS-AC-OPF model and the reduced Cloud-AC-OPF model constitutes a much richer test (than based on the optimal cost), thus setting better criteria for the assessment of model reduction. The configuration (optimal dispatches based) analysis of the Cloud-AC-OPF shows significant dependence on the loading regime and also strong sensitivity to the selection of the type of response in the model (a-c).

Fig. 5.5 shows details of the comparison of Cloud-AC-OPF-k ($k = a - c$) with the MS-AC-OPF in the low-loading regime.

The figure visualizes the response of a representative pair of generators. Output from MS-AC-OPF model is shown in terms of samples (blue dots). Affine response of different versions of the Cloud-AC-

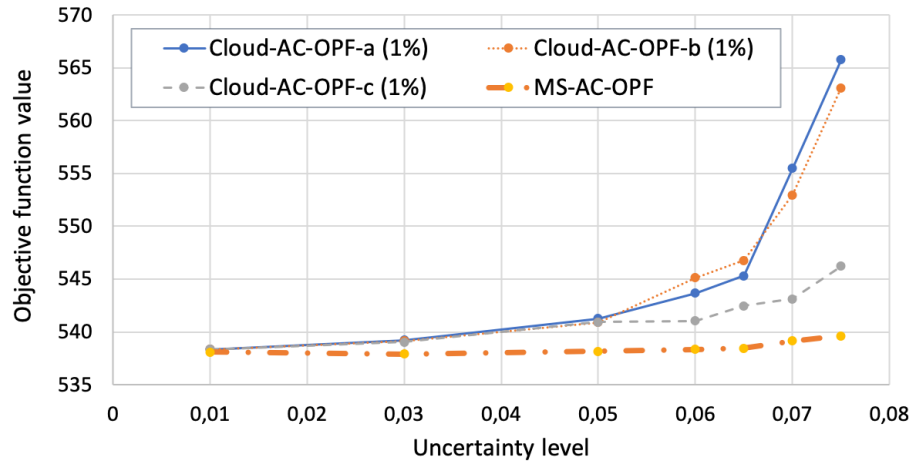


Figure 5.4: Obj. function comparison at high loading regime for different versions of the Cloud-AC-OPF-k. $\epsilon = 1\%$ for each model.

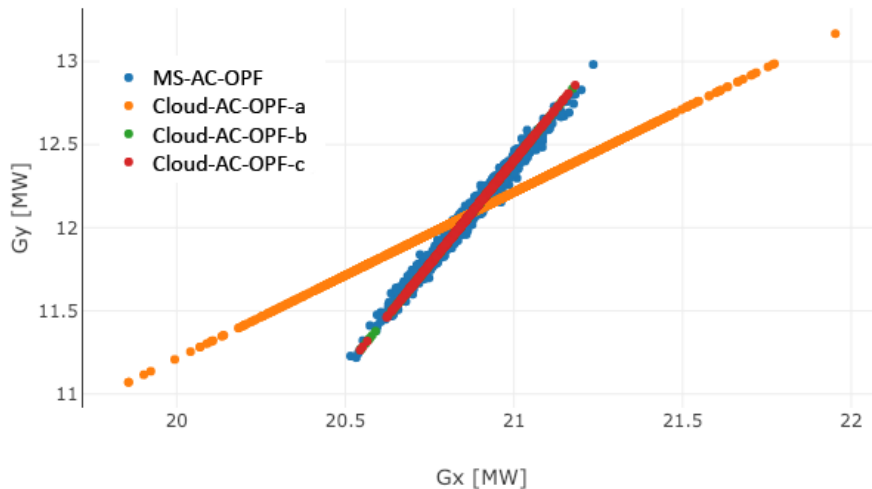


Figure 5.5: Illustration of the Cloud-AC-OPF solution quality in terms of the generation response to perturbations in the regime of low loading.

OPF-k is shown for the comparison. In Cloud-AC-OPF-a (orange) all generators participate equally, which is not relevant to the actual shape of the MS-AC-OPF state space. In Cloud-AC-OPF-b/c (green and purple) the response is optimized. Original state space is close to ($k = b$) model in the low loading regime (gens effectively respond to total power mismatch). Because of that, both Cloud-AC-OPF-b/c demonstrate good performance and matrix response model basically finds the same as vector response model.

In the regime of a high load, illustrated in Fig. 5.6, some constraints become active. This results in the fact that MS-AC-OPF state space of optimal configurations/dispatches is more complicated. We observe that in this case, the more constrained models Cloud-AC-OPF-a/b (green and orange) fail to represent MC-AC-OPF. However, one also observes that the solution quality of the more advanced

model reduction scheme, represented by Cloud-AC-OPF-c (purple), is still satisfactory. (Here, in the case of Cloud-AC-OPF-c, the probability of constraints violation over lines is increased to 10%, while the probability of all other violations is kept to the 5%).

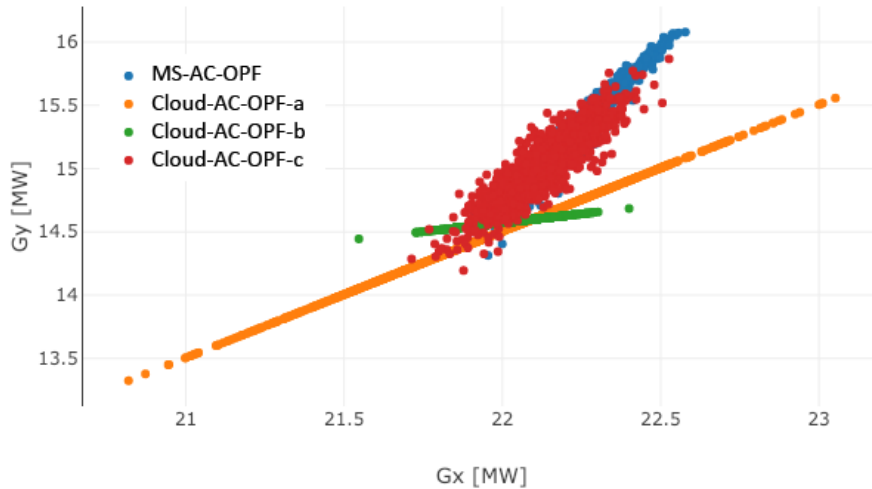


Figure 5.6: Illustration of the Cloud-AC-OPF solution quality in terms of the generation response to perturbations in the regime of high loading.

5.10 Summary

The complexity reduction approach is developed in this chapter for a set of close in the state space operational scenarios ("cloud"). The generalized version of CC-AC-OPF is used for that. It is demonstrated on the artificial example of 30-bus model and requires further analysis on a practical set of operational conditions but demonstrates good potential at the aggregated representation of multiple samples. It can be applied both in MS-AC-OPF problems and potentially at two-stage optimization problems as well.

Chapter 6

Multi-Cluster-AC-OPF: Model Reduction for Multi-Stage, Multi-Scenario Optimal Power Flows

This chapter applies an approach proposed in the previous chapter to RTS-GMLC 73 bus case, where time series of 105408 samples of operational conditions is provided, representing a year of operations sampled every 5 mins aiming to validate the potential for multi-stage, multi-scenario model reduction and then if it is successful, make next step to long-term, large-scale planning applications.

A variety of practical planning and operational problems in power systems require parallel processing of a large number of operating conditions, each corresponding to uncertain and varying with time configuration of renewable generation and load dependent on weather forecasts and different economic scenarios. Models representing these problems are usually stated as a family of single stage (covering short-term operational planning) or multi-stage (in the case of mid-to long-term operational and investment planning) optimizations accounting for as many conditions as possible *simultaneously* [86, 87, 83]. Each operating condition, representing exogenous parameters such as renewable generation output and load distribution, requires solving *unique* Alternating Current (AC) Optimal Power Flow (OPF) optimization over the model control variables (such as generation dispatch) conditioned to AC Power Flow (PF) equations, representing the power flow physics. Thus, we use the term *Multi-Stage, Multi-Scenario AC-OPFs* (MS-MS-AC-OPFs) to denote family of *parallel* optimizations accounting in combination for all the scenarios and all the time intervals explicitly. Even though significant progress has been made towards designing solution methods [84], and solvers [74, 85] for the basic AC-OPF problem, solving the MS-MS-AC-OPFs remains to be prohibitively expensive when the number of scenarios is large and extracting a sufficiently small subset of scenarios is problematic. We have suggested in [97] to resolve an oversimplified version of the problem, when all scenarios are relatively close to each other, by a probabilistic cloud of the size and location reconstructed from the available scenarios/samples.

In this chapter, we generalize the approach and build a multi-cluster one capable of efficiently representing a realistic setting with a larger and more diverse set of many clusters and multi-stage scenarios. In this novel construction, each cluster is represented by a probabilistic cloud parameterized in terms of its mean and covariance, which are learned from a large set of original scenarios. We parameterize the generation dispatch inside each cloud as an affine function of random parameters, which provides a conservative (i.e., possibly sub-optimal), but a feasible choice for generation control. The resulting Multi-Cluster-AC-OPF formulation is mathematically similar (considering each cluster), but conceptually different from the well-studied Chance-Constrained AC-OPF (CC-AC-OPF) formulation [88, 89, 90]. We investigate different approaches to clustering the data – i.e., different ways of splitting the set of original samples into clusters, which are then each modeled by its own cloud. We also explore (a) how many clusters are needed to represent the original data set (of multi-stage scenarios); (b) which cluster parametrization policy is the best in terms of the tradeoff between accuracy and performance.

6.1 Requirement for the model reduction

It is highly desirable to address the long-term investment planning in the power system transmission to take into account uncertainty of future operational conditions. However, the main difficulty in addressing such investment problems is related to variability and uncertainty of future operating conditions. A brute force approach for taking this variability into account consists in accounting for all possible operational conditions. This results in a two-stage optimization formulation where at the first stage one optimizes over capacity/investment decisions, and at the second stage one optimizes over the operational decisions (one set per scenario, per time interval) subject to constraints found at the first stage [70, 71, 82, 83]. There are two related problems with this approach: (1) the operational stage is extremely heavy, and (2) the investment planning stage lack feedback from the operational stage. An alternative would consist in reducing the complexity of the operational stage calculations, which would then allow for incorporating the reduced model into the long-term planning problem.

In this chapter, we take the alternative route but focus primarily on developing a model reduction approach for the operational stage of the bigger problem – operations aware investment planning. In other words, we consider here a setting where the investment variables are assumed fixed.

6.1.1 Multi-Stage Multi-Scenario AC-OPF

Let us first discuss the brute force approach, which consists in accounting for multiple operational scenarios, representing uncertainty and variability of conditions directly. A typical structure of this MS-MS-AC-OPF setting is schematically illustrated in the Fig. 6.1. The planning horizon is represented by T time intervals while each time interval (t) is operationally represented by $M(t)$ scenarios/conditions weighted by their probabilities. These scenarios are expected to cover operational

space for the given time interval, thus accounting for possible uncertainty and variability over the time horizon of interest (for the investment planning).

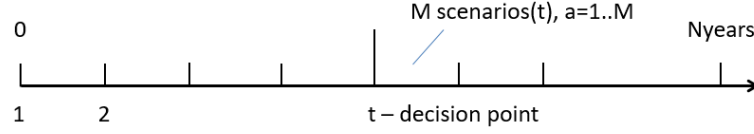


Figure 6.1: Illustration of the relation between number of scenarios, $M(t)$ (each associated with the time interval, t) and the number of time intervals, T . $N = \sum_{t=1}^T M(t)$ is the total number of constraints imposed (per line or per node) within the investment planning framework.

Formally (and also schematically), the MS-MS-AC-OPF problem can be stated as follows:

$$\text{MS-MS-AC-OPF}(x_u^{(t,a)} | \forall t, \forall a) = \min_{x_c^{(t,a)}} \sum_{t=1}^T \sum_{a=1}^{M(t)} C(x_c^{(t,a)}) \quad (6.1.1a)$$

$$\text{s.t. } \forall t, \forall a : \text{AC-PF}(x_c^{(t,a)}, x_u^{(t,a)}) = 0 \quad (6.1.1b)$$

$$\text{Constr}(x_c^{(t,a)}, x_u^{(t,a)}) \leq 0 \quad (6.1.1c)$$

Here, $x_c^{(t,a)}$, $x_u^{(t,a)}$ are controlled and, respectively, uncontrolled state variables. Values of the traditional generator dispatches are standard controlled variables. The output of renewable generators, as well as the consumption of many (aggregated) loads, are examples of the uncontrolled variables, which provide exogenous inputs. Some state variables, such as voltages and phases at all buses of the system (except for the slack bus), can be considered controlled but are uniquely determined by the AC-PF equations defined in (6.1.1b). Here, in (6.1.1), a indexes a sample, $a = 1, \dots, M(t)$, while $t = 1, \dots, T$ is time interval; the objective (6.1.1a) accounts for the cost of the traditional generation over the planning horizon; the inequalities in the conditions of (6.1.1c) express the constraints on line flows, voltages, etc, which are introduced to enforce safe operations. In the long-term investment planning all $N = \sum_{t=1}^T M(t)$ samples are included together to resolve the operational second-stage of the model constrained by the first-stage (investment planning) variables.

Let us clarify operational correlation of the considered samples. Each operational state inside time interval is considered to be individual in terms of its operational settings (basically each OPF is independent) but limited by available capacities of equipment at current time interval. It means that ramp activities are not accounted and not quite relevant to mid-term and long-term analysis and planning. In terms of spatial correlation – spatial effects accounted for each sample by transmission system model. And grouping of samples is available for only samples from a single time interval where the grid structure/equipment capacities are virtually fixed.

6.1.2 Concept of the model reduction

In many cases of practical interest, the number of samples, N , can be too large to allow for sufficient accuracy (when approached in a brute-force fashion). The stochastic, chance-constrained, methodology is a way to circumvent this significant computational obstacle. We model multiple scenarios and also system response to these scenarios in a reduced way. It consists in representing scenarios in a low-parametric, probabilistic form. This allows us to reduce the dimensionality of the problem dramatically while keeping the resulting dispatch sufficiently close to the truly controllable generation dispatches as if these were down for each operational sample. It is assumed (but not discussed in this Chapter) that this dramatic reduction of the multi-stage, multi-scenario operational model shall allow resolving the long-term investment planning problem in an operational aware way (with an advanced, nonlinear and covering the most part of the state space, operational stage). A high-level description of our model reduction scheme is illustrated in Fig.6.2.

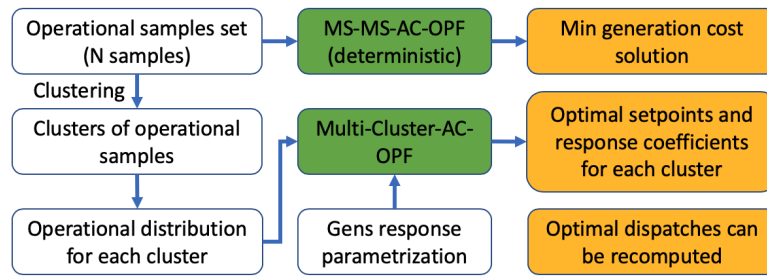


Figure 6.2: Schematic illustration of the complexity reduction offered by the Multi-Cluster-AC-OPF.

6.2 Multi-Cluster-AC-OPF

Basic principles of our Multi-Cluster-AC-OPF scheme are illustrated in the Fig. 6.3. Key elements of the approach we have started to develop in [97], and which is also detailed below, concern clustering the operational conditions, Section 6.2.1, modeling clusters, Section 6.2.2, reduced linear modeling of the controllable resources response, Section 6.2.3, and finally putting it all together in the Multi-Cluster-AC-OPF formulation in Sections 6.2.4,6.2.5.

One important point extracted from our experiments with the scheme, discussed in details down the road in Section 6.3, and which is worth to mention upfront, is that the operational points which are quite distant from each other in time domain (in terms of when they occur) may be placed by clustering algorithms quite close in the respective phase space (see Fig. 6.3). If there are linking constraints between the time intervals (e.g., incremental capacity of generation) clusters shall be determined individually for each time interval.

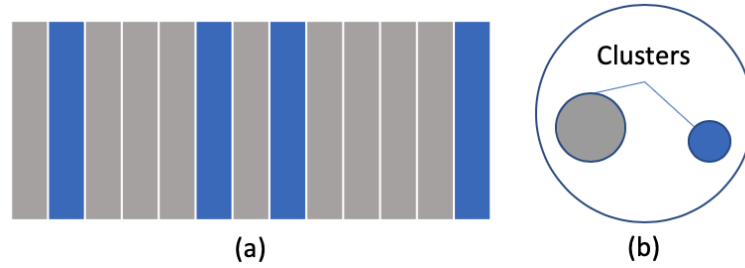


Figure 6.3: Schematic illustration of the relation between time series samples (a) and their phase-space clustering (b). We emphasize here (on the illustrative example of two clusters) that neighboring temporal samples are not necessarily close to each other in the phase-space metric used to identify clusters.

6.2.1 Clustering of the operational conditions

Two clustering approaches are explored. First, we consider time-domain clustering by the time of the day. For example, a cluster can be formed based on considerations of the summer off-peak or peak operational conditions on an hourly basis. Time correlation between uncertain variables is not considered in this case. Second, we consider mathematical clustering selected by an abstract state-of-the-art clustering algorithm. Our enabling example here is the K-means clustering of the vectors representing operational points in the state space. The result of K-means clustering is random, depends on the seed. The point of K-means clustering in this setting is to find “close” operational conditions much better than non-optimization approaches. And then analysis is performed on a given set. Basically, K-means can be performed ones, and the assignment can be stored for further computations. Analysis of clustering influence and various approaches for that is not considered to be the first important step.

We assume, in what follows, that the clustering is done as a pre-processing step resulting in discovery of K clusters and operational conditions assignments. Then, the next step consists in cluster modeling, that is finding a reduced way (in the sense of involving much fewer parameters than number of samples) to represent each of the already identified K clusters.

6.2.2 Cluster modelling

The key idea of our model reduction approach is in representing a cluster of similar samples by a single probabilistic cloud. Let $x_u^{(k,j)}$ be samples of uncontrolled operational conditions assigned to the cluster k and $j = 1..M_k$ (number of samples assigned to the cluster k). Then each sample $x_u^{(k,j)}$ represents an uncontrolled configuration assigned to the cluster. The mean \bar{x}_u^k and the standard deviation σ_u^k of the cluster for each uncontrolled bus can be computed according to:

$$\bar{x}_u^k = 1/M_k \sum_{j=1..M_k} x_u^{(k,j)}$$

$$\sigma_u^k = \sqrt{1/M_k \sum_{j=1..M_k} (x_u^{(k,j)} - \bar{x}_u^k)^2}$$

6.2.3 Reduced linear response modeling of the controllable resources

The main idea of the proposed complexity reduction approach is to parameterize the response of the controlled resources, x_c^k inside the cluster k , which are primary generators, Pg , to the fluctuating component of the uncertainty characteristic corresponding to shift from the mean of the cluster, $w \doteq x_u^k - \bar{x}_u^k$. We will be using x_c^k to represent all controlled variables and Pg to represent a subset of control degrees of freedom associated with generator dispatch of active power. We consider the following (three) response policies/parametrizations, similar to the policies in [93]:

- a) Response with a fixed (predefined) participation factor α of the controlled generators

$$Pg_i(w) = \overline{Pg}_i + \alpha_i \cdot \Omega \quad i = PV,$$

$$Pg_i(w) = \overline{Pg}_i + \alpha_i \cdot \Omega + \delta p(w) \quad i = \theta V,$$

$$\Omega = \sum_{i \in N} w_i, \quad \sum_{i \in N} \alpha_i = 1.$$

Here PV and θV represent, respectively, a set of buses where active power+voltage, and phase+voltage are kept fixed (the latter applies to the system's slack bus).

- b) A version of case a) where the linear response vector, α , is not fixed but is treated as an optimization variable.
- c) In the last, more general version, the linear response is parameterized by a matrix, α , such that each generator Pg responds separately to each component of w ,

$$Pg_i(w) = \overline{Pg}_i + \sum_{j \in N} \alpha_{ij} \cdot \omega_j \quad i = PV$$

$$Pg_i(w) = \overline{Pg}_i + \sum_{j \in N} \alpha_{ij} \cdot \omega_j + \delta p(w) \quad i = \theta V$$

$$\sum_{i \in N} \alpha_{ij} = 1 \quad \forall j \in N$$

Here, α is an optimization variable. The response is still an affine, but allows for more general response patterns.

We refer to the three policies in the following uniform form:

$$Pg(w, \alpha) = Resp^p(w, \alpha) \quad p = a, b, c, \forall w$$

Each of the parameterized policies is applied individually to each of the clusters $k = 1..M_k$.

6.2.4 Multi-Cluster-AC-OPF formulation

We are now in a position to formulate the reduced model. When clustering is performed, cluster model is defined, and parametrization of the response to the shift from the mean of the cluster is chosen, our next task becomes to find optimal setpoints of the controlled resources \bar{x}_c^k and the response coefficients α^k for each cluster ($k = 1..K$) accounting for the considered response policy $p = a, b, c$. When the task is accomplished, it allows us to recompute the state of each sample $j = 1..M_k$ assigned to the cluster k corresponding to the initial MS-MS-AC-OPF problem. Mathematically Multi-Cluster-AC-OPF (MC-AC-OPF) is stated in the following way:

$$\begin{aligned} & \mathbf{Multi-Cluster-AC-OPF}(\bar{x}_u^k, \sigma_u^k, k = 1..K) := \\ & \min_{\bar{x}_c^k, \alpha^k, k=1..K} \sum_{k=1}^K \mathbb{E}_w [Cost^k(\bar{x}_c^k + Resp^p(w, \alpha^k))] \\ & \text{s.t. } \forall k = 1..K : \mathbf{AC-PF}(\bar{x}_c^k, \bar{x}_u^k) = 0 \\ & \text{Prob}_w [\mathbf{Constr}(\bar{x}_c^k + \phi_c^k + Resp^p, \bar{x}_u^k + w) \geq 0] \leq \varepsilon \end{aligned} \tag{6.2.1}$$

where the expectation and the probabilistic expressions are given with respect to the uncertain/uncontrolled variable w for each of the clusters k . The functions $\phi_c^k = \phi_c(x_c^k, \bar{x}_u^k, w)$ describe variations of the controlled variables (other than $Pg(w, \alpha^k)$) as a function of the realization of w for each cluster k .

It is important to emphasize that although the formulation (6.2.1) is similar to the CC-AC-OPF (for each cluster) in, e.g., [88, 89], the relation between the MC-AC-OPF and the CC-AC-OPF is only formal. As explained above, MC-AC-OPF represents a reduced model, where the linear response coefficient(s) α^k in (6.2.1) can be understood as a (conservative) approximation of the generators ability to react to uncertainty. In general it is only the way to parameterize mathematically operational points inside a given cluster in a reduced way. On the contrary, the corresponding linear coefficients in CC-AC-OPF, see e.g., [88, 89], represent the actual automatic generation response to short term fluctuations.

6.2.5 Multi-Cluster-AC-OPF: analytic reformulation

Analytic reformulation of the MC-AC-OPF is similar to what we have suggested in [97]; however, it is now generalized to the multi-cluster case. The main ideas behind this approach are as follows. Each cluster, k , represents samples centered around $(\bar{x}_c^k, \bar{x}_u^k)$ for given operational conditions parameterized by w . Clusters are chosen such that their sizes are sufficiently small (or just moderate in size relative to the mean), which allows us to linearize the non-linear AC PF equations (around the mean) and expecting accurate representation of the response to the fluctuations ϕ_c^k . Linearization allows us to resolve probabilities in Eq. (6.2.1) analytically. Specifically, to obtain a tractable deterministic reformulation of the chance constraints in (6.2.1), we use the moment-based representation dependent only on the mean and standard deviation \bar{x}_u^k, σ_u^k . Notice that tracking only two first moments provides probabilistic guarantees for a much wider range of distributions with finite mean and variance [94], and can be understood, more generally, as a robust optimization with feasibility guarantees for uncertainty realizations [95].

With the assumptions on linearization of the AC power flow equations and on the moment-based chance constraint reformulation made, we arrive at the following version of (6.2.1)

$$\begin{aligned} \min_{\bar{x}_c^k, \alpha^k, k=1..K} & \sum_{k=1}^K Cost_1^k(\bar{x}_c^k) + \mathbb{E}_w [Cost_2^k(w, \alpha^k)] \\ \text{s.t. } \forall k = 1..K & : \text{AC-PF}(\bar{x}_c^k, \bar{x}_u^k) = 0 \\ & \text{Prob}_w [\text{Constr}(\bar{x}_c^k + G_w^k w + \text{Resp}^p(w, \alpha^k)) \geq 0] \leq \varepsilon \end{aligned} \quad (6.2.2)$$

where the adjustment of the controlled variables ϕ_c^k is parameterized by the sensitivity matrix G_w^k , describing the linear response of the controlled variables to variations in the uncontrolled variables

$$\phi_c^k = \left. \frac{\partial x_c^k}{\partial w} \right|_{\substack{x_c^k = \bar{x}_c^k \\ x_u^k = \bar{x}_u^k}} \times w \doteq G_w^k(\bar{x}_c^k, \bar{x}_u^k, \alpha^k) \times w.$$

Following [88, 89, 90] (and skipping some standard details for brevity) we are able to evaluate expectation and probabilities in (6.2.2) analytically. Moreover, the analytic evaluation returns explicit dependencies on \bar{x}_c^k and α^k for each considered cluster, thus stating the MC-AC-OPF (6.2.2) as the following tractable deterministic optimization

$$\begin{aligned} \min_{\bar{x}_c^k, \alpha^k} & \sum_{k=1}^K Cost_1^k(\bar{x}_c^k) + \mathbb{E}_w [Cost_2^k(w, \alpha^k)] \\ \text{s.t. } \forall k = 1..K & : \text{AC-PF}(\bar{x}_c^k, \bar{x}_u^k) = 0 \\ & \text{Constr}(\bar{x}_c^k, \bar{x}_u^k) \leq -\lambda^k(\bar{x}_c^k, \bar{x}_u^k, \alpha^k, \Sigma_w^k), \end{aligned} \quad (6.2.3)$$

Uncertainty margins, $\lambda^k(\bar{x}_c^k, \bar{x}_u^k, \alpha^k, \Sigma_w^k)$, are computed for each type of variables (γ), each type of bus/line (μ : PQ,PV, θV ,line) and for each cluster k as (here and below dependence on k is dropped to lighten notations)

$$\begin{aligned}\lambda_{\gamma:\mu} &= 0, V:\theta V, V:PV, P:PQ, Q:PQ \\ \lambda_{P:PV/\theta V}^i &= \Phi^{-1}(1 - \epsilon_\gamma) \times \|(G_{w(i,:)}^{\gamma:\mu} + \alpha_{(i,:)})\Sigma_w^{1/2}\|_2 \\ \lambda_{\gamma:\mu}^i &= \Phi^{-1}(1 - \epsilon_\gamma) \times \|(G_{w(i,:)}^{\gamma:\mu})\Sigma_w^{1/2}\|_2, V:PQ, Q:PV/\theta V, F:line\end{aligned}$$

where Φ^{-1} stands for the inverse cumulative distribution function of the standard normal distribution. Σ_w^k is the calculated covariance matrix for the cluster. (We remind that covariance is a parameter introduced for each cluster, k .) F is the squared apparent power at from/to side of the line. Correction of the objective function is also computed analytically, in the case of quadratic generation cost it is non zero term, depending on α and variances of the components of w . Transition from (6.2.1) to (6.2.3) is summarized in Fig. 6.4.

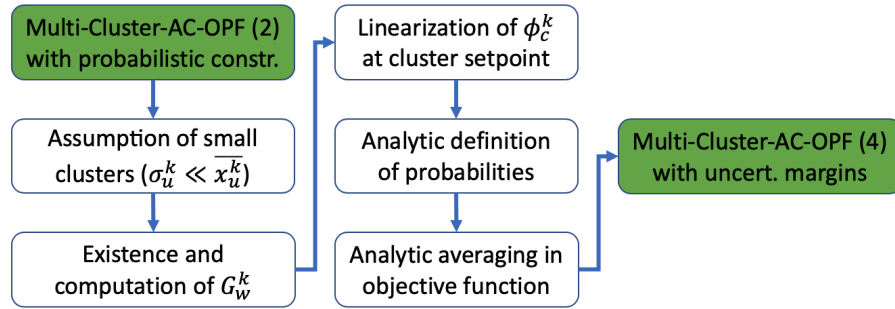


Figure 6.4: Analytic reformulation process from the original MC-AC-OPF with probabilistic constraints to the tractable model with deterministic constraints.

The problem (6.2.3) is very similar to the original problem MS-MS-AC-OPF (1) by the structure and constraints. But now, the number of constraints and variables is reduced significantly. MS-MS-AC-OPF simultaneously accounts for all the considered operational samples, while MC-AC-OPF simultaneously accounts for all the computed clusters. Notice that the reduction is made at the expense of the increased complexity of the model. Indeed, response to the shift from the centers of the clusters is parameterized, which requires adding response coefficients (more variables). Also, typical AC-OPF constraints are supplemented with new constraints associated with the uncertainty margins. See Table 6.1 for a summary of the MS-MS-AC-OPF and MC-AC-OPF comparison.

Here we assume that the planning horizon is split into T time intervals, and M samples are available per each time interval. Observe the possible dramatic reduction from $T * M = 10 * 10000 = 10^5$ samples to, e.g., $K = 10$ clusters is done on the expense of adding for each cluster a matrix of response coefficients (parametrization policy (c)) of size $N \times N$ (where N is the system size, measured in terms of the number of buses), and also of the constraints associated with the uncertainty margins $\lambda^{(k)}$. In general, the constraints associated with the uncertainty margins are complicated, as depend on

Table 6.1: Complexity comparison of the MS-MS-AC-OPF and MC-AC-OPF

Criteria	MS-MS-AC-OPF	MC-AC-OPF
State vars	$(V, \theta, P_c, Q_c)^{(a)}$	$(V, \theta, P_c, Q_c)^{(k)}$
# of states	$T * M$ (oper. points)	K (clusters)
Add. vars	-	$\alpha^{(k)}, k = 1..K$
Nonlinearity	AC-PF, Thermal constr.	AC-PF, Thermal constr., $\lambda^{(k)}$

the inverse of the system's Jacobian evaluated at the center of the cluster. However, when cluster sizes are reasonably small, we can find the constraints through a numerical procedure implemented at each iteration. Complex dependence of uncertainty margins on α and cluster set point is a big complication still. But overall, the methodology allows us to keep the structure of the resulting problem similar to the one of MS-MS-AC-OPF, however with a dramatically reduced number of states and only with a handful of additional response coefficients added.

6.3 Implementation and solution approach

We solve (6.2.3) via iterative algorithm implemented in Julia using JUMP [96], thus taking advantage of the modularity and automatic differentiation features of the software. The idea of the algorithm is to specify (current) $x^k \doteq (\bar{x}_c^k, \alpha^k)$ at each iteration step for each considered cluster. Then the sensitivity matrices G_w^k are evaluated at \bar{x}_c^k with analytical dependence only on α^k (because it is variable, the dependence on the setpoint is numerical if it is provided). Then the sensitivities are provided as an input to the optimization model. The uncertainty margins, λ^k are also computed for the provided setpoint for each cluster using analytical dependence on α . The schematic description of the algorithm is as follows:

1. Initialization. Set uncertainty margins $\lambda_P^{k-0} = \lambda_Q^{k-0} = \lambda_V^{k-0} = \lambda_F^{k-0} = 0$. Solve classical AC-OPF for each cluster, and set its argmin as \bar{x}_c^{k-0} . Set iteration number to $it = 1$.
2. Evaluate starting point for optimization variables. $\alpha^{k-start}$ - defined as the equal participation of each generator evaluated for each component of the w vector for each cluster.

$$\lambda_P^{k-start}, \lambda_Q^{k-start}, \lambda_V^{k-start}, \lambda_F^{k-start}$$

are computed using sensitivity matrices at $\bar{x}_c^{k,it-1}$ and $\alpha^{k-start}$.

$\bar{x}_c^{k-start}$ and auxiliary variables - take $it - 1$ solution (previous).

3. Define non-linear optimization model (6.2.3). Model variables are $\bar{x}_c^k = \bar{V}_c^k, \bar{\theta}_c^k, \bar{P}g_c^k, \bar{Q}g_c^k$ and α^k ; the auxiliary variables are $\lambda_P^{k-var}, \lambda_Q^{k-var}, \lambda_V^{k-var}, \lambda_F^{k-var}$ and $\bar{p}_{fr_c}^k, \bar{p}_{to_c}^k, \bar{q}_{fr_c}^k, \bar{q}_{to_c}^k$. Define constraints according to (6.2.3). Effectively model is similar to AC-OPF but with corrected by the uncertainty margins constraints, additional variables and modified objective - averaged over each cluster.

turned off at the base case so that without loss of generality, we account only for controllable generators (renewables can be included in the uncontrollable generation in the same way as uncontrollable demand).

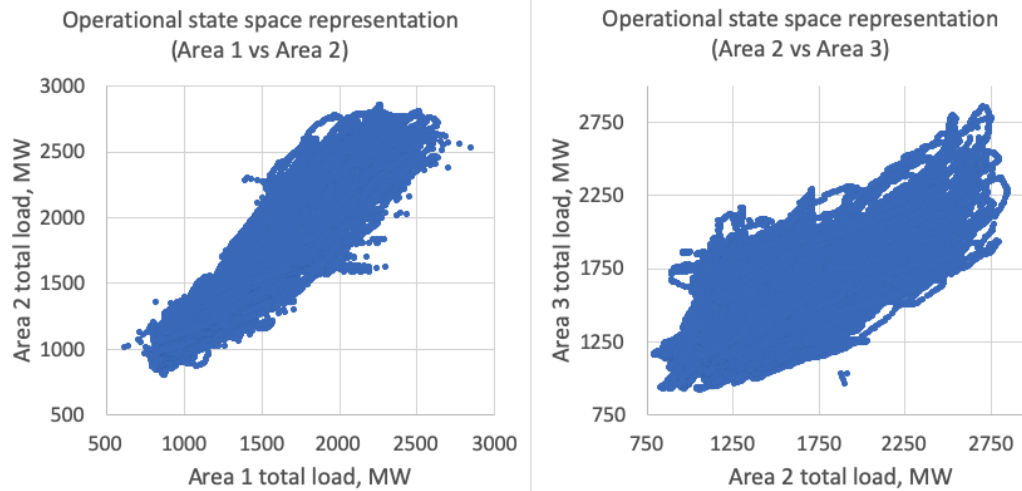


Figure 6.6: State space schematic illustration in terms of area loading. 105408 samples of operational conditions are totally provided and shown.

Fig. 6.6 illustrates the state space formed by the operational points in two projections of area loading. We observe that the operational space, which is rather large in terms of the demand realization, cannot be approximated by a single cluster as it was done in our previous studies on the case with significantly smaller sample diversity.

6.4.1 Clustering approaches

We utilize two approaches to cluster the data: (a) natural clustering by the time of the day and (b) mathematical clustering of the state space by the usage of the K-means algorithm. The comparison of the two approaches is shown in Figs. 6.7-6.8.

When the assignment of the state vectors to clusters is completed, the solution is illustrated in terms of the assignments of the aggregated area loadings. Each 3-dimensional point of power consumption at the three areas identified is expressed in terms of the 73-dimensional state vector. Area-1/Area-2 projection is shown.

One observes in Fig. 6.8 that the natural clustering on an hourly basis does not apply to the long-term horizon. We have attempted to improve the natural clustering by introducing an hourly clustering inside each season, which gave some improvement; however, still leaving us with clusters that are too big (for our model reduction approach). The problem was resolved with the introduction of the mathematical K-means clustering approach, which resulted in the identification of good distinct clusters of operational conditions, thus provided as an input to our reduced operational model. Cluster assignments are illustrated in colors in both (a) and (b) cases. Not to overload the image, we show

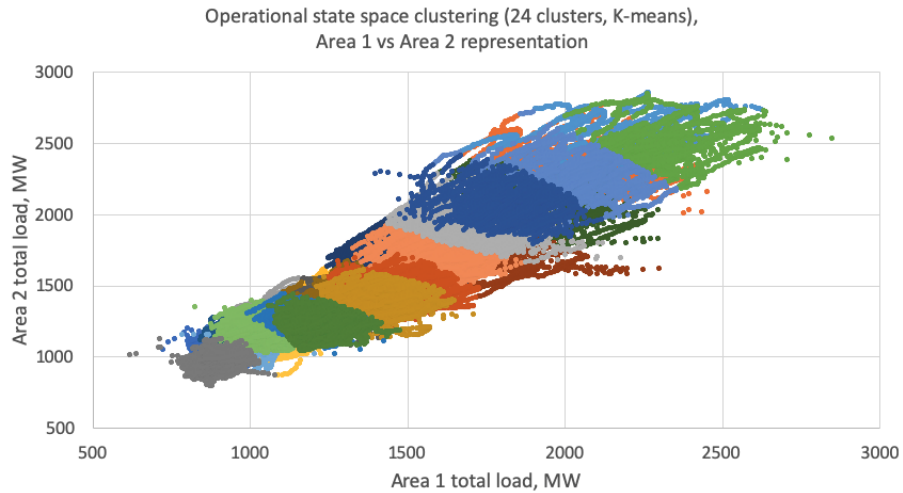


Figure 6.7: State space clustering of state vectors using K-means algorithm (24 clusters) and its' illustration on Areas loading diagram for 1 and 2 Areas.

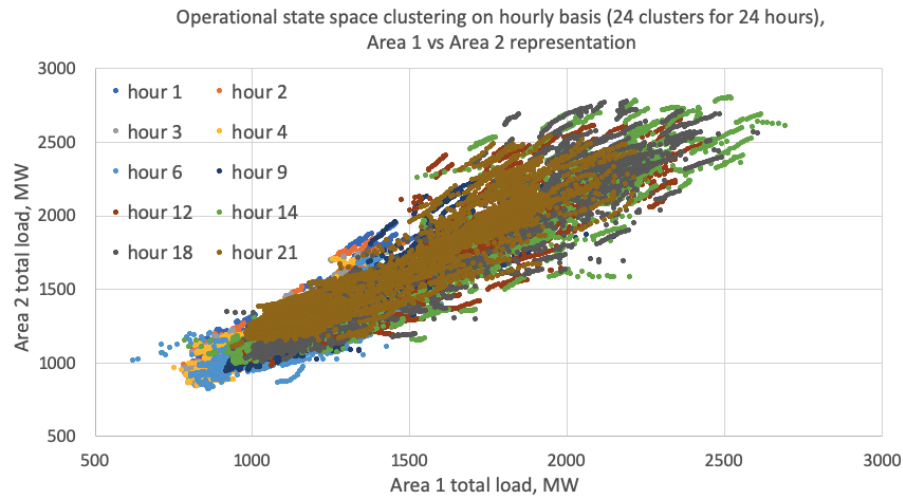


Figure 6.8: State space clustering of state vectors by 24 hours of the day and its' illustration on Areas loading diagram for 1 and 2 Areas.

only 10 clusters for the hourly case. One observes that in case (a), each cluster covers the whole space, while K-means clusters (case (b)) cover only a small part of the space each.

6.4.2 Ground truth solution

With no investment variables considered resolving MS-MS-AC-OPFs, setting the ground truth benchmark requires solving AC-OPF for each sample (each operational point for each time interval). These computations, performed on 3.3 GHz Core i7, 16Gb Ram laptop, took about 30000 seconds (8 hours). In our described approach pre-computing of OPFs is necessary only for the comparison with exact dispatches (they are not used in the algorithm). If pre-computing in terms of OPF is not feasible, again OPF without line capacity limits is possible (if initialization is required). Pre-computed OPFs can be

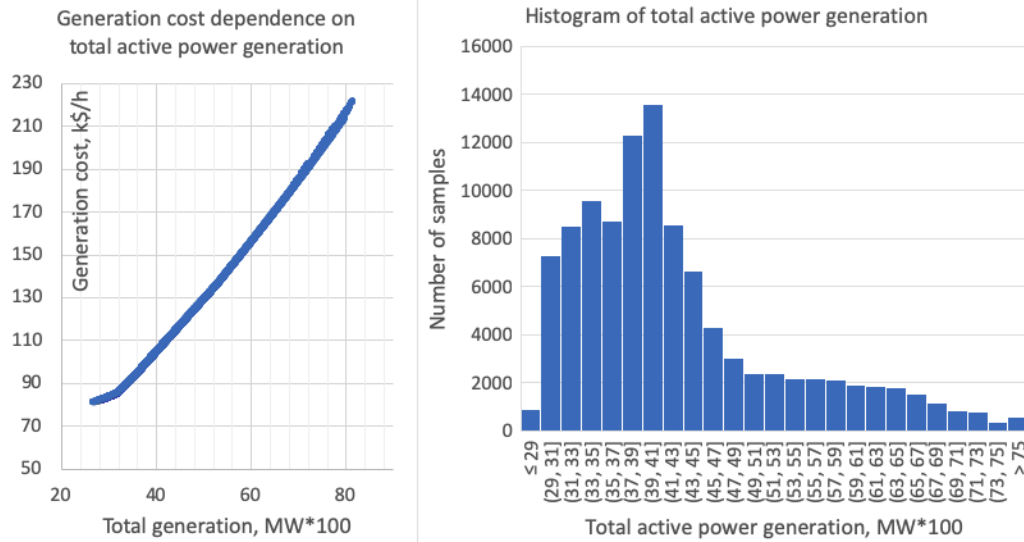


Figure 6.9: Ground truth solution - ACOPF computed individually for each sample. Left: generation cost depending on power generation, right: histogram showing number of samples with power generation from the given interval. Total computational time - 29665 sec (8.24 hours).

used for pre-computation of the parametrization of the response policy, which makes CC-optimization model way simpler. In terms of the grid configuration. Again, inside each time interval grid is globally fixed. An analysis of the ground truth solution is illustrated in the Fig. 6.9. The left part of the image shows generation cost depending on the optimal dispatch (all the optimal dispatches provide the solution for the MS-MS-AC-OPF), while the right part of the image illustrates an occurrence of each level of optimal power generation inside the state space. At higher loading levels (total generation 7500+ MW) we observe "noise" of cost for the same total generation. This is happening because of activation of line thermal constraints when optimal generation distribution is more dependent on the actual operational sample.

6.4.3 MC-AC-OPF solution analysis

We build and test a family of MC-AC-OPF solutions approximating the MS-MS-AC-OPF benchmark just described. The MC-AC-OPF solutions in the family have varying numbers of clusters and also obey one of the three parametrization policies. Distinct features of different MC-AC-OPF solutions in the hierarchy are summarized in Table 6.2.

We see, for example, that in the case of policy (a) and 20 clusters, our new scheme offers 170-fold acceleration. In this case, we are getting a good approximation of the average cost (within 1% accuracy); however individual dispatches are not accurate. This problem is corrected in case (b), also at the expense of speed – relative acceleration is 20-fold here. The third case offers the best quality (better than 0.1% cost quality), but it is also slowest with approximately 4 to 5-fold acceleration.

In all the cases, only 5 Iterations are enough to resolve the MC-AC-OPF. Average computational

Table 6.2: Features of the MS-AC-OPF solutions (20 clusters)

Criteria	MC-AC-OPF-a	MC-AC-OPF-b	MC-AC-OPF-c
Comp. time	1.7 sec	15 sec	80 sec
Application	only cost	dispatch@low	dispatch@high
Acceleration	x170	x20	x4-5
Obj. func. acc.	1%	0.5%	0.1%

time is shown per single cluster out of 20 considered and per single iteration of the developed algorithm. The additional trick which was used in cases (b) and (c) is that original base case line thermal limits were reduced by the uncertainty margins only for four potentially overloaded lines (see Fig. 6.5). Other thermal limits were considered constant as those lines are not overloaded for all the samples. All uncertainty margins are accounted for by the other constraints.

6.5 Summary

Overall, a combination of three introduced models can provide at least 10 times acceleration of MS-MS-AC-OPFs if used in combination - (a)/(b) for low loading clusters and (c) for higher loading levels. But the incorporation of optimal parametrization (especially in the matrix form) appeared to be very computationally demanding. We plan to look for some other approaches to this problem. One option for additional research is to pre-compute matrix aggregation from the known ground truth MS-MS-AC-OPF solution (if it is available).

Chapter 7

Summary, Conclusions and Recommendations for Future Research

7.1 Summary

This thesis proposes and discusses two directions to approach operational and uncertainty aware planning of power system. It is conceptually a new way to deal with mid-term to long-term planning problems, including investment planning. This is much harder computationally and methodology-wise compared to local and worst-case scenario planning but provides a great opportunity to analyze power system development in an uncertain environment (e.g., future operational conditions, renewables, availability of equipment) and accounting for operations at a planning stage. The introduced planning approach demonstrates that power system can operate in an efficient way with increased throughput and extended feasibility domain even when traditional upgrade opportunities (e.g., building new transmission lines, building new generation capacity locally) are expensive or limited/prohibited. When the potentially installed capacity of new equipment is considered as an additional degree of freedom together with available one, then significant additional flexibility can be achieved with comparably low cost.

The first part is related to operational and uncertainty aware planning with a stochastic modeling approach when future operational conditions are represented by a set of deterministic scenarios. The specific problem which is resolved is the placement and sizing of FACTS devices, but a similar approach can be used for the introduction of other degrees of freedom to the system as well.

Chapter 2 develops an advanced placement and sizing multiple-scenario model and solution methodology for that. Exact AC computations are incorporated here, which allows to account for reactive power flows and state and solve practical problems when detailed power flows representation is necessary. Chapters 3 and 4 demonstrate scalability of the solution methodology and developed algorithms to large-scale practical problems (e.g. Polish system from Matpower) including multi-scenario multi-time intervals planning case studies. These chapters also provide a broad analysis of the solutions and

discuss opportunities and problems related to the developed approach.

The second part is related to probabilistic modeling of future operational conditions by chance constrained optimization. We question if it is possible to shift from deterministic planning models with a limited number of representable scenarios to broader probabilistic consideration of the whole state space at planning. Furthermore, do it for practical size problems with a good level of detailization as well. Chapter 5 discusses the aggregation of multiple AC-OPF solutions of close in the operational state-space operational points. This is an important problem as many practical planning and operational applications in power systems require (including the extension to long-term planning problems) simultaneous consideration of a large number of operating conditions or Multi-Scenario AC-Optimal Power Flow (MS-AC-OPF) solution. We propose a tractable formulation and implementation and illustrate our construction on the example of 30-bus IEEE model. Chapter 6 explores the application of the developed reduction at the practical RTS-GMLC 73 bus case, where time series of 105408 samples of operational conditions is provided, representing a year of operations sampled every 5 mins. We discuss a model reduction approach, Multi-Cluster-AC-OPF, which performs clustering of a large and diverse set of multi-stage operational samples and then replaces a collection of samples assigned to each cluster by their compact representation in terms of its mean and standard deviation. The essence of our approach is in substituting parallel evaluation of many generation dispatch optimizations (each per sample, per time period) by a much smaller number (correspondent to the number of clusters) chance-constrained optimizations where samples are split into clouds, and each cloud is represented by an affine function of random parameters.

7.2 Conclusions

The main observations and results achieved in the first part of the thesis are the following:

A novel optimization framework for placing and sizing FACTS devices that accounts for future operations under uncertain conditions is developed. The framework takes into account AC-PF equations. The most important features of the newly developed framework are the scalability of the algorithm, allowing to resolve congestion over practical (thousands of buses) size transmission systems, and the ability of the algorithm to resolve multiple scenarios simultaneously. Introduced optimization setting can also be considered as generalizing the standard AC-OPF: it seeks a balance between installation and operations. The optimization objective includes the cost of operations over an extended time horizon as well as the cost of installation of the FACTS devices, represented in the form of an l_1 norm to promote sparsity of the resulting solutions. Optimization variables include capacities of the FACTS devices and respective operational settings associated with each scenario, where the latter is bounded by the former.

The proposed solution algorithm was tested in different regimes on a midsize model (30-bus IEEE) and a realistic size (Polish grid) model. It is observed that the output is spatially sparse, i.e., a very

small number of FACTS devices is sufficient, and that the output is nonlocal, i.e., a typical new installation resolves congestion at multiple locations that can be rather far from the newly installed devices. Also, it is observed that under highly loaded conditions, FACTS devices are beneficial in reducing the total cost of generation. Optimal installation of the devices helps to resolve infeasibilities that are projected to become even more severe in the future as well due to loading and operational variability growth.

The main technical achievement is the development of the algorithm that constitutes an efficient heuristic for solving nonlinear and nonconvex optimization. The algorithm is sequential—it constructs a convergent sequence of convex and analytic formulations (QP with linear constraints) where each constraint is represented explicitly through exact/analytic linearization of the original nonlinear constraints (e.g., representing power balance at nodes and apparent power line limits) over all the degrees of freedom (including FACTS corrections) around the current operational point.

To represent uncertainty in the expected growth of the system (loads), a scenario sampling methodology is introduced. Long-term planning examples were demonstrated at the IEEE 30-bus system and practical size Polish system. The application of the developed methodology was justified in detail on several examples on both systems. It is evident from experimental results that the developed framework/approach has a practical value for planning transmission grid expansion - it simultaneously provides the growing operational economy and resolves emerging congestion and infeasibility problems. The development of convenient and flexible software for web visualization of transmission system states and FACTS installations has become a side benefit of the project as well.

An optimization framework for algorithmic resolution of placement and sizing of FACTS devices in large transmission grids was generalized for accounting of multiple time intervals of the planning horizon as well. Additional algorithmic improvements (e.g., cutting plane, experiments with solvers, and settings) were introduced to resolve a large-scale problem. Overall, the results show an advanced level of the development of the methodology for operational and uncertainty aware planning with operational conditions represented by a set of deterministic scenarios/samples both in a technical and conceptual sense.

The second part of the thesis achieves the following:

The results demonstrate that the cloud-based approach has a strong potential in model reduction applications. The significant reduction in the computational effort is achieved due to the fact that the Cloud-AC-OPF modeling, implemented via generalized chance constraints, allows representing infinitely many realistic configurations with a small number of decision variables. The resulting solutions demonstrate good approximation quality when compared with the ground truth, set by the multiple scenarios AC OPF (MS-AC-OPF), in terms of the optimal objective. The best approximation quality in terms of actual generation dispatch reconstruction is achieved when the reduced model is represented by a matrix response, where each generator responds to each variable source (i.e., each network node with significant variability) independently. The results are encouraging as they open

a multitude of opportunities to handle more complex and challenging settings, such as two-level and multi-stage planning problems of the type discussed in [86, 87, 98].

A summary of technical contributions:

1. We develop the Cloud-AC-OPF approach, which applied the CC-OPF methodology [88, 89, 90] to model reduction of the computationally prohibitive MS-AC-OPF.
2. The approach takes advantage of an affine parameterization of the decision variables.
3. We show the practicality of the approach on the examples of moderate size (IEEE 30 bus model) where validation against the MS-AC-OPF, providing the ground truth, is still feasible.

We also apply the developed multi-scenario complexity reduction methodology to the practical operationally diverse case of RTS-GMLC system. And formulate and solve Multi-Cluster-AC-OPF. Parallel evaluation of OPFs over multiple operational scenarios over many temporal stages, e.g., in the long-term planning, is replaced by evaluation of separate clusters in a state space, represented in a probabilistic form with mean and standard deviation. MC-AC-OPF reduction methodology is introduced, solution algorithm is developed and evaluated on practical in terms of diversity and number of samples test case. The approximation demonstrates good performance and appropriate accuracy.

7.3 Recommendations for future research

The research performed in this thesis provides not only answers but also questions and directions for future research. The most important methodological question which is not resolved by now is the accounting for security constraints. It is a really important problem as mid-term to long-term planning is considered. One option is to account for some additional margins, which should be additionally defined. Another option is to add scenarios representing failure events to the set of conditions. This opportunity is also limited as adding of all events will be intractable. The probabilistic approach to modeling the operational part of the problem can help to potentially approach this problem.

A probabilistic setting for planning shows very good potential, but operational complexity reduction models are quite complex analytically and require additional exploration. Simultaneous optimization of the cluster dispatch and response parametrization appeared extremely computationally demanding. One possible option is to compute parametrization separately. Another important question is the probabilistic guarantees. At a current point we have not explored this question. Also, for example 1% violation was selected experimentally as providing good approximation but demonstrating visible difference between three parametrizations of uncertainty inside the cluster. If taking too small probability violation algorithm becomes quite conservative. Additional research is required for that as well. Additionally, we look into improved approaches for clusters selection and also an analytical simplification of the problem reduction methodology. After that, the second installation stage of

the planning problem should be added. The model should be validated, and a case study analysis has to be performed.

When this is done, new planning problems will be considered. We look forward to generation capacity upgrade planning analysis and storage planning problem, which is potentially a resolution of a multitude of operational problems as approach a natural feature of power grids of the real-time supply-demand balance.

Chapter 8

Appendix

In this chapter, we describe steady-state power system modeling and formulate Power Flow (PF), Optimal Power Flow (OPF), and Chance-Constrained AC Optimal Power Flow (CC-AC-OPF) problems as main base models of steady-state operations. We provide details on analytical linearization of FACTS placement and sizing problem and analytical reformulation of generalized CC-AC-OPF. We also discuss the long-term operations of the power transmission system. Methodology of analytical linearization of non-linear constraints in AC based multiple scenarios two-stage optimization was first introduced in [72].

8.1 Power system modelling

First, we describe the AC model and then the simplified DC model. The main components of the power system are:

- Branches or power lines
- Generators
- Loads

Matpower [74] is the open-source package, which allows to test/run all of the standard steady-state models typically used for power flow analysis. According to Matpower's documentation, all transmission lines, transformers, and phase shifters are modeled with a common branch model, consisting of a standard π transmission line model, with series impedance $z = r + jx$ and total charging susceptance b , in series with an ideal phase-shifting transformer [1]. Each line has two sides, one called from, and another one is to. The transformer, whose tap ratio has magnitude τ and phase shift angle θ_{shift} , is located at the from the end of the branch, as shown in Fig. 8.1

The complex current injections i_f and i_t at the from and to ends of the branch, respectively, can be expressed in terms of the 2×2 branch admittance matrix Y_{br} and the respective terminal voltages v_f and v_t (from [1]):

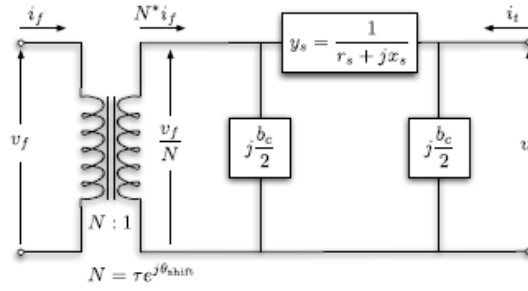


Figure 8.1: Branch model illustration from [1].

$$\begin{bmatrix} \dot{i}_f \\ \dot{i}_t \end{bmatrix} = Y_{br} \begin{bmatrix} v_f \\ v_t \end{bmatrix} \quad (8.1.1)$$

With the series admittance element in the π model denoted by $y = 1/z$, the branch admittance matrix can be written as follows [1]:

$$Y_{br} = \begin{bmatrix} (y + j\frac{b}{2})\frac{1}{\tau^2} & -y\frac{1}{\tau \exp(-j\theta_{shift})} \\ -y\frac{1}{\tau \exp(j\theta_{shift})} & (y + j\frac{b}{2}) \end{bmatrix} \quad (8.1.2)$$

For simplicity we do not take into account phase shifters and tap-changers for now (this can be easily added to the model), Thus setting $\tau = 1$ and $\theta_{shift} = 0$ we get the following complex current flowing through the line $a - b$ (in the direction from a to b):

$$i_{ab} = \left(\frac{1}{r + jx} + j * \frac{b}{2} \right) * v_a - \frac{1}{r + jx} * v_b \quad (8.1.3)$$

Taking into account the fact that complex voltage $v_a = V_a e^{j\theta_a}$, the apparent power flowing through the line satisfies:

$$S_{ab} = v_a i_{ab}^* \quad (8.1.4)$$

$$S_{ab} = \frac{rV_a^2 - rV_aV_b \cos(\theta_a - \theta_b) + xV_aV_b \sin(\theta_a - \theta_b)}{r^2 + x^2} + j\frac{xV_a^2 - rV_aV_b \sin(\theta_a - \theta_b) - xV_aV_b \cos(\theta_a - \theta_b)}{r^2 + x^2} - j\frac{b}{2}V_a^2 \quad (8.1.5)$$

Now, if phase shifting transformers are considered. A transformer breaks the symmetry between the “from” end, positioned next to the transformer, and the “to” end of the line. The so-called π -model from [74] is utilized here as well. Parameters of the line model are the series impedance, $z = r + jx$, the total charging susceptance, b , the transformation ratio, τ , and the shift angle θ_{shift} .

Explicit expressions for apparent powers injected at the “from” end and the “to” end of the line in terms of voltages and phases are

$$S_f(V_f, \theta_f, V_t, \theta_t, x) = \frac{V_f (rV_f - \tau V_t (r \cos \Delta + x \sin \Delta))}{\tau^2 l} - j \frac{V_f}{2\tau^2 l} \left(V_f (-2x + bl) + 2\tau V_t (x \cos \Delta + r \sin \Delta) \right) \quad (8.1.6)$$

$$S_t(V_f, \theta_f, V_t, \theta_t, x) = \frac{V_t (r\tau V_t - V_f (r \cos \Delta + x \sin \Delta))}{\tau^2 l} - j \frac{V_t}{2\tau l} \left(\tau V_t (-2x + bl) + 2V_f (x \cos \Delta - r \sin \Delta) \right) \quad (8.1.7)$$

where $\forall i : v_i = V_i e^{j\theta_i}$, $\Delta = \theta_f - \theta_t - \theta_{\text{shift}}$ and $l = r^2 + x^2$.

While lines transfer active and reactive power through the system, there are two other players - generators and loads which produce or consume electricity.

A generator is modeled as a complex power injection at a specific bus. For generator i , the injection is:

$$S_i^g = P_i^g + Q_i^g \quad (8.1.8)$$

where, P_i^g is active power positive injection and Q_i^g - reactive power injection, which can be both positive or negative.

Constant power loads are modeled as a specified quantity of real and reactive power consumed at a bus. For bus i , the load is

$$S_i^l = P_i^l + Q_i^l \quad (8.1.9)$$

where, P_i^l is active power negative consumption and Q_i^l - reactive power negative consumption.

Eq. 8.1.5 defines active and reactive powers flowing through an edge of the system. It can be seen that the function is complex and depends on many variables (predefined constants for the system are just line parameters x , r , and b if there are no any adjustable compensation devices used). We are going to adjust x - inductance of the transmission line. Then fixed parameters will be only r and b .

When an optimization problem is formulated, one includes these non-linear and non-convex functions in the constraints for power system state definition by Kirchhoff's circuit laws [99].

Thus, during our initial research, we simplified the task and worked within reasonable for transmission systems DC-approximation, which is defined according to the following three assumptions:

- Branches can be considered lossless. In particular, branch resistances r and charging capacitances b are negligible:
- All bus voltage magnitudes are close to their nominal value or 1 p.u.
- Voltage angle differences across branches are small enough that $\sin(\theta_f - \theta_t) \approx \theta_f - \theta_t$

In DC-approximation the apparent power S_{ab} will be:

$$\begin{aligned}
 S_{ab} = v_a i_{ab}^* &= V_a e^{j\theta_a} * \left(\left(\frac{1}{r + jx} + j * \frac{b}{2} \right) * V_a e^{j\theta_a} - \frac{1}{r + jx} * V_b e^{j\theta_b} \right)^* \approx \\
 &\approx e^{j\theta_a} * \left(\frac{1}{jx} * e^{j\theta_a} - \frac{1}{jx} * e^{j\theta_b} \right)^* = \frac{j}{x} (1 - e^{j(\theta_a - \theta_b)}) = \\
 &= \frac{j}{x} * (1 - \cos(\theta_a - \theta_b) - j \sin(\theta_a - \theta_b)) \approx \frac{\theta_a - \theta_b}{x} \quad (8.1.10)
 \end{aligned}$$

Which is much simpler than Eq. 8.1.5. Only active power flows in the system, and for each line is defined by the phase difference between the ends and line inductance, the function still nonlinear (if x is adjusted).

8.2 Power Flow (PF) and Optimal Power Flow (OPF) problems

The standard Power Flow (PF) problem outputs voltages and flows in a network for a given profile of consumption/injections at loads, and generators [1]. For the known structure of the network, branch parameters and values of generation and consumption of power solving PF means finding voltages, phases, and active in reactive power flows in the system.

By convention, a single largest generator is typically chosen as a reference bus, also called the slack bus. The reference/slack bus is assumed to provide a slack of generation. Thus input/output of active and reactive power at the slack bus is a parameter to allow consistency of PF equations in balancing the global power budget. Other generators are typically classified as PV buses, with the values of voltage magnitude and generator real power injection given [1]. Loads are specified as PQ buses with given power consumption and unknown voltage and phase values.

The solution of the AC-PF problem is a solution of the PF equations representing Kirchhoff's laws. Stated in their standard form, the PF equations are usually split into active and reactive parts. At each

node of the system, actual active and reactive power injection or consumption is equal to the sum of flows going to lines connected to the given node:

$$P_i = \sum_{j \sim i} \frac{r_{ij}V_i^2 - r_{ij}V_iV_j \cos(\theta_i - \theta_j) + x_{ij}V_iV_j \sin(\theta_i - \theta_j)}{r_{ij}^2 + x_{ij}^2} \quad (8.2.1)$$

$$Q_i = \sum_{j \sim i} \left(\frac{x_{ij}V_i^2 - r_{ij}V_iV_j \sin(\theta_i - \theta_j) - x_{ij}V_iV_j \cos(\theta_i - \theta_j)}{r_{ij}^2 + x_{ij}^2} - \frac{b_{ij}}{2}V_i^2 \right) \quad (8.2.2)$$

We use Matpower toolbox to solve the AC PF equations, and when needed for embedding in higher level (optimization) problem, develop our own solver (computational framework).

Another important standard for power systems is Optimal Power Flow problem (OPF). This task involves searching for the optimal active and reactive power dispatch of generation, minimizing the value of the power generation cost function. The optimization vector x for the standard AC OPF problem consists of the $n_b \times 1$ (n_b - number of nodes or buses) vectors of voltage angles Θ and magnitudes V and the $n_g \times 1$ (n_g - number of generators) vectors of generator real and reactive power injections P_{gen} and Q_{gen} .

$$x = \begin{bmatrix} \Theta \\ V \\ P_{gen} \\ Q_{gen} \end{bmatrix} \quad (8.2.3)$$

The objective function in the OPF is a sum of costs of active and reactive power injections at the generators C_p^i and C_q^i .

Finally, the AC-OPF problem is formulated as follows:

$$\begin{aligned} \min_x \quad & \sum_{i=1..n_g} C_p^i(p_g^i) + C_q^i(q_g^i) \\ \text{s.t.} \quad & \\ & V_{\min} \leq V \leq V_{\max} \\ & Q_{\min-gen} \leq Q_{gen} \leq Q_{\max-gen} \\ & P_{\min-gen} \leq P_{gen} \leq P_{\max-gen} \\ & \sqrt{(P_{ij})^2 + (Q_{ij})^2} \leq S_{\max}^{ij} \quad \forall i \sim j \\ & P_i + iQ_i = \sum_{j \sim i} (S_{ij}) \quad \forall i = 1..n_b \end{aligned} \quad (8.2.4)$$

The optimization constraints above have the following meaning:

- voltage amplitude at each node is within an appropriate range defined by minimum and maximum levels
- reactive power generation is limited
- active power generation is limited
- lines thermal limits for each pair of connected nodes
- active and reactive power balance at each node (network equations)

This problem is very important and has a significant value in power systems research. In our study, we extend this problem formulation to include placement and sizing of FACTS devices which will be described in the following sections.

8.3 FACTS devices

FACTS are selected to be a transmission system upgrade option for the planning methodology development and analysis. Let us introduce the FACTS concept and motivation for the installation from [72].

In addition to traditional ways to balance AC-flows and meet the demand through generation dispatch, a number of new technological solutions are now available. In particular, installation of the so-called Flexible Alternating Current Transmission System (FACTS) adds an important new option to the mix of other available control options, see e.g. [14, 100, 15, 20, 24] and references therein. Serial Compensation (SC) and Static VAR Compensation (SVC) are FACTS devices of a new type [31, 33, 34, 30] which generally represent a way to compensate lines or loads respectively. Planning installation of new FACTS devices with sufficient capacity and flexibility to meet requirements of multiple demand scenarios, e.g., accounting for seasonal variations and growth of demands, various network configurations, and different generators on-line, is a challenging optimization problem discussed in the past by many other authors, e.g., [14, 100, 15, 20, 24].

According to [2] Flexible AC Transmission System (FACTS) is a generic term for a group of technologies that dramatically increase the capacity of the existing transmission network - by as much as 50 percent or more - while maintaining or improving voltage stability grid reliability and energy security. FACTS technologies have a small footprint and minimal impact on the environment. Project implementation times are considerably faster, and investment costs substantially lower than the alternative of building more transmission lines or new power generation facilities. FACTS technologies are traditionally divided into the two categories of series compensation and shunt compensation. All four technologies that make up the two categories are fixed series compensation, and thyristor-controlled series compensation in the former, SVC and STATCOM/SVC Light in the latter [2].

Series Compensation devices

Series compensation is defined as the insertion of reactive power elements into transmission lines [101]. Series compensation is a well-established technology that is primarily used to reduce transfer reactances, most notably in bulk transmission corridors. The result is a significant increase in the transient and voltage stability in transmission systems [2]. The main principle of SC devices is to modify the reactance of a transmission line by series connection of capacitors. There are two types of devices - Fixed SCs and Thyristor controlled SCs (TCSC). For us, more interesting is a second, adjustable type of SC devices, which can do both - increase or decrease the overall inductance of a power line. As TCSC enables rapid dynamic modulation of the inserted reactance, we can use them for the improvement of power system operations globally by adding setting of the installed device to the OPF problem, for instance. An example of the installed TCSC is shown in Fig. 8.2.



Figure 8.2: TCSC for stable transmission of surplus power from Eastern to Western India from [2].

Static Var Compensation devices

A SVC is a high voltage system that controls dynamically the network voltage at its coupling point. Its main task is to keep the network voltage constantly at a set reference value [101]. SVC is connected in parallel to a consumer in a transmission system and injects the reactive power. The SVC consists of a number of fixed or switched branches, so it can be dynamically adjustable. At least one branch includes thyristors, and the combination of branches can be varied a lot depending on requirements. An SVC typically includes a combination of at least two of the given items below (most common topologies for SVCs are: TCR/FC or TCR/TSC/FC):

- Thyristor controlled reactor (TCR)
- Thyristor switched capacitor (TSC)
- Harmonic filter (FC)
- Mechanically switched capacitor bank (MSC) or reactor bank (MSR)

Example of an installed SVC is given in Fig. 8.3.



Figure 8.3: SVC system enable and support remote variable generation from [3].

The devices are large, complicated, and expensive. The installation time is 1-2 years, and thus usage decisions should be well planned and reasoned.

Steady-state modeling

In our introduced models FACTS devices are described by two variables - first is capacity, second is setting. They represent the first stage degree of freedom - installed capacity and the second - operational.

Series Compensation (SC) device capacity and setting for the line $\{i, j\} \in \mathcal{E}$:

$$\overline{\Delta x_{ij}} \tag{8.3.1}$$

$$-\overline{\Delta x_{ij}} \leq \Delta x_{ij} \leq \overline{\Delta x_{ij}} \tag{8.3.2}$$

Static Var Compensation (SVC) device capacity and setting for the load node $i \in \mathcal{V}_l$:

$$\overline{\Delta Q_i} \tag{8.3.3}$$

$$-\overline{\Delta Q_i} \leq \Delta Q_i \leq \overline{\Delta Q_i} \tag{8.3.4}$$

Motivation for FACTS installation

FACTS devices of SC and SVC types can be utilized for multiple purposes. Series Compensation devices can be used in order to [101]:

- Reduce line voltage drops
- Limit load-dependent voltage drop

- Influence load flow in parallel transmission lines
- Increase transfer capability
- Reduce transmission angle
- Increase system stability

Functions of Static Var Compensation devices are [101]:

- Voltage control
- Reactive power control
- Damping of power oscillations
- Unbalance control

In principle, some of the modern (and expensive) FACTS devices can be used on a fast time scale to mitigate dynamical problems. Even though dynamic applications are important, they are still exotic (lacking practical applications). Therefore we limit our study and analysis solely to the static setting(s). In this study, we analyze how to use FACTS devices of both types to:

- Reduce overall generation cost

Each available generator in the power system has some cost function for power generation, and there is a procedure called Optimal Power Flow (OPF) which the system operator uses to define generation levels for generators to minimize the overall cost. And there is a possibility that for highly loaded configurations of the power system, some "cheap" generators will not be able to produce a maximum amount of electric power due to line congestion around them. As the devices can influence the distribution of power flows by modification of inductance of transmission lines, we can use that ability in order to increase system throughput and support "cheap" power to go to the demand places. This can be renewable energy or just energy from some modern or really large generators.

- Improve power system reliability

This means that we can use FACTS devices to reinforce power system to withstand the disturbances and to reduce the risk of power outages. An emergency situation occurs when some elements (for example, transmission lines) are overloaded. If one considers huge power outages in the US (for example, Northeast blackout of 2003) they started from simple line faults [102]. When the OPF solution is infeasible, the only way to resolve that is to use load scheduling or turn of the customers. We are aiming to find a way of extending the feasibility region for the system operation by using FACTS devices.

- Reduce congestion

Again, if some line is overloaded, we can try to use compensation devices to resolve that. The question is how to do that because generation redispatch is also one of the options. We need to develop a procedure on how to choose from all the possibilities the right one or a number of them.

Installation approaches

The approach to device installation discussed in this thesis is more of a forward looking "theoretical" type. However, let us first discuss current industry practice. As of now, SVC and SC devices are mainly installed to resolve support and transmission congestion problems, respectively. Guidance for installation is typically local - related to historical observations at the given localized portion of the grid. In [4] the installation of fixed SCs is discussed, and the authors state that the main impact on the system is improved voltage and angular stability of power lines, shown in Fig. 8.4.

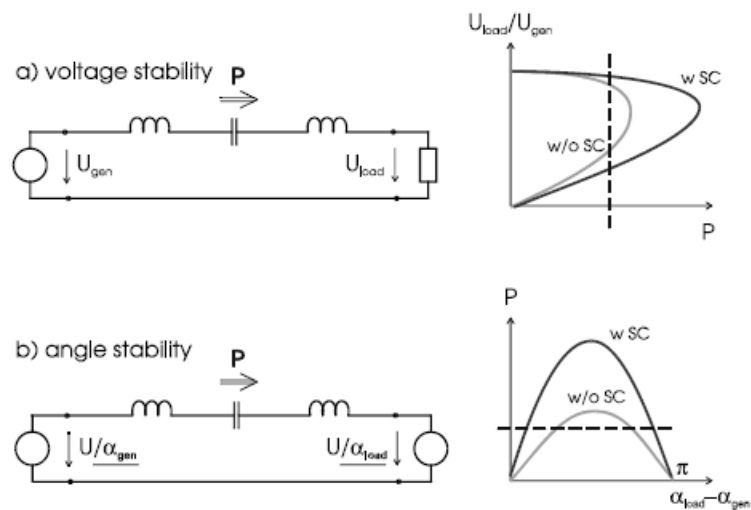


Figure 8.4: The impact of SC on a) voltage and b) angular stability [4].

In Fig. 8.4 two curved lines illustrate the stability region with and without SC installation, and the dashed line shows the operational state. It is clearly seen that SC devices improve both the voltage and angular stability of a power line, thus allowing more power to be transported through the line without loss of steady-state stability. Producers of FACTS devices also give a number of examples of successful installations of SVCs for reactive power support and voltage control [103]. Overview of FACTS devices [104], the effect of the installed FACTS devices [105], local control problems and effect of coordinated control [24], planning of placement of the devices with appropriate characteristics and suitable for various loading configurations problem [16] and the economic effect caused by compensation [106],[107] are among subjects broadly discussed in research papers representing a scientific point of view on the FACTS installation.

8.4 Equations for general optimization problem of FACTS placement and sizing

All the notations are introduced in Section 2.1 and power system modelling is discussed in Section 8.1.

Here again, a - number of the scenario, i,j - numbering of nodes in the grid. We use π -model of the transmission power line with charge capacitance taken into account. For each line r - resistance, x - inductance and b - capacitance are known.

Using π -model of the line (no tap changers and phase shifters), the dependence between the current on the ends and voltages on the ends can be derived:

$$i_{ij} = \left(\frac{1}{r + jx} + j * \frac{b}{2} \right) * v_i - \frac{1}{r + jx} * v_j \quad (8.4.1)$$

Then apparent power flowing at each end can be calculated:

$$S_{ij} = \frac{rV_i^2 - rV_iV_j\cos(\theta_i - \theta_j) + xV_iV_j\sin(\theta_i - \theta_j)}{r^2 + x^2} + \\ + j \frac{xV_i^2 - rV_iV_j\sin(\theta_i - \theta_j) - xV_iV_j\cos(\theta_i - \theta_j)}{r^2 + x^2} - j \frac{b}{2} V_i^2 \quad (8.4.2)$$

We introduce three parameters in order to write equations for thermal limits limitations for the lines and network equations (power balance at each node):

- $F_{ij} = \sqrt{(P_{ij}^{(a)})^2 + (Q_{ij}^{(a)})^2}$ - squared absolute value of the power flow from the node i to the node j
- P_i - active power injection/consumption at the node i
- Q_i - reactive power injection/consumption at the node i

This can be expressed in terms of state variables (V, θ, P, Q, x) as it is shown below:

$$F_{ij} = \frac{V_i^4 + V_i^2V_j^2 - 2V_i^3V_j\cos(\theta_i - \theta_j)}{r_{ij}^2 + x_{ij}^2} - \\ - \frac{b(x_{ij}V_i^4 - x_{ij}V_i^3V_j\cos(\theta_i - \theta_j) - r_{ij}V_i^3V_j\sin(\theta_i - \theta_j))}{r_{ij}^2 + x_{ij}^2} + \\ + \frac{b_{ij}^2V_i^4}{4} \quad (8.4.3)$$

$$P_i = \sum_{j \sim i} \frac{r_{ij}V_i^2 - r_{ij}V_iV_j \cos(\theta_i - \theta_j) + x_{ij}V_iV_j \sin(\theta_i - \theta_j)}{r_{ij}^2 + x_{ij}^2} \quad (8.4.4)$$

$$Q_i = \sum_{j \sim i} \left(\frac{x_{ij}V_i^2 - r_{ij}V_iV_j \sin(\theta_i - \theta_j) - x_{ij}V_iV_j \cos(\theta_i - \theta_j)}{r_{ij}^2 + x_{ij}^2} - \frac{b_{ij}}{2}V_i^2 \right) \quad (8.4.5)$$

These equations define non-linear constraints in the general optimization problem for FACTS placement which is formulated in Section 2.2. For the convenience, we also rewrite it here:

$$\min_{\overline{\Delta x}, \overline{\Delta Q}; \text{state}^{(a)}, \forall a} \text{COST}(\overline{\Delta x}, \overline{\Delta Q}; \text{state}^{(a)}) \quad (8.4.6)$$

$$\begin{aligned} \text{COST} &\doteq (C_{SC} \sum_{\{i,j\} \in \mathcal{E}} \overline{\Delta x}_{ij} + C_{SVC} \sum_{i \in \mathcal{V}_l} \overline{\Delta Q}_i \\ &+ N_y \sum_{a=1..N} T_a * C_a(P^{(a)})) \end{aligned} \quad (8.4.7)$$

$$\text{state}^{(a)} \doteq (x^{(a)}, v^{(a)}, \theta^{(a)}, Q^{(a)}, P^{(a)}), \forall a$$

$$x^{(a)} = x_0^{(a)} + \Delta x^{(a)} \quad \forall a$$

$$Q_{load}^{(a)} = Q_{load-0}^{(a)} + \Delta Q_{load}^{(a)}, \forall a$$

$$-\overline{\Delta x} \leq \Delta x^{(a)} \leq \overline{\Delta x}, \forall a$$

$$-\overline{\Delta Q} \leq \Delta Q_{load}^{(a)} \leq \overline{\Delta Q}, \forall a$$

$$V_{\min}^{(a)} \leq V^{(a)} \leq V_{\max}^{(a)}, \forall a$$

$$Q_{\min-gen}^{(a)} \leq Q_{gen}^{(a)} \leq Q_{\max-gen}^{(a)}, \forall a$$

$$P_{\min-gen}^{(a)} \leq P_{gen}^{(a)} \leq P_{\max-gen}^{(a)}, \forall a$$

$$\sqrt{(P_{ij}^{(a)})^2 + (Q_{ij}^{(a)})^2} \leq S_{\max}^{(a)} \quad \forall a; \forall \{i, j\} \in \mathcal{E}^{(a)}$$

$$P_i^{(a)} + iQ_i^{(a)} = \sum_{j: \{i,j\} \in \mathcal{E}^{(a)}} \left(S_{ij}^{(a)} \right), \forall i \in \mathcal{V}^{(a)}, \forall a$$

We develop an iterative algorithm, which finds a solution for a given problem starting from specified initial states for the scenarios and improves it consequently by solving Quadratic Programming (QP) with linear constraints on each step. The linearization of constraints is done analytically, on each step we calculate Jacobian matrices and use them to define constraints for the QP solver.

8.5 Equations for linearized optimization problem

We illustrate the linearization procedure for one scenario. For multiple scenarios, it is generalized by constructing block matrices out of Jacobian matrices calculated for each scenario. Firstly, we calculate partial derivatives used for the Jacobian matrices calculations:

$$\begin{aligned}
\frac{\partial F_{ij}}{\partial x_{ij}} &= -\frac{b_{ij}(V_i^4 - V_i^3 V_j \cos(\theta_i - \theta_j))}{r_{ij}^2 + x_{ij}^2} - \\
&- 2x_{ij} \frac{V_i^4 + V_i^2 V_j^2 - 2V_i^3 V_j \cos(\theta_i - \theta_j)}{(r_{ij}^2 + x_{ij}^2)^2} - \\
&- 2x_{ij} b_{ij} \frac{(x_{ij} V_i^4 - x_{ij} V_i^3 V_j \cos(\theta_i - \theta_j) - r_{ij} V_i^3 V_j \sin(\theta_i - \theta_j))}{(r_{ij}^2 + x_{ij}^2)^2}
\end{aligned} \tag{8.5.1}$$

$$\begin{aligned}
\frac{\partial F_{ij}}{\partial V_i} &= b_{ij}^2 V_i^3 + \frac{4V_i^3 + 2V_i V_j^2 - 6V_i^2 V_j \cos(\theta_i - \theta_j)}{r_{ij}^2 + x_{ij}^2} - \\
&- b_{ij} \frac{4V_i^3 x_{ij} - 3V_i^2 V_j x_{ij} \cos(\theta_i - \theta_j) - 3r_{ij} V_i^3 V_j \sin(\theta_i - \theta_j)}{r_{ij}^2 + x_{ij}^2}
\end{aligned} \tag{8.5.2}$$

$$\begin{aligned}
\frac{\partial F_{ij}}{\partial V_j} &= \frac{2V_i^2 V_j - 2V_i^3 \cos(\theta_i - \theta_j)}{r_{ij}^2 + x_{ij}^2} - \\
&- b_{ij} \frac{-V_i^3 x_{ij} \cos(\theta_i - \theta_j) - r_{ij} V_i^3 \sin(\theta_i - \theta_j)}{r_{ij}^2 + x_{ij}^2}
\end{aligned} \tag{8.5.3}$$

$$\begin{aligned}
\frac{\partial F_{ij}}{\partial \theta_i} &= \frac{2V_i^3 V_j \sin(\theta_i - \theta_j)}{r_{ij}^2 + x_{ij}^2} - \\
&- b_{ij} \frac{-r_{ij} V_i^3 V_j \cos(\theta_i - \theta_j) + x_{ij} V_i^3 V_j \sin(\theta_i - \theta_j)}{r_{ij}^2 + x_{ij}^2}
\end{aligned} \tag{8.5.4}$$

$$\begin{aligned}
\frac{\partial F_{ij}}{\partial \theta_j} &= -\frac{2V_i^3 V_j \sin(\theta_i - \theta_j)}{r_{ij}^2 + x_{ij}^2} - \\
&- b_{ij} \frac{r_{ij} V_i^3 V_j \cos(\theta_i - \theta_j) - V_i^3 V_j x_{ij} \sin(\theta_i - \theta_j)}{r_{ij}^2 + x_{ij}^2}
\end{aligned} \tag{8.5.5}$$

The important thing here is that each line has two ends and then two different values of apparent power on each end. There is a list of partial derivatives which is calculated for F_{ji} in the same way.

DFm is a matrix of corresponding partial derivatives calculated in the "previous" point for power flows. It is constructed in the way that multiplication on the change of state vector y gives a vector representing ΔF for every line (two values for each for both ends). Linearized thermal limit inequalities around the "previous" point for each given scenario will be written in the following way:

$$F_Prev + DFm(y - y_{prev}) \leq F^{max} \tag{8.5.6}$$

Here y is vector of the variables, $y = (x, V, \theta, Q, P)$ (again for one given scenario)

Partial derivatives for P and Q at the nodes will be:

$$\frac{\partial P_i}{\partial x_{ij}} = \sum_{j \sim i} \left[\frac{V_i V_j \sin(\theta_i - \theta_j)}{r_{ij}^2 + x_{ij}^2} - 2x_{ij} \frac{r_{ij} V_i^2 - r_{ij} V_i V_j \cos(\theta_i - \theta_j) + V_i V_j x_{ij} \sin(\theta_i - \theta_j)}{(r_{ij}^2 + x_{ij}^2)^2} \right] \quad (8.5.7)$$

$$\frac{\partial P_i}{\partial V_i} = \sum_{j \sim i} \left[\frac{2r_{ij} V_i - r_{ij} V_j \cos(\theta_i - \theta_j) + V_j x_{ij} \sin(\theta_i - \theta_j)}{r_{ij}^2 + x_{ij}^2} \right] \quad (8.5.8)$$

$$\frac{\partial P_i}{\partial V_j} = \sum_{j \sim i} \left[\frac{-r_{ij} V_i \cos(\theta_i - \theta_j) + V_i x_{ij} \sin(\theta_i - \theta_j)}{r_{ij}^2 + x_{ij}^2} \right] \quad (8.5.9)$$

$$\frac{\partial P_i}{\partial \theta_i} = \sum_{j \sim i} \left[\frac{V_i V_j x_{ij} \cos(\theta_i - \theta_j) + r_{ij} V_i V_j \sin(\theta_i - \theta_j)}{r_{ij}^2 + x_{ij}^2} \right] \quad (8.5.10)$$

$$\frac{\partial P_i}{\partial \theta_j} = \sum_{j \sim i} \left[\frac{-V_i V_j x_{ij} \cos(\theta_i - \theta_j) - r_{ij} V_i V_j \sin(\theta_i - \theta_j)}{r_{ij}^2 + x_{ij}^2} \right] \quad (8.5.11)$$

$$\frac{\partial P_i}{\partial P_i} = 1 \quad (8.5.12)$$

$$\frac{\partial Q_i}{\partial x_{ij}} = \sum_{j \sim i} \left[\frac{V_i^2 - V_i V_j \cos(\theta_i - \theta_j)}{r_{ij}^2 + x_{ij}^2} - 2x_{ij} \frac{x_{ij} V_i^2 - x_{ij} V_i V_j \cos(\theta_i - \theta_j) - r_{ij} V_i V_j \sin(\theta_i - \theta_j)}{(r_{ij}^2 + x_{ij}^2)^2} \right] \quad (8.5.13)$$

$$\frac{\partial Q_i}{\partial V_i} = \sum_{j \sim i} \left[-b_{ij} V_i + \frac{2x_{ij} V_i - x_{ij} V_j \cos(\theta_i - \theta_j) - V_j r_{ij} \sin(\theta_i - \theta_j)}{r_{ij}^2 + x_{ij}^2} \right] \quad (8.5.14)$$

$$\frac{\partial Q_i}{\partial V_j} = \sum_{j \sim i} \left[\frac{-x_{ij} V_i \cos(\theta_i - \theta_j) - V_i r_{ij} \sin(\theta_i - \theta_j)}{r_{ij}^2 + x_{ij}^2} \right] \quad (8.5.15)$$

$$\frac{\partial Q_i}{\partial \theta_i} = \sum_{j \sim i} \left[\frac{-V_i V_j r_{ij} \cos(\theta_i - \theta_j) + x_{ij} V_i V_j \sin(\theta_i - \theta_j)}{r_{ij}^2 + x_{ij}^2} \right] \quad (8.5.16)$$

$$\frac{\partial Q_i}{\partial \theta_j} = \sum_{j \sim i} \left[\frac{V_i V_j r_{ij} \cos(\theta_i - \theta_j) - x_{ij} V_i V_j \sin(\theta_i - \theta_j)}{r_{ij}^2 + x_{ij}^2} \right] \quad (8.5.17)$$

$$\frac{\partial Q_i}{\partial Q_i} = 1 \quad (8.5.18)$$

if i-load node, then P_i is fixed ($P_{Prev_i} = P_i$) and around the previous point, for each $j \sim i$:

$$0 = \left(\frac{\partial P_i}{\partial x_{ij}}, \frac{\partial P_i}{\partial V_i}, \frac{\partial P_i}{\partial V_j}, \frac{\partial P_i}{\partial \theta_i}, \frac{\partial P_i}{\partial \theta_j} \right)' * \quad (8.5.19)$$

$$*(x_{ij} - x_{Prev_{ij}}, V_i - V_{Prev_i}, V_j - V_{Prev_j}, \theta_i - \theta_{Prev_i}, \theta_j - \theta_{Prev_j}) \quad (8.5.20)$$

$$1 * (Q_i - Q_{Prev_i}) = \left(\frac{\partial Q_i}{\partial x_{ij}}, \frac{\partial Q_i}{\partial V_i}, \frac{\partial Q_i}{\partial V_j}, \frac{\partial Q_i}{\partial \theta_i}, \frac{\partial Q_i}{\partial \theta_j} \right)' * \quad (8.5.21)$$

$$*(x_{ij} - x_{Prev_{ij}}, V_i - V_{Prev_i}, V_j - V_{Prev_j}, \theta_i - \theta_{Prev_i}, \theta_j - \theta_{Prev_j}) \quad (8.5.22)$$

if i-generator node, then around the previous point, for each $j \sim i$:

$$(P_i - P_{Prev_i}) = \left(\frac{\partial P_i}{\partial x_{ij}}, \frac{\partial P_i}{\partial V_i}, \frac{\partial P_i}{\partial V_j}, \frac{\partial P_i}{\partial \theta_i}, \frac{\partial P_i}{\partial \theta_j} \right)' *$$

$$*(x_{ij} - x_{Prev_{ij}}, V_i - V_{Prev_i}, V_j - V_{Prev_j}, \theta_i - \theta_{Prev_i}, \theta_j - \theta_{Prev_j})$$

$$(Q_i - Q_{Prev_i}) = \left(\frac{\partial Q_i}{\partial x_{ij}}, \frac{\partial Q_i}{\partial V_i}, \frac{\partial Q_i}{\partial V_j}, \frac{\partial Q_i}{\partial \theta_i}, \frac{\partial Q_i}{\partial \theta_j} \right)' *$$

$$*(x_{ij} - x_{Prev_{ij}}, V_i - V_{Prev_i}, V_j - V_{Prev_j}, \theta_i - \theta_{Prev_i}, \theta_j - \theta_{Prev_j})$$

The same linearized equations for active and reactive power in vector notation:

$$0 = \left(\frac{\partial P_i}{\partial x_{ij}}, \frac{\partial P_i}{\partial V_i}, \frac{\partial P_i}{\partial V_j}, \frac{\partial P_i}{\partial \theta_i}, \frac{\partial P_i}{\partial \theta_j}, -\frac{\partial P_i}{\partial P_i} \right)' *$$

$$*(x_{ij} - x_{Prev_{ij}}, V_i - V_{Prev_i}, V_j - V_{Prev_j}, \theta_i - \theta_{Prev_i}, \theta_j - \theta_{Prev_j}, P_i - P_{Prev_i})$$

$$0 = \left(\frac{\partial Q_i}{\partial x_{ij}}, \frac{\partial Q_i}{\partial V_i}, \frac{\partial Q_i}{\partial V_j}, \frac{\partial Q_i}{\partial \theta_i}, \frac{\partial Q_i}{\partial \theta_j}, -\frac{\partial Q_i}{\partial Q_i} \right)' *$$

$$*(x_{ij} - x_{Prev_{ij}}, V_i - V_{Prev_i}, V_j - V_{Prev_j}, \theta_i - \theta_{Prev_i}, \theta_j - \theta_{Prev_j}, Q_i - Q_{Prev_i})$$

Then we can rewrite all the linearized active and reactive power balance equations in the matrix form:

$$DPM(y - y_{prev}) = 0 \quad (8.5.23)$$

Here y is vector of the variables, $y = (x, V, \theta, Q, P)$

Cost functions for each generator are usually polynomial functions of the 2nd order. Optimization over sum of quadratic form and linear function will be used in order to solve the following problem on each iteration step from y_{Prev} to new state y :

$$\begin{aligned}
& \min_{\substack{\Delta x, \Delta Q \\ \text{state}^{(a)}, \forall a = 1, \dots, N}} C_{SC} \sum_{\{i,j\} \in \mathcal{E}} \overline{\Delta x_{ij}} + C_{SVC} * \sum_{i \in \mathcal{V}_l} \overline{\Delta Q_i} + N_y \sum_{a=1..N} T_a * C_a(P^{(a)}) \\
\text{s.t. } & \text{state}^{(a)} = y^{(a)} = (x^{(a)}, V^{(a)}, \theta^{(a)}, Q^{(a)}, P^{(a)}) \quad \forall a = 1, \dots, N \\
& x^{(a)} = x_0^{(a)} + \Delta x^{(a)} \quad \forall a = 1, \dots, N \\
& Q_{load}^{(a)} = Q_{load-0}^{(a)} + \Delta Q_{load}^{(a)} \quad \forall a = 1, \dots, N \\
& -\overline{\Delta x} \leq \Delta x^{(a)} \leq \overline{\Delta x} \quad \forall a = 1, \dots, N \\
& -\overline{\Delta Q} \leq \Delta Q_{load}^{(a)} \leq \overline{\Delta Q} \quad \forall a = 1, \dots, N \\
& V_{\min}^{(a)} \leq V^{(a)} \leq V_{\max}^{(a)} \quad \forall a = 1, \dots, N \\
& Q_{\min-gen}^{(a)} \leq Q_{gen}^{(a)} \leq Q_{\max-gen}^{(a)} \quad \forall a = 1, \dots, N \\
& P_{\min-gen}^{(a)} \leq P_{gen}^{(a)} \leq P_{\max-gen}^{(a)} \quad \forall a = 1, \dots, N \\
& F_Prev^{(a)} + DFm^{(a)}(y^{(a)} - y_{prev}^{(a)}) \leq F_{(a)}^{max} \\
& DPM^{(a)}(y^{(a)} - y_{prev}^{(a)}) = 0
\end{aligned} \tag{8.5.24}$$

where $C_a(P^{(a)})$ stands for the function representing the cost of generation for scenario a , and we use the following notation for the complex voltage/potential: $v_i^{(a)} = V_i^{(a)} \exp(i\theta_i^{(a)})$, $\forall a = 1, \dots, N$, $i \in \mathcal{V}^{(a)}$.

8.6 Multiple-scenarios optimization generalization (deterministic)

In the case of multiple scenario optimization, each scenario is defined by occurrence probability, grid structure, load configuration, and uniform loading parameter α . We optimize over all input scenarios simultaneously, so, on each iteration, we linearize constraints for each scenario as it is described above. But capacity variables are the same for all the scenarios. There are various ways how to deal with it. We implement a solution when the solver operates with variables vector X :

$$X = (\overline{\Delta Q}, \overline{\Delta x} | x^1, V^1, \Theta^1, Q^1, P^1 | \dots | x^N, V^N, \Theta^N, Q^N, P^N |)'; \tag{8.6.1}$$

We construct block matrices DFm_mult and DPM_mult corresponding to X vector so that linear approximations of lines thermal constraints and active and reactive power balances at each node written in a matrix form are valid for all the scenarios simultaneously.

8.7 Chance-Constrained Optimal Power Flow (CC-OPF)

8.7.1 Problem statement and analytic reformulation

Problem AC-OPF is a deterministic model finding optimal controllable dispatch for given deterministic uncontrollable buses. Now assume the existence of stochastic uncontrollable buses in the system - wind farms (uncontrollable generators) or fluctuating loads (which have distributed renewable generation at distribution level). In general, it could be the same system but with the uncertain realization of generation/demand at uncertain buses. Fluctuations of active power at uncontrolled buses are modeled by vector w (with length $kbus$), which has 0 mean value and given standard deviation. Expected power value is provided and considered separately as deterministic generation/demand. If there are no fluctuations at bus then the corresponding standard deviation is zero, and the bus becomes deterministic. In this model, it is important that there are controllable generators available in the system for responding to power disbalance and providing frequency control. The response to fluctuations is modeled by AGC control with given participation factors on controllable generators (α) in the following form:

$$\begin{aligned}
 Pg_i(w) &= \overline{Pg}_i + \alpha_i \cdot \Omega & i = PV, \\
 Pg_i(w) &= \overline{Pg}_i + \alpha_i \cdot \Omega + \delta p(w) & i = \theta V, \\
 \Omega &= \sum_{i \in N} w_i, \quad \sum_{i \in N} \alpha_i = 1.
 \end{aligned} \tag{8.7.1}$$

Here PV and θV represent, respectively, a set of buses where active power+voltage, and phase+voltage are kept fixed (the latter applies to the system's slack bus).

CC-AC-OPF model considers response to fluctuations for the predicted period of time made by the controllable resources and provides probabilistic guarantees for the constraints violation (i.e., voltage is less than maximum with probability 99 % means that only 1 % of time voltage is allowed to violate the constraint). CC-AC-OPF finds such setpoint that generation cost is minimized (can be generalized to minimization of the expected value of generation cost), and constraints are probabilistic:

$$\min_{(V, \theta, Pg, Qg)^{set}} \sum_{i=1..kgen} GenCost_i(Pg_i^{set}) \tag{8.7.2}$$

subject to:

$$\begin{aligned}
f_i(V(w), \theta(w), P(w), Q(w)) &= 0 && \forall i = 1..kb \\
Pr(Pg_i(w) \leq Pg_i^{max}) &\geq 1 - \epsilon_p && \forall i = 1..kg \\
Pr(Pg_i(w) \geq Pg_i^{min}) &\geq 1 - \epsilon_p && \forall i = 1..kg \\
Pr(Qg_i(w) \leq Qg_i^{max}) &\geq 1 - \epsilon_q && \forall i = 1..kg \\
Pr(Qg_i(w) \geq Qg_i^{min}) &\geq 1 - \epsilon_q && \forall i = 1..kg \\
Pr(V_i(w) \leq V_i^{max}) &\geq 1 - \epsilon_V && \forall i = 1..kb \\
Pr(V_i(w) \geq V_i^{min}) &\geq 1 - \epsilon_V && \forall i = 1..kb \\
Pr(F_{ij}(w) \leq F_{ij}^{max}) &\geq 1 - \epsilon_F && \forall i - j : line \\
\theta_i &= 0 && i = \theta V, \forall w \\
F_{ij}(w) &= P_{ij}(w)^2 + Q_{ij}(w)^2 && \forall i - j : line \\
f_i(w) &= P_i(w) + iQ_i(w) - \sum_{j \sim i} (S_{ij}) && \forall i = 1..kbus \\
Pg_i(w) &= AGC(w, \alpha) && \forall i = PV, \theta V
\end{aligned}$$

Here AGC is represented by Eq. 8.7.1. All the constraints are similar to the deterministic AC-OPF problem but have a probabilistic form considering any realization of uncertainty w . F_{ij} stands for the squared value of the apparent power flowing at i end of the line. f_i stands for the power balance constraint at each bus. ϵ is allowed probability of constraint violation for the given type of variable.

Using methodology provided in [90] problem [8.7.2] is reformulated analytically to the problem with deterministic constraints using introduced uncertainty margins (λ):

$$\min_{x=(V,\theta,Pg,Qg)^{set}} \sum_{i=1..kgen} GenCost_i(Pg_i^{set}) \tag{8.7.3}$$

subject to:

$$f_i(V^{set}, \theta^{set}, P^{set}, Q^{set}) = 0 \quad \forall i = 1..kbus \quad (8.7.4)$$

$$Pg_i^{min} + \lambda_p^i(x) \leq Pg_i^{set} \leq Pg_i^{max} - \lambda_p^i(x) \quad \forall i = 1..kgen \quad (8.7.5)$$

$$Qg_i^{min} + \lambda_q^i(x) \leq Qg_i^{set} \leq Qg_i^{max} - \lambda_q^i(x) \quad \forall i = 1..kgen \quad (8.7.6)$$

$$V_i^{min} + \lambda_V^i(x) \leq V_i^{set} \leq V_i^{max} - \lambda_V^i(x) \quad \forall i = 1..kbus \quad (8.7.7)$$

$$F_{ij} \leq F_{ij}^{max} - \lambda_F^{ij}(x) \quad \forall i - j : line \quad (8.7.8)$$

$$\theta_i = 0 \quad i = \theta V \quad (8.7.9)$$

$$F_{ij} = P_{ij}^2 + Q_{ij}^2 \quad \forall i - j : line \quad (8.7.10)$$

$$f_i = P_i + iQ_i - \sum_{j \sim i} (S_{ij}) \quad \forall i = 1..kbus \quad (8.7.11)$$

We generalize the formulation and approach to the case when AGC response coefficients are not provided but found by the optimization model. The details of the generalized model and approach for the solution is the following:

8.7.2 Generalized Chance-Constrained OPF

Now α is not given, and it is a matrix in general such that AGC response is generalized to mathematical response to fluctuation vector w . This formulation is not aiming to change AGC control which is well known. It generalizes response to fluctuation in order to increase degrees of freedom to respond to change of conditions. This formulation will be used and discussed then as Cloud-AC-OPF considering various parametrization of the responses to fluctuations.

$$\begin{aligned} Pg_i(w) &= Pg_i^{set} + \sum_{j=1..kbus} \alpha_{ij} * \omega_j & i = PV, \forall w \\ Pg_i(w) &= Pg_i^{set} + \sum_{j=1..kbus} \alpha_{ij} * \omega_j + \delta p(w) & i = \theta V, \forall w \end{aligned} \quad (8.7.12)$$

The problem is mathematically formulated in the following way. The objective function is expected value of the generation cost considering response of generators and there is additional set of variables representing response matrix α .

$$\min_{(V,\theta,Pg,Qg)^{set},\alpha} \sum_{i=1..kgen} \langle GenCost_i(Pg_i(w,\alpha)) \rangle \quad (8.7.13)$$

subject to:

$$\begin{aligned} f_i(V(w,\alpha),\theta(w,\alpha),P(w,\alpha),Q(w,\alpha)) &= 0 & \forall i = 1..kb \\ Pr(Pg_i(w,\alpha) \leq Pg_i^{max}) &\geq 1 - \epsilon_p & \forall i = 1..kg \\ Pr(Pg_i(w,\alpha) \geq Pg_i^{min}) &\geq 1 - \epsilon_p & \forall i = 1..kg \\ Pr(Qg_i(w,\alpha) \leq Qg_i^{max}) &\geq 1 - \epsilon_q & \forall i = 1..kg \\ Pr(Qg_i(w,\alpha) \geq Qg_i^{min}) &\geq 1 - \epsilon_q & \forall i = 1..kg \\ Pr(V_i(w,\alpha) \leq V_i^{max}) &\geq 1 - \epsilon_V & \forall i = 1..kb \\ Pr(V_i(w,\alpha) \geq V_i^{min}) &\geq 1 - \epsilon_V & \forall i = 1..kb \\ Pr(F_{ij}(w,\alpha) \leq F_{ij}^{max}) &\geq 1 - \epsilon_F & \forall i - j : line \\ \theta_i &= 0 & i = \theta V, \forall w \\ F_{ij}(w,\alpha) &= P_{ij}(w,\alpha)^2 + Q_{ij}(w,\alpha)^2 & \forall i - j : line \\ f_i(w,\alpha) &= P_i(w,\alpha) + iQ_i(w,\alpha) - \sum_{j \sim i} (S_{ij}(w,\alpha)) & \forall i = 1..kbus \\ Pg_i(w,\alpha) &= Resp(w,\alpha) & \forall i = 1..kg \end{aligned}$$

Here $Resp((w,\alpha))$ is the response to uncertainty represented by Eq. 8.7.12.

Problem again can be processed to deterministic analytically:

$$\min_{x=(V,\theta,Pg,Qg)^{set},\alpha} \sum_{i=1..kgen} \langle GenCost_i(Pg_i(w)) \rangle \quad (8.7.14)$$

subject to:

$$\begin{aligned}
f_i(V^{set}, \theta^{set}, P^{set}, Q^{set}) &= 0 & \forall i \in N \\
Pg_i^{min} + \lambda_p^i(x, \alpha) &\leq Pg_i^{set} \leq Pg_i^{max} - \lambda_p^i(x, \alpha) & \forall i \in G \\
Qg_i^{min} + \lambda_q^i(x, \alpha) &\leq Qg_i^{set} \leq Qg_i^{max} - \lambda_q^i(x, \alpha) & \forall i \in G \\
V_i^{min} + \lambda_V^i(x, \alpha) &\leq V_i^{set} \leq V_i^{max} - \lambda_V^i(x, \alpha) & \forall i \in N \\
F_{ij} &\leq F_{ij}^{max} - \lambda_F^{ij}(x, \alpha) & \forall ij \in L \\
\theta_i &= 0 & i = \theta V \\
F_{ij} &= P_{ij}^2 + Q_{ij}^2 & \forall ij \in L \\
f_i &= P_i + iQ_i - \sum_{j \sim i} (S_{ij}) & \forall i \in N
\end{aligned}$$

Here N,G,L is set of buses, generators and lines. Now let us detail the procedure of analytic computation of the uncertainty margins.

8.7.3 Definition of uncertainty margins ($\lambda(x, \alpha)$)

The detailed procedure for dealing with PQ, PV, and θV buses for determining the sensitivity matrices to fluctuations which are used for the corresponding uncertainty margins calculation is presented in [9] for the provided α . Here the formal definition procedure is described (considering types of buses), assuming that AC-PF solution exists at the operating point $y = (\theta, V, P, Q)$ and Jacobian matrices can be computed at y . α is taken to be a matrix to represent the generalized CC-AC-OPF.

1) Jacobians are evaluated at y : $J_{vars}^{PQ-constr}(y)$, $J_{vars}^{Ffr}(y)$, $J_{vars}^{Fto}(y)$. Order of variables used for the following sensitivity matrices calculation (according to bus types in the system) is

$$vars = [\theta[PQ], \theta[PV], V[PQ], \theta[\theta V], V[PV], V[\theta V]].$$

Order of PQ-constraints is: $[P[PQ], P[PV], P[\theta V], Q[PQ], Q[PV], Q[\theta V]]$.

Ffr and Fto are squared apparent power at from and to ends of the lines.

$$J^* = J_{vars}^{PQ-constr}(y)[:, 1 : (2kPQ + kPV)] \quad (8.7.15)$$

$$J^{Ffr} = J_{vars}^{Ffr}(y)[:, 1 : (2kPQ + kPV)] \quad (8.7.16)$$

$$J^{Fto} = J_{vars}^{Fto}(y)[:, 1 : (2kPQ + kPV)] \quad (8.7.17)$$

J^* is the same $J_{vars}^{PQ-constr}(y)$ Jacobian but only for variables $[\theta[PQ], \theta[PV], V[PQ]]$. Similar for J^{Ffr} and J^{Fto} .

J^{p-PQ} , J^{p-PV} , $J^{p-\theta V}$, J^{q-PQ} , J^{q-PV} , $J^{q-\theta V}$ are rows of J^* corresponding to specified constraints (p-PQ means active power constraint on PQ buses, etc).

2) Response matrix Ψ with a size $N \times N$ is determined in the following way through α :

$$\Psi = \begin{bmatrix} \alpha_{11} - 1 & \alpha_{12} & \alpha_{13} & \dots & \alpha_{1N} \\ \alpha_{21} & \alpha_{22} - 1 & \alpha_{23} & \dots & \alpha_{2N} \\ \vdots & \vdots & \vdots & \ddots & \vdots \\ \alpha_{N1} & \alpha_{N2} & \alpha_{N3} & \dots & \alpha_{NN} - 1 \end{bmatrix} \quad (8.7.18)$$

and again Ψ^{PQ} , Ψ^{PV} , $\Psi^{\theta V}$ - matrices with rows corresponding to PQ, PV and θV buses.

$$\Psi 1 = \begin{bmatrix} \Psi^{PQ} \\ \Psi^{PV} \\ 0^{kPQ \times N} \end{bmatrix} \quad (8.7.19)$$

$$G1 = inv\left(\begin{bmatrix} J^{p-PQ} \\ J^{p-PV} \\ J^{q-PQ} \end{bmatrix} \right) \times \Psi 1 \quad (8.7.20)$$

Here, the important point is that inversion of a square matrix is done numerically when operational point y is specified. If α is specified, then all sensitivity matrices and uncertainty margins are numerically defined. If not, then it can be found by optimization, but the operational point should be specified for that.

3) Then sensitivity matrix to uncertainty vector w for each variable and for each type of bus is determined in the following way (generator parameterized response is not included to sensitivity response, i.e. $G_w^{p-PV} = 0$, as it is predefined by Eq. 8.7.12 and its impact to uncertainty margin is

computed similarly):

$$G_w^{p-PQ} = 0 \quad (8.7.21)$$

$$G_w^{p-PV} = 0 \quad (8.7.22)$$

$$G_w^{p-\theta V} = J^{p-\theta V} \times G1 - \Psi^{\theta V} \quad (8.7.23)$$

$$G_w^{q-PQ} = 0 \quad (8.7.24)$$

$$G_w^{q-PV} = J^{q-PV} \times G1 \quad (8.7.25)$$

$$G_w^{q-\theta V} = J^{q-\theta V} \times G1 \quad (8.7.26)$$

$$G_w^{V-PQ} = G1[kPQ + kPV + 1 : 2kPQ + kPV, :] \quad (8.7.27)$$

$$G_w^{V-PV} = 0 \quad (8.7.28)$$

$$G_w^{V-\theta V} = 0 \quad (8.7.29)$$

$$G_w^{Ffr} = J^{Ffr} \times G1 \quad (8.7.30)$$

$$G_w^{Fto} = J^{Fto} \times G1 \quad (8.7.31)$$

4) Finally, uncertainty margins for each variable and for each type of bus case be defined around y . If γ is considered system parameter and it is probabilistically constrained $Pr(\gamma_i(w, \alpha) \leq \gamma_i^{max}) \geq 1 - \epsilon_\gamma$ (for a bus i) then dependence on uncertainty vector and generators response policy coefficients can be linearized for a small uncertainty $Pr(\gamma_i^{set} + G_{w(i,:)}^\gamma(y, \alpha) \times w \leq \gamma_i^{max}) \geq 1 - \epsilon_\gamma$ which is equivalent to (for Gaussian distribution of uncertainty) to:

$$\gamma_i \leq \gamma_i^{max} - F^{-1}(1 - \epsilon_\gamma) \sqrt{(G_{w(i,:)}^\gamma(y, \alpha))^T \Sigma_w G_{w(i,:)}^\gamma(y, \alpha)} \quad (8.7.32)$$

Here the reduction of maximum value is the definition of the uncertainty margin $\lambda_\gamma^i(y, \alpha)$. $F^{-1}(1 - \epsilon_\gamma)$ is the inverse cumulative distribution function of the standard normal distribution evaluated at $1 - \epsilon_\gamma$. Σ_w is the covariance matrix of the fluctuation vector w .

8.7.4 Analytic averaging of cost over uncertainty set

There is a generator response for each realization of uncertainty such that $Pg(w) = Pg^{set} + \xi(w)$. Usually generation cost is represented by a quadratic function $GenCost = ap^2 + bp + c$. Mean value of fluctuations is zero then

$$\langle GenCost(w) \rangle = a(Pg^{set})^2 + bPg^{set} + c + a \langle \xi^2 \rangle$$

Using the response policy (3) with $\xi = Resp^3(w, \alpha)$ we obtain the following:

$$i - PV : \langle \xi^2 \rangle = \sum_{j=1..N} \alpha_{ij}^2 \times Var(w_j) \quad (8.7.33)$$

$$i - \theta V : \langle \xi^2 \rangle = \sum_{j=1..N} (\alpha_{ij} + (G_w^{p-\theta V})_{1j})^2 \times Var(w_j) \quad (8.7.34)$$

Here $G_w^{p-\theta V}$ is 1-row matrix (single slack bus in the system) and $Var(w_j)$ is variance of the j-component of the uncertainty vector.

Bibliography

- [1] “Matpower users manual, <http://www.pserc.cornell.edu/matpower/manual.pdf>.”
- [2] “Flexible ac transmission systems (facts), abb, <http://new.abb.com/facts>.”
- [3] A. Martin Gross, Global Head of Grid Systems Business, “Flexible power transmission, <http://www.powersystemsdesign.com/flexible-power-transmission>.”
- [4] R. Grunbaum and G. Ingestrom, “765 kv series capacitors for increasing power transmission capacity to the cape region .”
- [5] [Online]. Available: <https://www.statista.com>
- [6] [Online]. Available: <https://ec.europa.eu>
- [7] [Online]. Available: <https://www.eia.gov/>
- [8] [Online]. Available: <https://en.wikipedia.org/>
- [9] L. Roald, “Optimization methods to manage uncertainty and risk in power system operation,” *Ph.D. dissertation*, 2016.
- [10] “Russian generation capacity upgrade analysis,” https://www.kommersant.ru/doc/3758063?utm_source=kommersant&utm_medium=partner_verh&utm_campaign=siemens.
- [11] A. H. Fuldner, “Upgrading transmission capacity for wholesale electric power trade,” http://www.eia.doe.gov/cneaf/pubs_html/feat_trans_capacity/w_sale.html, accessed: 2016-11-16.
- [12] L. Gyugyi, “Unified power-flow control concept for flexible ac transmission systems,” *Generation, Transmission and Distribution, IEE Proceedings C*, vol. 139, no. 4, pp. 323–331, 1992.
- [13] M. Noroozian and G. Andersson, “Power flow control by use of controllable series components,” *Power Delivery, IEEE Transactions on*, vol. 8, no. 3, pp. 1420–1429, 1993.
- [14] M. Noroozian, L. Angquist, M. Ghandhari, and G. Andersson, “Use of upfc for optimal power flow control,” *Power Delivery, IEEE Transactions on*, vol. 12, no. 4, pp. 1629–1634, oct 1997.

- [15] D. Gotham and G. Heydt, "Power flow control and power flow studies for systems with facts devices," *Power Systems, IEEE Transactions on*, vol. 13, no. 1, pp. 60–65, feb 1998.
- [16] S. Gerbex, R. Cherkaoui, and A. Germond, "Optimal location of multi-type facts devices in a power system by means of genetic algorithms," *Power Systems, IEEE Transactions on*, vol. 16, no. 3, pp. 537–544, aug 2001.
- [17] A. Oudalov, R. Cherkaoui, and A. Germond, "Application of fuzzy logic techniques for the coordinated power flow control by multiple series facts devices," in *Power Industry Computer Applications, 2001. PICA 2001. Innovative Computing for Power - Electric Energy Meets the Market. 22nd IEEE Power Engineering Society International Conference on*, 2001, pp. 74–80.
- [18] T. Orfanogianni and R. Bacher, "Steady-state optimization in power systems with series facts devices," *Power Systems, IEEE Transactions on*, vol. 18, no. 1, pp. 19–26, feb 2003.
- [19] W. Wu and C. Wong, "Facts applications in preventing loop flows in interconnected systems," in *Power Engineering Society General Meeting, 2003, IEEE*, vol. 1, july 2003, p. 4 vol. 2666.
- [20] G. Glanzmann and G. Andersson, "Using facts devices to resolve congestions in transmission grids," in *CIGRE/IEEE PES, 2005. International Symposium*, oct. 2005, pp. 347–354. [Online]. Available: [\url{http://www.eeh.ee.ethz.ch/uploads/tx_ethpublications/Glanzmann_CIGRE_05.pdf}](http://www.eeh.ee.ethz.ch/uploads/tx_ethpublications/Glanzmann_CIGRE_05.pdf)
- [21] W. Shao and V. Vittal, "Lp-based opf for corrective facts control to relieve overloads and voltage violations," *Power Systems, IEEE Transactions on*, vol. 21, no. 4, pp. 1832–1839, nov. 2006.
- [22] M. Santiago-Luna and J. Cedeno-Maldonado, "Optimal placement of facts controllers in power systems via evolution strategies," in *Transmission Distribution Conference and Exposition: Latin America, 2006. TDC '06. IEEE/PES*, aug. 2006, pp. 1–6.
- [23] K. Lee, M. Farsangi, and H. Nezamabadi-pour, "Hybrid of analytical and heuristic techniques for facts devices in transmission systems," in *Power Engineering Society General Meeting, 2007. IEEE*, june 2007, pp. 1–8.
- [24] C. Rehtanz and U. Hager, "Coordinated wide area control of facts for congestion management," in *Electric Utility Deregulation and Restructuring and Power Technologies, 2008. DRPT 2008. Third International Conference on*, april 2008, pp. 130–135.
- [25] H. Sauvain, M. Lalou, Z. Styczynski, and P. Komarnicki, "Optimal and secure transmission of stochastic load controlled by wacs #x2014; swiss case," in *Power and Energy Society General Meeting - Conversion and Delivery of Electrical Energy in the 21st Century, 2008 IEEE*, july 2008, pp. 1–5.

- [26] Q. Wu, Z. Lu, M. Li, and T. Ji, "Optimal placement of facts devices by a group search optimizer with multiple producer," in *Evolutionary Computation, 2008. CEC 2008. (IEEE World Congress on Computational Intelligence)*. IEEE Congress on, june 2008, pp. 1033 –1039.
- [27] J. Filho, N. Martins, and D. Falcao, "Identifying power flow control infeasibilities in large-scale power system models," *Power Systems, IEEE Transactions on*, vol. 24, no. 1, pp. 86 –95, feb. 2009.
- [28] M. Sahraei-Ardakani and S. Blumsack, "Market equilibrium for dispatchable transmission using fact devices," in *Power and Energy Society General Meeting, 2012 IEEE*, 2012, pp. 1–6.
- [29] P. Albrecht and G. Breuer, *Flexible ac transmission systems (FACTS): scoping study*, ser. Flexible Ac Transmission Systems (FACTS): Scoping Study. General Electric Company. Power Systems Engineering Dept and Electric Power Research Institute, 1991, no. v. 2, pt. 1. [Online]. Available: <http://books.google.com/books?id=UPwJAQAAMAAJ>
- [30] "Flexible ac transmission systems (facts)," http://en.wikipedia.org/wiki/Flexible_AC_transmission_system.
- [31] A. Edris, "Proposed terms and definitions for flexible ac transmission system (facts)," *Power Delivery, IEEE Transactions on*, vol. 12, no. 4, pp. 1848 –1853, oct 1997.
- [32] N. Hingorani and L. Gyugyi, *Understanding FACTS: Concepts and Technology of Flexible AC Transmission Systems*. Wiley-IEEE Press, 1999.
- [33] ———, *Understanding FACTS concepts and technology of flexible AC transmission systems*. IEEE Press, New York, 2000.
- [34] R. Mathur and R. Varma, *Thyristor-based FACTS controllers for electrical transmission systems*. IEEE Press, Piscataway, 2002.
- [35] K. Dvijotham, S. Backhaus, and M. Chertkov, "Operations-Based Planning for Placement and Sizing of Energy Storage in a Grid With a High Penetration of Renewables," *ArXiv e-prints*, Jul. 2011.
- [36] E. J. Candes, M. B. Wakin, and S. Boyd, "Enhancing sparsity by reweighted l1 minimization," *Journal of Fourier Analysis and Applications*, vol. 14, no. 5, pp. 877–905, 2008.
- [37] J. Johnson and M. Chertkov, "A majorization-minimization approach to design of power transmission networks," in *Decision and Control (CDC), 2010 49th IEEE Conference on*, dec. 2010, pp. 3996 –4003.
- [38] M. Chertkov, F. Pan, and M. Stepanov, "Predicting failures in power grids: The case of static overloads," *IEEE Transactions on Smart Grids*, vol. 2, p. 150, 2010.

- [39] M. Chertkov, M. Stepanov, F. Pan, and R. Baldick, “Exact and efficient algorithm to discover extreme stochastic events in wind generation over transmission power grids,” *CDC-ECC*, pp. 2174–2180, dec. 2011.
- [40] F. Dörfler, M. Chertkov, and F. Bullo, “Synchronization in Complex Oscillator Networks and Smart Grids,” *Proceedings of National Academy of Sciences*, vol. 10.1073/pnas.1212134110, 2013. [Online]. Available: [\url{http://arxiv.org/abs/1208.0045}](http://arxiv.org/abs/1208.0045)
- [41] J. Lavaei and S. Low, “Zero duality gap in optimal power flow problem,” *IEEE Transactions on Power Systems*, 2012.
- [42] D. Bienstock, M. Chertkov, and S. Harnett, “Chance-constrained optimal power flow: Risk-aware network control under uncertainty,” *SIAM Review*, vol. 56, no. 3, pp. 461—495, 2014.
- [43] S. Bose, D. Gayme, K. M. Chandy, and S. Low, “Quadratically constrained quadratic programs on acyclic graphs with application to power flow,” in *arXiv:1203.5599*, 2012.
- [44] C. Coffrin, P. van Hentenryck, and R. Bent, “Approximating line losses and apparent power in ac power flow linearizations,” in *Power Engineering Society General Meeting 2012*, 2012, pp. 1–8.
- [45] S. L. Programming, “[http://en.wikipedia.org/wiki/Successive_linear_programming.](http://en.wikipedia.org/wiki/Successive_linear_programming)”
- [46] D. P. Bertsekas, *Nonlinear Programming*. Athena Scientific, 1999.
- [47] M. Avriel, *Nonlinear Programming: Analysis and Methods*. Dover Publications, 2003.
- [48] D. Chattopadhyay, K. Bhattacharya, and J. Parikh, “Optimal reactive power planning and its spot-pricing: an integrated approach,” *IEEE Trans. Power Syst.*, vol. 10, no. 4, pp. 2014–2020, Nov. 1995.
- [49] A. Lashkar Ara, A. Kazemi, and S. A. Nabavi Niaki, “Multiobjective optimal location of FACTS shunt-series controllers for power system operation planning,” *IEEE Trans. Power Del.*, vol. 27, no. 2, pp. 481–490, Dec. 2011.
- [50] S. J. Galloway, I. M. Elders, G. M. Burt, and B. Sookananta, “Optimal flexible alternative current transmission system device allocation under system fluctuations due to demand and renewable generation,” *IET Gen. Trans. Distrib.*, vol. 4, no. 6, pp. 725–735, June 2010.
- [51] K. Aoki, M. Fan, and A. Nishikori, “Optimal VAR planning by approximation method for recursive mixed-integer linear programming,” *IEEE Trans. Power Syst.*, vol. 3, no. 4, pp. 1741–1747, Nov. 1988.

- [52] G. Y. Yang, G. Hovland, R. Majumder, and Z. Y. Dong, "TCSC allocation based on line flow based equations via mixed-integer programming," *IEEE Trans. Power Syst.*, vol. 22, no. 4, pp. 2262–2269, Nov. 2007.
- [53] Y. T. Hsiao, C. C. Liu, H. D. Chiang, and Y. L. Chen, "A new approach for optimal VAR sources planning in large scale electric power systems," *IEEE Trans. Power Syst.*, vol. 8, no. 3, pp. 988–996, Aug. 1993.
- [54] R. Minguez, F. Milano, R. Zarate-Miano, and A. J. Conejo, "Optimal network placement of SVC devices," *IEEE Trans. Power Syst.*, vol. 22, no. 4, pp. 1851–1860, Nov. 2007.
- [55] E. Ghahremani and I. Kamwa, "Optimal placement of multiple-type FACTS devices to maximize power system loadability using a generic graphical user interface," *IEEE Trans. Power Syst.*, vol. 28, no. 2, pp. 764–778, Aug. 2013.
- [56] R. S. Wibowo, N. Yorino, M. Eghbal, Y. Zoka, and Y. Sasaki, "FACTS devices allocation with control coordination considering congestion relief and voltage stability," *IEEE Trans. Power Syst.*, vol. 26, no. 4, pp. 2302–2310, Nov 2011.
- [57] J. G. Singh, P. Guha Thakurta, and L. Soder, "Load curtailment minimization by optimal placements of SVC/STATCOM," *Int. Trans. Elect. Energy Syst.*, vol. 25, no. 11, pp. 2769–2780, Sept. 2014.
- [58] F. Dong, B. H. Chowdhury, M. L. Crow, and L. Acar, "Improving voltage stability by reactive power reserve management," *IEEE Trans. Power Syst.*, vol. 20, no. 1, pp. 338–345, Feb. 2005.
- [59] E. A. Leonidaki, D. P. Georgiadis, and N. D. Hatziargyriou, "Decision trees for determination of optimal location and rate of series compensation to increase power system loading margin," *IEEE Trans. Power Syst.*, vol. 21, no. 3, pp. 1303–1310, Jul. 2006.
- [60] F. G. M. Lima, F. D. Galiana, I. Kockar, and J. Munoz, "Phase shifter placement in large-scale systems via mixed integer linear programming," *IEEE Trans. Power Syst.*, vol. 18, no. 3, pp. 1029–1034, Aug. 2003.
- [61] S. Rahimzadeh, M. Tavakoli, and B. A. H. Viki, "Simultaneous application of multi-type FACTS devices to the restructured environment: achieving both optimal number and location," *IET Gen. Trans. Distrib.*, vol. 4, no. 3, pp. 349–362, Mar. 2010.
- [62] S. Gerbex, R. Cherkaoui, and A. J. Germond, "Optimal location of multi-type FACTS devices in a power system by means of genetic algorithms," *IEEE Trans. Power Syst.*, vol. 16, no. 3, pp. 537–544, Aug. 2001.

- [63] P. Paterni, S. Vitet, M. Bena, and A. Yokoyama, “Optimal location of phase shifters in the French network by genetic algorithm,” *IEEE Trans. Power Syst.*, vol. 14, no. 1, pp. 37–42, Feb. 1999.
- [64] L. Ippolito and P. Siano, “Selection of optimal number and location of thyristor-controlled phase shifters using genetic based algorithms,” *IEE Proc. Gen. Trans. Distrib.*, vol. 151, no. 5, pp. 630–637, Sept. 2004.
- [65] N. K. Sharma, A. Ghosh, and R. K. Varma, “A novel placement strategy for facts controllers,” *IEEE TRANSACTIONS ON POWER DELIVERY*, vol. 18, no. 3, 2003.
- [66] D. Gaur and L. Mathew, “Optimal placement of facts devices using optimization techniques: A review,” *3rd International Conference on Communication Systems (ICCS-2017)*, 2017.
- [67] J. Huang, Z. Jiang, and M. Negnevitsky, “Loadability of power systems and optimal svc placement,” *Electrical Power and Energy Systems*, vol. 45, 2013.
- [68] J. G. Singh, S. N. Singh, and S. C. Srivastava, “Placement of facts controllers for enhancing power system loadability,” *2006 IEEE Power India Conference*, 2006.
- [69] C. Duan, W. Fang, L. Jiang, and S. Niu, “FACTS devices allocation via sparse optimization,” *IEEE Trans. Power Syst.*, vol. 31, no. 2, pp. 1308–1319, Mar. 2016.
- [70] V. Frolov, S. Backhaus, and M. Chertkov, “Efficient algorithm for locating and sizing series compensation devices in large power transmission grids: I. model implementation,” *New Journal of Physics*, vol. 16, no. 10, p. 105015, 2014. [Online]. Available: <http://stacks.iop.org/1367-2630/16/i=10/a=105015>
- [71] —, “Efficient algorithm for locating and sizing series compensation devices in large power transmission grids: Ii. solutions and applications,” *New Journal of Physics*, vol. 16, no. 10, p. 105016, 2014. [Online]. Available: <http://stacks.iop.org/1367-2630/16/i=10/a=105016>
- [72] V. Frolov, “Placement and sizing of series compensation (sc) and static var compensation (svc) devices in transmission grids: The case of ac power flows,” *MSc thesis, Skoltech*, 2016.
- [73] “Mosek, <https://www.mosek.com/>.”
- [74] R. D. Zimmerman and C. E. Murillo-Sanchez, “A matlab power system simulation package, <http://www.pserc.cornell.edu/matpower/>.”
- [75] D. L. Donoho, “For most large underdetermined systems of linear equations the minimal 1-norm solution is also the sparsest solution,” *Communications on pure and applied mathematics*, vol. 59, pp. 797—829, 2006.

- [76] “Interior point optimizer, <https://projects.coin-or.org/Ipopt>.”
- [77] H. Lee Willis, *Power Distribution Planning Reference Book*. New York: Marcel Dekker, Inc, 2004.
- [78] “Ibm cplex optimizer, <http://www-01.ibm.com/software/commerce/optimization/cplex-optimizer/>.”
- [79] C. Coffrin, R. Bent, K. Sundar, Y. Ng, and M. Lubin, “Powermodels.jl: An open-source framework for exploring power flow formulations,” *Power Systems Computation Conference (PSCC)*, 2018.
- [80] V. Frolov, P. Guha Thakurta, S. Backhaus, J. Bialek, and M. Chertkov, “Optimal Placement and Sizing of FACTS Devices to Delay Transmission Expansion,” *arxiv*., 2016.
- [81] “[online] julia/jump package for steady-state power network optimization,” <https://github.com/lanl-ansi/PowerModels.jl>, accessed: 2017-06-17.
- [82] V. Frolov, P. Guha Thakurta, S. Backhaus, J. Bialek, and M. Chertkov, “Scalable Optimal Placement and Sizing of FACTS Devices Using AC Power Flow Model,” *arXiv:1608.04467*, submitted *IEEE CONES*, 2016.
- [83] V. A. Frolov and M. Chertkov, “Methodology for multi-stage, operations- and uncertainty-aware placement and sizing of FACTS devices in a large power transmission system,” *arXiv:1707.03686*, *IREP/2017*, 2017.
- [84] D. K. Molzahn and I. A. Hiskens, “A survey of relaxations and approximations of the power flow equations,” *Foundations and Trends® in Electric Energy Systems*, vol. 4, no. 1-2, pp. 1–221, 2019. [Online]. Available: <http://dx.doi.org/10.1561/3100000012>
- [85] A. Wächter and L. T. Biegler, “On the implementation of a primal-dual interior point filter line search algorithm for large-scale nonlinear programming,” *Mathematical Programming*, vol. 106, pp. 25–57, 2006.
- [86] B. G. Gorenstin, N. M. Campodonico, J. P. Costa, and M. V. F. Pereira, “Power system expansion planning under uncertainty,” *IEEE Transactions on Power Systems*, vol. 8, no. 1, pp. 129–136, Feb 1993.
- [87] F. D. Munoz and J.-P. Watson, “A scalable solution framework for stochastic transmission and generation planning problems,” *Computational Management Science*, vol. 12, no. 4, pp. 491–518, Oct 2015. [Online]. Available: <https://doi.org/10.1007/s10287-015-0229-y>

- [88] L. Roald, F. Oldewurtel, T. Krause, and G. Andersson, “Analytical reformulation of security constrained optimal power flow with probabilistic constraints,” in *2013 IEEE Grenoble Conference*, June 2013, pp. 1–6.
- [89] D. Bienstock, M. Chertkov, and S. Harnett, “Chance-constrained optimal power flow: Risk-aware network control under uncertainty,” *SIAM Review*, vol. 56, no. 3, pp. 461–495, 2014. [Online]. Available: <https://doi.org/10.1137/130910312>
- [90] L. Roald and G. Andersson, “Chance-constrained ac optimal power flow: Reformulations and efficient algorithms,” *IEEE Transactions on Power Systems*, vol. 33, no. 3, pp. 2906–2918, May 2018.
- [91] A. Venzke, L. Halilbasic, A. Barré, L. Roald, and S. Chatzivasileiadis, “Chance-constrained ac optimal power flow integrating hvdc lines and controllability,” *arXiv:1810.09218*, 2018.
- [92] K. Sundar, H. Nagarajan, M. Lubin, L. Roald, S. Misra, R. Bent, and D. Bienstock, “Unit commitment with n-1 security and wind uncertainty,” in *Power Systems Computation Conference (PSCC), 2016*. IEEE, 2016, pp. 1–7.
- [93] L. Roald, T. Krause, and G. Andersson, “Integrated balancing and congestion management under forecast uncertainty,” in *2016 IEEE International Energy Conference (ENERGYCON)*. IEEE, 2016, pp. 1–6.
- [94] L. Roald, F. Oldewurtel, B. Van Parys, and G. Andersson, “Security constrained optimal power flow with distributionally robust chance constraints,” *arXiv:1508.06061*, 2015.
- [95] A. Ben-Tal, L. El Ghaoui, and A. Nemirovski, *Robust optimization*. Princeton University Press, 2009, vol. 28.
- [96] I. Dunning, J. Huchette, and M. Lubin, “Jump: A modeling language for mathematical optimization,” *SIAM Review*, vol. 59, no. 2, pp. 295–320, 2017.
- [97] V. Frolov, L. Roald, and M. Chertkov, “Cloud-ac-opf: Model reduction technique for multi-scenario optimal power flow via chance-constrained optimization,” *arXiv:1905.10455, POWERTECH/2019*, 2019.
- [98] A. Moreira, D. Pozo, A. Street, and E. Sauma, “Reliable renewable generation and transmission expansion planning: Co-optimizing system’s resources for meeting renewable targets,” *IEEE Transactions on Power Systems*, vol. 32, no. 4, pp. 3246–3257, July 2017.
- [99] “Kirchhoff’s circuit laws, http://en.wikipedia.org/wiki/Kirchhoff's_circuit_laws.”

- [100] M. Noroozian, L. Angquist, M. Ghandhari, and G. Andersson, "Improving power system dynamics by series-connected facts devices," *Power Delivery, IEEE Transactions on*, vol. 12, no. 4, pp. 1635–1641, 1997.
- [101] "Flexible ac transmission systems (facts), siemens, <http://www.energy.siemens.com/hq/en/power-transmission/facts/>."
- [102] "Northeast blackout of 2003, http://en.wikipedia.org/wiki/Northeast_blackout_of_2003."
- [103] "Fast-track facts project completed in time for christmas peak load, <http://www.abb.com/cawp/seitp202/b6f6ffd8620ff668c1257db2003587c3.aspx>."
- [104] R. K. Bindal, "A review of benefits of {FACTS} devices in power system," *International Journal of Engineering and Advanced Technology (IJEAT)*, vol. 3, pp. 105 – 108, 2014. [Online]. Available: <http://www.ijeat.org/attachments/File/v3i4/D2903043414.pdf>
- [105] "2012 state of the market report for the miso electricity markets, https://www.misoenergy.org/Library/Repository/Report/IMM/2012%20SOM_Analytic%20Appendix.pdf," 2012.
- [106] N. Mithulananthan and N. Acharya, "A proposal for investment recovery of {FACTS} devices in deregulated electricity markets," *Electric Power Systems Research*, vol. 77, no. 5.6, pp. 695 – 703, 2007. [Online]. Available: <http://www.sciencedirect.com/science/article/pii/S0378779606001507>
- [107] R. Suman, C. Lal, M. Kumar, I. Alam, and A. Goswami, "Cost-benefit analysis of tcsc installation to power system operation," in *Energy, Automation, and Signal (ICEAS), 2011 International Conference on*, Dec 2011, pp. 1–6.